Exceptionally preserved shark fossils from Mexico elucidate the long-standing enigma of the Cretaceous elasmobranch Ptychodus

Romain Vullo, Eduardo Villalobos-Segura, Manuel Amadori, Jürgen Kriwet, Eberhard Frey, Margarito González González, José Padilla Gutiérrez, Christina Ifrim, Eva Stinnesbeck, Wolfgang Stinnesbeck

Exceptionally preserved shark fossils from Mexico elucidate the long-standing enigma of the Cretaceous elasmobranch *Ptychodus*

Romain Vullo[1], Eduardo Villalobos-Segura[2], Manuel Amadori[2], Jürgen Kriwet[2,3], Eberhard Frey[4], Margarito A. González González[5], José M. Padilla Gutiérrez[6], Christina Ifrim[7], Eva S. Stinnesbeck[8] and Wolfgang Stinnesbeck[9]

[1]Univ Rennes, CNRS, Géosciences Rennes, UMR 6118, Rennes, France

[2]Department of Palaeontology, Faculty of Earth Sciences, Geography and Astronomy, University of Vienna, Vienna, Austria

[3]Vienna Doctoral School of Ecology and Evolution, University of Vienna, Vienna, Austria

[4]Sonnenbergstraße 27, Pforzheim, Germany

[5]Calle Josefa Ortiz de Domínguez 165 norte, Colonia Bella Vista, Sabinas Hidalgo, Mexico

[6]Museo del Desierto, Parque de las Maravillas, Nuevo Centro Metropolitano, Saltillo, Mexico

[7]Staatliche Naturwissenschaftliche Sammlungen Bayerns, Jura-Museum, Willibaldsburg, Eichstätt, Germany

[8]Steinmann-Institut für Geologie, Mineralogie und Paläontologie, Rheinische Friedrich-Wilhelms-Universität, Bonn, Germany

[9]Institute für Geowissenschaften, Ruprecht-Karls-Universität, Heidelberg, Germany

Author for correspondence:

Romain Vullo

e-mail: romain.vullo@univ-rennes.fr

DOI: 10.1098/rspb.2024.0262

ABSTRACT

The fossil fish *Ptychodus* Agassiz, 1834, characterized by a highly distinctive grinding dentition and an estimated gigantic body size (up to around 10 m), has remained one of the most enigmatic extinct elasmobranchs (i.e. sharks, skates and rays) for nearly two centuries. This widespread Cretaceous taxon is common in Albian to Campanian deposits from almost all continents. However, specimens mostly consist of isolated teeth or more or less complete dentitions, whereas cranial and post-cranial skeletal elements are very rare. Here we describe newly discovered material from the early Late Cretaceous of Mexico, including complete articulated specimens with preserved body outline, which reveals crucial information on the anatomy and systematic position of *Ptychodus*. Our phylogenetic and ecomorphological analyses indicate that ptychodontids were high-speed (tachypelagic) durophagous lamniforms (mackerel sharks), which occupied a specialized predatory niche previously unknown in fossil and extant elasmobranchs. Our results support the view that lamniforms were ecomorphologically highly diverse and represented the dominant group of sharks in Cretaceous marine ecosystems. *Ptychodus* may have fed predominantly on nektonic hard-shelled prey items such as ammonites and sea turtles rather than on benthic invertebrates, and its extinction during the Campanian, well before the end-Cretaceous crisis, might have been related to competition with emerging blunt-toothed globidensine and prognathodontine mosasaurs.

Keywords: Chondrichthyes, Lamniformes, Ptychodontidae, ecomorphology, Late Cretaceous, Vallecillo fossil Lagerstätte

1. Introduction

Ptychodus Agassiz, 1834 (Elasmobranchii: Ptychodontidae) is a cosmopolitan group of fossil sharks occurring in Albian–Campanian (*ca* 105 to 75 million years old) marine deposits of all continents except Antarctica (e.g. [1–10]). This diverse Cretaceous genus, including at least 16 species, is primarily known from isolated teeth and partial dentitions. Two species groups, which often co-occur with each other, can be distinguished: species with low-crowned (uncuspidate) teeth and species with high-crowned (cuspidate) teeth, such as *Ptychodus decurrens* and *P. mammillaris*, respectively (e.g. [8,10]). Teeth were arranged in a way that they formed large dental plates supported by elongated, V-shaped jaws [1,8,9,11–14]. It is generally accepted that ptychodontids had a durophagous predatory lifestyle, using their massive grinding dentitions to prey on shelled bottom-dwelling animals such as bivalves, brachiopods and crustaceans, but also to hunt ammonites and other pelagic animals in the open water column [8,9,12,14–21]. Although complete specimens of *Ptychodus* have not been reported so far, the body size of this extinct predator was estimated to have reached or even exceeded 10 m in total length based on jaw elements and dentitions (e.g. [12,13]), making *Ptychodus* the largest durophagous shark that ever roamed the oceans, being even bigger than modern apex shark predators.

Since its first report in the first half of the 18th century based on some isolated teeth from the English Chalk [22,23], numerous researchers attempted to identify the relationships of this fascinating predator resulting in sometimes very contradictory interpretations ranging from representing durophagous bony fishes such as porcupinefishes as well as various cartilaginous fishes [23]. Although *Ptychodus* has been unanimously acknowledged to be a chondrichthyan

since the seminal work of Agassiz [24], its exact affinities remained dubious for decades, and it was assumed to belong either to extinct hybodont sharks, modern sharks, or even rays [1,5,12,23,25–33]. Closer relationships to living mackerel sharks were already proposed by Hamm [34], but without providing substantial information or figures. Later, the same author [35] placed the family Ptychodontidae (i.e. *Ptychodus* and *Paraptychodus*; [36]) in its own order, Ptychodontiformes, with unresolved relationships to other sharks. The new complete skeletons described here help resolve the long-standing enigma of *Ptychodus*. This material allows detailed phylogenetic and morphological analyses, which were implemented to identify the systematic relationships of *Ptychodus* and characterize the predatory lifestyle of this peculiar durophagous shark.

2. Material and methods

(a) Repository of specimens

The six *Ptychodus* specimens examined for this study are part of the Colección Paleontológica de Coahuila (CPC) and are permanently housed in two Mexican public museums: the Museo La Milarca, San Pedro Garza García, Nuevo León (MMSP) and the Museo del Desierto, Saltillo, Coahuila (MUDE).

(b) Geological setting

All the specimens studied here come from the quarries near Vallecillo (26°39.32’N, 100°00.82’W), Nuevo León, northeastern Mexico. In this region, the uppermost Cenomanian–middle Turonian Vallecillo Member comprises ca. 8 m of pinkish platy limestone intercalated in the monotonous marl-limestone series of the Agua Nueva Formation [37]. These beds were deposited in an open marine shelf environment [37,38] and include a unit of thin laminated

layers rich in inoceramid bivalves, ammonites, and vertebrates (e.g. [17,39]). The latter are represented by exquisitely preserved fossils of fishes (elasmobranchs, actinopterygians, and actinistians) and marine reptiles (protostegid turtles, mosasauroids and polycotylid plesiosaurs) (e.g. [39–42]) (see electronic supplementary material, figure S1).

(b) Phylogenetic analysis

We explored the phylogenetic relationships of the genus *Ptychodus* Agassiz, 1834 within the elasmobranchs using a modified version of Jambura *et al.*'s [43] data matrix. In order to provide a broader context of these relations, several Palaeozoic, Mesozoic, Cenozoic and Recent chondrichthyan taxa were additionally included as outgroups, with *Pucapampella* and *Doliodus* serving as the root. To accommodate the inclusion of these groups, several modifications and additional characters from previous works were added to the present data matrix (e.g. [44–56]; see electronic supplementary material for additional references). The resulting data matrix was assembled in Mesquite 3.81 [57] and includes 221 characters (see electronic supplementary material and [58]).

The parsimony analysis was carried out in TNT v.1.6 [59], under Goloboff *et al.*'s [60] protocol, considering the inclusion of inapplicable characters. A traditional parsimony search with step matrices ('smatrix &') was conducted with the command 'mult' using TBR (tree bisection and reconnection) as the algorithm for branch permutations for 10000 iterations holding ten trees for each iteration. This protocol was repeated ten times using the command 'loop' with different random seeds to evaluate if the tree space was adequately explored by the parameters. All ten searches recovered a similar number of most parsimonious trees (MPT's) (633-636) and the same strict consensus (see electronic supplementary material), suggesting an adequate search in the tree space. All MPT's recovered in these ten searches were included in the same file, from which a global strict consensus was generated. Jackknife and Bremer

analyses were used to estimate clade support using the "resample" and "jak" commands. For the support analysis under a regular Jackknife analysis (i.e. with independent deletion), 10000 replications were carried out, from which the absolute frequencies of the groups on the strict consensus tree were estimated, leaving the remaining parameters in the default settings. The Bremer support was calculated based on suboptimal topologies 50 steps larger than the ones found in the parsimony analysis, collapsing groups with support lower than one (see scripts in [58]).

(c) Ecomorphological analysis

The measurement data (see electronic supplementary material) for the extant species used to assess the ecomorphotype of *Ptychodus* were assembled from the literature [61–64]. We followed Sternes & Shimada's [65] strategy by using illustrations of reference books (i.e. FAO publications, authored by internationally recognized experts) to determine some morphometric measurements sometimes not provided in the literature and thus not available for all species included in the present analysis. Sternes and Shimada [65] demonstrated the high degree of similarity between the book illustrations and actual shark samples, thus showing that such drawings can be reliably used for interspecific morphometric analyses. Measurements of specimen MMSP CPC 3063 (142 cm TL) were used to infer measurements of medium-, large- and giant-sized *Ptychodus* sp. with three distinct maximum TL (2, 5 and 10 m, respectively). All measurements were log-transformed in order to improve normality and homogeneity of variance.

Using 11 linear body measurements (PCL, P1H, D1H, D2H, CFL, PD1, PD2, PP1, PP2, CDM, CPV) (electronic supplementary material, figure S10), we compared *Ptychodus* sp. to 42 modern shark species belonging to the eight main ecomorphotypes (i.e. probenthic,

leptobenthic, squatinobenthic, littoral, bathic, microceanic, macroceanic, tachypelagic) defined by Compagno [66]. For each ecomorphology, we selected several species (all with two dorsal fins) representative of the size range and body proportions of the category (see electronic supplementary material, table S3). Two non-parametric tests revealed statistically significant differences between the ecomorphotypes (ANOSIM: $R = 0.463$, $p = 0.0001$; PERMANOVA: $F = 12.46$, $p = 0.0001$) (see electronic supplementary material, tables S4 and S5 for pairwise comparisons). A Linear Discriminant Analysis (LDA) was performed using Paleontological Statistics (PAST software, version 4.04; [67]) to maximize differences among a priori groups and predict the ecomorphotype of *Ptychodus* sp. The LDA matrix consists of 11 quantitative variables (log-transformed linear body measurements) and one qualitative variable (ecomorphotype category, here used as grouping variable) scored for 42 living shark species (assigned to eight given groups) plus *Ptychodus* sp. (with no given group). As the ecomorphotype of the latter is unknown, a "?" was scored in the group column; thus, *Ptychodus* sp. was not included in the discriminant analysis itself, but was classified (see electronic supplementary material).

3. Systematic palaeontology

Class Chondrichthyes Huxley, 1880

Subclass Elasmobranchii Bonaparte, 1838

Infraclass Neoselachii Compagno, 1977

Clade Selachimorpha Nelson, 1984

Superorder Galeomorphii Compagno, 1973

Order Lamniformes Berg, 1937

Family Ptychodontidae Jaekel, 1898

Genus ***Ptychodus*** Agassiz, 1834

Type species. *Ptychodus schlotheimii* Agassiz, 1834 (*nomen oblitum*), a senior synonym of *Ptychodus latissimus* Agassiz, 1835 (*nomen protectum*).

(a) Material examined

MMSP CPC 3063, *Ptychodus* sp., complete well-preserved specimen (1420 mm total length (TL)) exposed in right lateral view, showing almost all skeletal elements, dentition, phosphatized muscle remains, and body outline displaying all fins (figures 1*a*,*b* and S2). MMSP CPC 3064, *P.* sp., almost complete juvenile specimen (565 mm TL) exposed in right laterodorsal view, showing jaws, dentition, vertebral column, pectoral, first dorsal and caudal fins, and most of the body outline (except second dorsal and anal fins) (figures 1*c*,*d* and S3). MUDE CPC 3065, *P.* sp., a partial skeleton exposed in right lateral view, showing part of the neurocranium, scleral capsule, jaws, teeth, branchial elements, anterior vertebral column, and some dorsal fin radials (figures 2*a* and S4). MMSP CPC 3066, *P.* sp., incomplete skeleton missing tail in left lateral view, showing neurocranial remains, scleral capsule, jaws, teeth, vertebral column, branchial elements, pectoral and first dorsal fins, phosphatized muscle remains and most of the body outline (figures 2*b* and S5). MMSP CPC 3067, *P.* sp., slightly disarticulated almost complete skeleton (~890 mm TL) exposed in left lateral view, showing some jaw elements (Meckel's cartilages), teeth, most of the vertebral column, first dorsal and caudal fins, phosphatized muscle remains and most of the body outline (figures 2*c* and S6). MMSP CPC 3068, *P. decurrens*, almost complete skeleton (~2030 mm TL) in dorsal view,

showing neurocranial remains, scleral capsule, jaws, dentition, pectoral and caudal fins, and vertebral column (figures 2*d* and S7).

(b) Locality and horizon

Vallecillo Lagerstätte (26°39.32'N, 100°00.82'W), Nuevo León, Mexico, lower Turonian (*Pseudaspidoceras flexuosum* Zone) platy limestone of the Vallecillo Member, Agua Nueva Formation, Upper Cretaceous.

(c) Amended diagnosis of genus

Medium-sized to gigantic fusiform-bodied sharks with large and long head. Presence of two dorsal fins and an anal fin. Occipital region of the neurocranium with a prominent nuchal crest; occipital condyles extending posteriorly and surrounding at least two cervical vertebral centra. Scleral capsules with tesserae densely mineralized and organized. Palatoquadrate presenting a large otic process on the quadrate portion along with a large process articulating with the Meckel's cartilage. Meckel's cartilage presenting a well-developed facet with surface for articulation with the palatoquadrate process. Posterior part of the Meckel's cartilage with a slender, sigmoidal extension posterior to the articulation facet. Meckel's cartilage becoming progressively wider toward its posterior portion. Palatoquadrate–Meckel's cartilage articulation well posterior to the occiput. Pectoral fins large and semifalcate with narrowly rounded tips. Pectoral fins plesodic with long distal radial segments. Three pectoral basals, with metapterygial axis present. Pectoral girdle with a well-developed, dorsally directed scapular process. Pelvic fins small. First dorsal fin rounded, with high semiplesodic fin skeleton, and significantly larger than the second dorsal fin. First dorsal fin origin located slightly posterior to pectoral fins origin, and second dorsal fin origin located slightly anterior to anal fin origin.

Segmented dorsal basals; no basal plates and spines. Anal fin small (similar in size to the second dorsal fin) and lacking any evidence of basal cartilages. Caudal fin lunate or semilunate with high heterocercal angle (up to 45º) (lower angle in juveniles). Hypochordal rays well developed and directed ventrally (high hypochordal ray angle, lower in juveniles). Vertebral centra strongly calcified and exhibiting concentric rings and numerous parallel lamellae, which run radially from the centre to the external margin. Dentition composed of molariform teeth arranged in numerous (up to 23) anteroposterioly directed files and forming convex dental plates. Dental plates semi-elliptical in shape and narrow anteriorly. Occlusal crown surface showing transverse or radial ridges, granulations, wrinkles, and a possible single cusp. Dentition showing different degrees of heterodonty. Largest teeth of the dentition from the lower symphysial (medial) file. Lateral teeth gradually shrinking and losing bilateral symmetry across each dental plate mesiodistally. Anaulacorhize root massive and always bilobate (i.e. basal face slightly concave in labial view) except in upper symphysial teeth.

(d) General comparative description

The head is very large and long (ca. 34% of TL and 1.6 times the distance between pectoral and pelvic fin bases), with a subterminal mouth extending posteriorly behind the orbits (figure 1). A similar elongated head is known in the megamouth shark (*Megachasma*) [53,68]. In all *Ptychodus* specimens available, the neurocranium and rostral cartilages are crushed, and anatomical structures are not easily discernible. An occipital crest is present. The eyeballs were encapsulated by rigid scleral capsules showing an external surface covered by tessellated calcified cartilage (figure 3*a*). The jaws are well developed, with long palatoquadrates and Meckel's cartilages articulating with each other well posterior to the occiput (reaching the level of the tenth vertebra), like in most lamniforms [69,70] (figure 1). The Meckel's cartilage is a massive and deep element, with a markedly convex ventral border. The toothed portion of the

jaws is restricted to about the anterior half of the palatoquadrates and Meckel's cartilages (figures 1 and 3*b*). The tooth morphology, characterized by a massive crown with several transverse ridges, is typical of the genus [5] and confirms the assignment of the specimens studied (figures 3*c* and S9). Elements of the hyoid arch (hyomandibular and ceratohyal) cannot be identified with certainty. The branchial arches are well separated from each other, and some of their elements (epibranchials and ceratobranchials) are elongated, suggesting large gill openings like in many lamniforms [63].

The total vertebral count is ~160, with precaudal vertebral count ranging from 89 to 92. The vertebral centra are circular and short, with a length/diameter ratio ranging from 0.52 (anterior precaudal) to 0.39 (posterior precaudal). This is similar to the range observed in other Cretaceous lamniform taxa [71]. The vertebral column is thick for its length, i.e. the maximum centrum diameter is 2.5% of the precaudal vertebral column length (like in *Lamna*; [72]). They are strongly calcified and show the concentric rings and numerous bands running radially from the centre to the external margin [1,8,73] (figure 3*d*).

The mesopterygium, which is subtriangular in shape, is the largest element of the three basal cartilages. The metapterygium is more elongated and extends posteriorly with a series of segments (metapterygial axis). The pectoral fins are well developed, straight and relatively narrow-tipped. There are 16 longitudinal series of pectoral radials. The radials seem to be composed of two segments. Some distal radials bifurcate distally and reach the end of the pectoral fin (plesodic condition). The pelvic fins are markedly smaller that the pectoral fins.

There are two dorsal fins devoid of spines and basal plates. The first dorsal fin is relatively low (i.e. slightly longer than high) and apically rounded, and its origin is located slightly posterior to the origin of the pectoral fins. It is semiplesodic (*sensu* [53,74]) and shows segmented basals. There are at least 20 radials, some of them bifurcating distally. The second dorsal fin is much smaller, and its origin is located slightly anterior to the anal fin origin. The

first dorsal fin shape and skeleton as well as the position and respective sizes of both dorsal fins resemble those observed in modern lamnid sharks (e.g. *Lamna*; [63,69]). The anal fin is apically angular, slightly higher than long, and similar in size to the second dorsal fin. Its origin is located slightly posterior to the second dorsal fin origin.

The caudal fin shows a lunate or semilunate shape (heterocercal angle up to ~45°), with a moderately elongated dorsal lobe and a shorter subvertical ventral lobe (high hypocercal angle). The longest hypochordal rays, which are located in the anterior portion of the caudal fin, are robust, laterally flattened and ventrally directed, thus forming a high hypochordal ray angle (128°) similar to that observed in *Lamna* (up to 122°) and *Cretoxyrhina* (133°) [75]. Specimen REG 2544 P.F. 839 indicates that juveniles did not have a lunate caudal fin, with lower heterocercal and hypochordal ray angles (~30° and ~90°, respectively) and a less vertical ventral lobe (lower hypocercal angle). This ontogenetic difference is known in some modern lamnid and cetorhinid lamniforms [76,77]. The caudal fin of *Ptychodus* corresponds in its proportions to the type 4 (type 2 in juveniles) defined for lamniform sharks [75]. Although not preserved in any specimen, a terminal lobe may have been present, as in all living lamniforms [63] and in Cretaceous lamniform specimens with well-preserved caudal fins [78].

The squamation consists of minute, densely arranged ridged dermal denticles (= placoid scales). Best preserved skin portions are located on the dorsal, anal and pectoral fins of specimen MMSP CPC 3063, where placoid scales are leaf-shaped (~180 µm long and ~140 µm wide), with a slightly swollen apical crown surface showing five longitudinal ridges bounded by shallow grooves (inter-ridge distance = 40 µm) (figure S8). Their morphology is consistent with that of some placoid scales previously described in *Ptychodus rugosus* [12,34], and similar in size and morphology to that described in the extant lamnid *Isurus oxyrinchus* [79].

Some portions of the lateral trunk musculature, i.e. myomeres and myospeta, are preserved in several specimens. Muscle fibers, composing each myomere, can be observed in

situ or as scattered isolated elements (likely a result of the decay process) (figures 1 and 3*e*,*f*). In specimen MMSP CPC 3063, a brownish area located inside the abdominal cavity might represent remnants of the iron-rich liver tissues (figure 1).

4. Results and discussion

(a) Phylogenetic relationships

The parsimony analysis recovered 6349 most parsimonious trees (MPT's) of 691 steps and a Consistency Index (CI) of 0.47 and a Retention Index (RI) of 1. The phylogenetic analysis conducted in the present study provides new insights into the long-standing debate of the systematic affiliation of *Ptychodus*, placing this taxon within Neoselachii (crown elasmobranchs), as a member of Lamniformes within Galeomorphii. In the following section, only the characters observed in the new *Ptychodus* specimens or accounted for the genus in the literature are considered (see electronic supplementary material and [58] for full synapomorphy list and character reconstructions).

The clade Neoselachii (crown elasmobranchs) (figure 4; Clade 119) is well supported in the present study with a Jackknife value (JV) of 99% and a Bremer value (BV) of 10. *Ptychodus* affiliation within Neoselachii is supported by the following features (in specimens or in literature): the lack of an internasal plate separating the palatoquadrates (character 4:0), the reduced number of cartilages connecting the basipterygium and the clasper cartilage (character149:1), the presence of an occipital hemicentrum (character 154:1), the presence of calcified vertebral centra in the different regions on the body (characters 155:1 and 158:1), and the presence of multilayered enameloid on the teeth [33,80] (character 209:1).

The clade Selachimorpha (figure 4; Clade 118) has a relatively low support in the present analysis (JV of 55% and BV of 1). The placement of *Ptychodus* within Selachimorpha

is supported by a suite of characters that include an enlarged and broad mesopterygium (character 134:2), the presence of a propterygium, which is reduced, not elongated anteriorly and containing radials (characters 135:1, 136:3 and 137:0).

The clade Galeomorphii (figure 4; Clade 131) presents a high support (JV: 73% and BV: 3). The placement of *Ptychodus* within Galemorphii is based on the reduced or lack of supraneurals (character 169:0). Within Galeomorphii, the clade [Orectolobiformes + (Carcharhiniformes + Lamniformes)] (figure 4; Clade 135) has a relatively low support of 59% (JV) and a BV of 2. The affiliation of *Ptychodus* to this clade is supported by the presence of secondary calcification in the vertebral centra and the presence of radii radiating from the notochordal sheath (characters 166:1 and 167:0), the lack of dorsal fin basal cartilages (basal plates) (segmented *sensu* [69]) (character 176:2) and the lack of dorsal fin spines (character 202:0). These features clearly separate *Ptychodus* from heterodontiforms, another group of durophagous galeomorph sharks.

The clade Lamniformes (figure 4; Clade 139) has high support (JV: 88% and BV: 4). The assignment of *Ptychodus* to Clade 139 is supported by the presence of an occipital crest (character 30:2), the presence of a large process on the otic region (quadrate portion) of the palatoquadrate (character 84:1), with a deep groove for the abductor mandibularis (character 83:1). Within Lamniformes, *Ptychodus* is included in a polytomic group (figure 4; Clade 140). This group has low support (JV: 51% and BV: 1) and is based on the presence of a plesodic dorsal fin (character 175:1) (some trees also recovered the presence of plesodic pectoral fins (character 121:0) and the presence of homocercal caudal fin (character 177:1) as additional characters for this clade). It is worth mentioning that all characters supporting the lamniform affiliation do not necessarily represent synapomorphies for the lamniforms as they are also present in other taxa. For instance, a large process in the quadrate portion of the palatoquadrate also occurs in *Hexanchus*, *Heptranchias*, *Notorynchus* and *Orthacanthus* among others

(character 84:1), but in these taxa this process also forms part of the postorbital articulation (see [81]), which is not present in Lamniformes. However, those taxa do not present the same combination of shared features leading to the clade Lamniformes and placing *Ptychodus* as a member of this group.

(b) Ecomorphological specializations

The LDA morphospace defined by the first three LD axes shows good discrimination among ecomorphological groups (figure 5). The living species were assigned to an ecomorphotype category with high accuracy (correct classification = 90.48%; electronic supplementary material, table S6). The positions of *Ptychodus* with distinct maximum TL are close to that of the tachypelagic group. This is confirmed by the LDA classifier, which assigns medium-, large- and giant-sized *Ptychodus* species to the tachypelagic group based on the minimal Mahalanobis distance to the group mean (electronic supplementary material, table S7).

Ptychodus shares several morphological features with tachypelagic lamnids (e.g. *Carcharodon*, *Lamna*), such as a first dorsal fin placed in a markedly anterior position, just posterior to the origin of the pectoral fins, a minute second dorsal fin, and a lunate caudal fin (Compagno 1990b, 2001). Additional features present in *Ptychodus* also characterize tachypelagic lamnids, such as high heterocercal and hypochordal ray angles [75], a vertebral column that is thick for its length [72], and scleral capsules that are covered by noticeably discrete and well-organized tesserae [82,83]. All these features are found in living fast-swimming species, and are therefore consistent with the assignment of *Ptychodus* to the tachypelagic ecomorphotype.

Ptychodus, like all other lamniforms, exhibits a morphology and body proportions clearly different from those characterizing extant durophagous sharks, which are all demersal forms (e.g. *Heterodontus* and *Nebrius* in the probenthic and littoral ecomorphotype categories,

respectively) [66]. However, the massive dentitions of *Ptychodus*, composed of numerous ornamented molariform teeth, unambiguously indicate a durophagous diet (see [8,9,14,32]). Another aspect of the anatomy of *Ptychodus* that clearly separates it from all other extinct and extant durophagous sharks is its gigantic size (e.g. [12,13,73]). Shimada *et al.* [12,13] estimated the size of various species of *Ptychodus* using the proportions between anteroposterior jaw length, symphysial tooth size and total body length (based on the assumption that jaw length is 7–8.5% of TL). For instance, Shimada *et al.* [13] found that *P. mortoni* could have reached 11.2 m TL. However, the jaw length is 18% and 21% of TL in specimens MMSP CPC 3063 and MMSP CPC 3068, respectively, indicating that the total lengths proposed by Shimada *et al.* [12,13] were overestimated. Here, we obtained the proportion between lower symphysial tooth length and TL from the dental and skeletal remains preserved in specimen MMSP CPC 3063. Assuming that these proportions are maintained across various species, different ontogenetic stages and between sexes, we propose revised body size estimates using the best-preserved known *Ptychodus* dentitions (electronic supplementary material, table S2). According to our results, the maximum TL for the genus would be 9.7 m based on an associated dentition of *P. latissimus* from Italy [20], with a corresponding jaw length of roughly 1.9 m. The maximum body length of *ca* 2.5 m (possibly 3.5 m) so far documented for the largest living durophagous shark (*Stegostoma fasciatum*; see [63]) pales in comparison to the gigantic sizes reached by some uncuspidate species of *Ptychodus* such as *P. latissimus*, *P. martini*, *P. mediterraneus* and *P. polygyrus* (see also electronic supplementary material). Furthermore, such sizes have rarely been exceeded during the long and complex evolutionary history of sharks, with the few exceptions being restricted to apex predators and planktivorous forms (e.g. the extinct megatooth shark, *Otodus megalodon*, and the living whale shark, *Rhincodon typus*) [66]. Therefore, the lamnid-like morphology of *Ptychodus* combined with its massive pavement-like dentition and its large to gigantic size, make it a unique meso- to apex predator, as well as

probably the largest durophagous shark that ever existed. The tachypelagic ecomorphotype revealed by the newly discovered material from Mexico challenges the widely held view that the durophagous genus *Ptychodus* was a group of bottom-dwelling sharks (e.g. [12,13]) feeding mainly on shelled benthic invertebrates such as inoceramid bivalves (e.g. [15,16,21]). New evidence indicates that *Ptychodus* was an open-water, fast-swimming predator that preyed on well-armored pelagic organisms such as large ammonites and sea turtles (figure 6), thus confirming the more active nektonic lifestyle previously suggested based on morphological features of vertebral centra and placoid scales [33,34]. At Vallecillo, the presence cracked shells of the spinose ammonite *Pseudaspidoceras flexuosum* may have resulted from predation *Ptychodus*, as previously hypothesized [17].

Lamniformes show a wide range of diets, especially when fossil taxa are taken into account [84]. While extant lamniform sharks are superpredators (*Carcharodon*), fish/cephalopod-eating predators (e.g. *Alopias*, *Carcharias*, *Isurus*, *Lamna*) or filter-feeders (*Cetorhinus*, *Megachasma*) [63], the systematic position of *Ptychodus* indicates that durophagy evolved within a Cretaceous lineage of lamniforms, making this order one of the most diverse in terms of feeding strategies. Hard-prey specialists were so far unknown among extant and extinct lamniform sharks, with the exception of *Ptychocorax*, a poorly known Late Cretaceous (Coniacian–Campanian) anacoracid genus characterized by a unique dentition consisting of anterior cutting teeth and lateroposterior grinding teeth [5]. Interestingly, this short-lived experimentation with durophagous habits, somewhat similar to that observed in ptychodontids, emphasizes the capacity of rapid acquisition of trophic specializations in lamniform sharks. Our study confirms that Cretaceous lamniforms exhibited particularly diverse ecomorphologies and diets, with ptychodontids adding to other highly specialized groups of the order such as anacoracids [5], johnlongines [85], haimirichiids [86] and aquilolamnids [87]. Our findings also show that the development of durophagous specializations within elasmobranchs occurred

several times independently in most major extant groups (orders) and in distinct ecomorphotype categories. Furthermore, the gigantic sizes reached by the last (Campanian) representatives of *Ptychodus* suggest that the availability of space and nektonic shelled prey items may have been a more important factor than previously assumed. During the Campanian, ptychodontid sharks would have been in direct competition with the members of mosasaur clades Globidensini and Prognathodontini (Squamata: Mosasauridae), two emerging groups of pelagic predators with powerful crushing dentitions and therefore probably targeting the same nektonic shelled prey items [88].

Ethics. All specimens examined for this study are part of the Colección Paleontológica de Coahuila (CPC) and are permanently housed in two Mexican public museums: the Museo La Milarca, San Pedro Garza García, Nuevo León (MMSP) and the Museo del Desierto, Saltillo, Coahuila (MUDE). As indicated above, the collection numbers of the six specimens are: MMSP CPC 3063; MMSP CPC 3064; MUDE CPC 3065; MMSP CPC 3066; MMSP CPC 3067; MMSP CPC 3068.

Data accessibility. All the data relevant to this study can be found in the electronic supplementary material [89] and downloaded from the Dryad Digital Repository: https://doi.org/10.5061/dryad.12jm63z5n [58].

Authors' contributions. R.V.: conceptualization, data curation, formal analysis, methodology, investigation, writing—original draft, writing—review and editing; E.V.-S: data curation, formal analysis, methodology, investigation, writing—original draft, writing—review and editing; M.A.: data curation, formal analysis, methodology, investigation, writing—original draft, writing—review and editing; J.K.: funding acquisition, investigation, writing—review and editing; E.F.: investigation, writing—review and editing; M.A.G.G.: investigation, writing—review and editing; J.M.P.G.: investigation, writing—review and editing; C.I.,

investigation, writing—review and editing; E.S.: investigation, writing—review and editing; W.S.: conceptualization, funding acquisition, investigation, writing—review and editing.

Conflict of interest declaration. The authors declare no competing interests.

Funding. This research was funded in part by Géosciences Rennes, UMR CNRS 6118 to R. Vullo and by the Austrian Science Fund (FWF) [P33820] to J. Kriwet.

Acknowledgements. We are grateful to M. Fernández Garza, who donated five of the specimens described here to the Museo La Milarca and thus made them accessible for scientific research. We also thank two anonymous reviewers for their constructive comments, and F. Spindler for the life reconstruction of *Ptychodus*.

References

1. Woodward AS. 1912 The fossil fish of the English Chalk, Part VII. *Monogr. Palaeontogr. Soc.* **65**, 225–264.

2. Tan K. 1949 *Ptychodus latissimus* Agassiz from the Upper Cretaceous of Hokkaidô. *Proc. Jap. Acad.* **25(8)**, 18–20.

3. Hoch E. 1992 First Greenland record of the shark genus *Ptychodus* and the biogeographic significance of its fossil assemblage. *Palaeogeogr. Palaeoclimatol. Palaeoecol.* **92**, 277– 281.

4. Siverson M. 1999 A new large lamniform shark from the uppermost Gearle Siltstone (Cenomanian, Late Cretaceous) of Western Australia. *Earth Environ. Sci. Trans. R. Soc. Edinb.* **90**, 49–66.

5. Cappetta H. 2012 Chondrichthyes. Mesozoic and Cenozoic Elasmobranchii: Teeth. In *Handbook of paleoichthyology*, vol. 3E (ed. H-P Schultze), München, Germany: Pfeil.

6. Verma O, Prasad GVR, Goswami A, Parmar V. 2012 *Ptychodus decurrens* Agassiz (Elasmobranchii: Ptychodontidae) from the Upper Cretaceous of India. *Cret. Res.* **33**, 183–188.

7. Carillo-Briceño JD, Lucas SG. 2013 The first tooth set of *Ptychodus atcoensis* (Elasmobranchii: Ptychodontidae), from the Cretaceous of Venezuela. *Swiss J. Palaeontol.* **132**, 69–75.

8. Hamm SA. 2020 Stratigraphic, geographic and paleoecological distribution of the Late Cretaceous shark genus *Ptychodus* within the Western Interior Seaway, North America. *Bull. N. M. Mus. Nat. Hist. Sci.* **81**, 1–94.

9. Amadori M, Kindlimann R, Fornaciari E, Giusberti L, Kriwet J. 2022a A new cuspidate ptychodontid shark (Chondrichthyes; Elasmobranchii), from the Upper Cretaceous of Morocco with comments on tooth functionalities and replacement patterns. *J. Afr. Earth Sci.* **187**, 104440.

10. Amadori M, Solonin SV, Vodorezov AV, Shell R, Niedźwiedzki R, Kriwet J. 2022b The extinct shark, *Ptychodus* (Elasmobranchii: Ptychodontidae) in the Upper Cretaceous of central-western Russia—The road to easternmost peri-Tethyan seas. *J. Vert. Paleontol.* **42**, e2162909.

11. Woodward AS. 1904 On the jaws of *Ptychodus* from the Chalk. *Quart. J. Geol. Soc.* **60**, 133–136.

12. Shimada K, Rigsby, CK, Kim S. 2009 Partial skull of the Late Cretaceous durophagous shark, *Ptychodus occidentalis* (Elasmobranchii: Ptychodontidae), from Nebraska, U.S.A. *J. Vert. Paleontol.* **29**, 336–349.

13. Shimada K, Everhart MJ, Decker R, Decker PD. 2010 A new skeletal remain of the durophagous shark, *Ptychodus mortoni*, from the Upper Cretaceous of North America: an indication of gigantic body size. *Cret. Res.* **31**, 249–254.

14. Amadori M, Amalfitano J, Giusberti L, Fornaciari E, Carnevale G, Kriwet J. 2020a A revision of the Upper Cretaceous shark *Ptychodus mediterraneus* Canavari, 1916 from northeastern Italy, with a reassessment of *P. latissimus* and *P. polygyrus* Agassiz, 1835 (Chondrichthyes, Elasmobranchii). *Cret. Res.* **110**, 104386.

15. Kauffman EG. 1972 *Ptychodus* predation upon a Cretaceous *Inoceramus*. *Palaeontology* **15**, 439–444.

16. Diedrich CG. 2013 Facies related phylostratigraphy of the benthic neoselachian *Ptychodus* from the Late Cretaceous (Cenomanian/Turonian) of the Pre-North Sea Basin of Europe. *Cret. Res.* **41**, 17–30.

17. Ifrim C. 2013 Paleobiology and paleoecology of the early Turonian (Late Cretaceous) ammonite *Pseudaspidoceras flexuosum*. *Palaios* **28**, 9–22.

18. Everhart MJ. 2017 *Oceans of Kansas: a natural history of the Western Interior Sea*, 2nd ed. Bloomington, USA: Indiana University Press.

19. Amadori M, Amalfitano J, Giusberti L, Fornaciari E, Luciani V, Carnevale G, Kriwet J. 2019 First associated tooth set of a high-cusped *Ptychodus* (Chondrichthyes, Elasmobranchii) from the Upper Cretaceous of northeastern Italy, and resurrection of *Ptychodus altior* Agassiz, 1835. *Cret. Res.* **93**, 330–345.

20. Amadori M, Amalfitano J, Giusberti L, Fornaciari E, Carnevale G, Kriwet J. 2020b The Italian record of the Cretaceous shark, *Ptychodus latissimus* Agassiz, 1835 (Chondrichthyes, Elasmobranchii). *PeerJ* **8**, e10167.

21. Mazurek D, Antczak M. 2023 Late Cretaceous coprolite from the Opole area (southern Poland) as evidence for a variable diet in shell-crushing shark *Ptychodus* (Elasmobranchii: Ptychodontidae). *PeerJ* **11**, e16598.

22. Woodward J. 1729 *A catalogue of the English fossils in the collection of J. Woodward M. D.* Tome 1, part 2. London, UK: Fayram, Senex, Osborn and Longman.

23. Brignon A. 2019 Le diodon devenu requin: l'histoire des premières découvertes du genre *Ptychodus* (Chondrichthyes). Bourg-la-Reine, France: Published by the author.

24. Agassiz JLR. 1839 *Recherche sur les poissons fossiles, 10^e^ et 12^e^ livraisons* (April 1839), Neuchâtel, Switzerland: Petitpierre et Nicolet.

25. Woodward AS. 1887 On the dentition and affinities of the selachian genus *Ptychodus*, Agassiz. *Quart. J. Geol. Soc.* **43**, 121–131.

26. Casier E. 1953 Origine des ptychodontes. *Mém. Inst. Roy. Sci. Nat. Belgique (2^ème^ sér.)* **49**, 1–51.

27. Patterson C. 1966 British Wealden sharks. *Bull. Br. Mus. (Nat. Hist.) Geol.* **11**, 283–350.

28. Maisey JG. 1982 The anatomy and interrelationships of Mesozoic hybodont sharks. *Am. Mus. Novit.* **2724**, 1–48.

29. Cuny G. 2008 Mesozoic hybodont sharks from Asia and their relationships to the genus *Ptychodus*. *Acta Geol. Pol.* **58**, 211–216.

30. Müller A. 2008 Ein artikulierte Fund von *Ptychodus* aus dem Obercenoman von Westfalen. *Geol. Paläont. Westf.* **70**, 55–63.

31. Nicholls E-L. 2010 The miserable story of *Ptychodus*—will we ever know? *Programs and Abstracts of the 2010 Symposium of Vertebrate Palaeontology and Comparative Anatomy*, Cambridge, UK, p. 30.

32. Shimada K. 2012 Dentition of Late Cretaceous shark, *Ptychodus mortoni* (Elasmobranchii, Ptychodontidae). *J. Vert. Paleontol.* **32**, 1271–1284.

33. Hoffman BL, Hageman SA, Claycomb GD. 2016 Scanning electron microscope examination of the dental enameloid of the Cretaceous durophagous shark *Ptychodus* supports neoselachian classification. *J. Paleontol.* **90**, 741–762.

34. Hamm SA. 2010 The Late Cretaceous shark, *Ptychodus rugosus*, (Ptychodontidae) in the Western Interior Sea. *Trans. Kansas Acad. Sci.* **113**, 44–55.

35. Hamm SA. 2019 First associated tooth set of *Ptychodus anonymus* (Elasmobranchii: Ptychodontidae) in North America from the Jetmore Chalk in Kansas. *Trans. Kansas Acad. Sci.* **113**, 44–55.

36. Hamm SA. 2015 *Paraptychodus washitaensis* n. gen. et n. sp., of ptychodontid shark from the Albian of Texas, USA. *Cret. Res.* **54**, 60–67.

37. Ifrim C. 2006 The fossil *Lagerstätte* at Vallecillo, north-eastern Mexico: Pelagic *Plattenkalks* related to Cenomanian–Turonian boundary anoxia. PhD thesis, University of Karlsruhe, Germany.

38. Ifrim C, Götz S, Stinnesbeck W. 2011 Fluctuations of oxygen minimum zone at the end of Oceanic Anoxic Event 2 reflected by benthic and planktic fossils. *Geology* **39**, 1043–1046.

39. Ifrim C, Stinnesbeck W, Frey E. 2007 Upper Cretaceous (Cenomanian–Turonian and Turonian–Coniacian) open marine plattenkalk deposits in NE Mexico. *N. Jb. Geol. Paläont. Abh.* **245**, 71–81.

40. Blanco A, Stinnesbeck W, López-Oliva JG, Frey E, Adatte T, González AH. 2001 Vallecillo, Nuevo León: una nueva localidad fosilífera del Cretácico Tardío en el noreste de México. *Rev. Mex. Cienc. Geol.* **18**, 186–199.

41. Smith KT, Buchy M-C. 2008 A new aigialosaur (Squamata: Anguimorpha) with soft tissue remains from the Upper Cretaceous of Nuevo León, Mexico. *J. Vert. Paleontol.* **28**, 85–94.

42. Frey E, Mulder EWA Stinnesbeck W, Rivera-Sylva HE, Padilla-Gutiérrez, González-González. 2017 A new polycotylid plesiosaur with extensive soft tissue preservation from the early Late Cretaceous of northeast Mexico. *Bol. Soc. Geol. Mex.* **69**, 86–134.

43. Jambura PL, Villalobos-Segura E, Türtscher J, Begat A, Staggl MA, Stumpf S, Kindlimann R, Klug S, Lacombat F, Pohl B, Maisey J, Naylor GJP, Kriwet J. 2023 Systematics and phylogenetic interrelationships of the enigmatic Late Jurassic shark *Protospinax annectans* Woodward, 1918 with comments of the shark–ray sister group relationship. *Diversity* **15**, 311.

44. Allis EP. 1923 The cranial anatomy of *Chlamydoselachus anguineus*. *Acta Zool.* **4**, 123–221.

45. Holmgren N. 1940 Studies on the head of fishes – Embryological, morphological, and phylogenetical researches. Part I: Development of the skull in sharks and rays. *Acta Zool.* **21**, 51–266.

46. Holmgren N. 1941 Studies on the head of fishes – Embryological, morphological, and phylogenetical researches. Part II: Comparative anatomy of the adult selachian skull, with remarks on the dorsal fins in sharks. *Acta Zool.* **22**, 1–100.

47. Patterson C. 1965 The phylogeny of chimaeroids. *Phil. Trans. R. Soc. Lond. B* **249**, 101–219.

48. Schaeffer B. 1981 The xenacanth shark neurocranium, with comments on elasmobranch monophyly. *Bull. Am. Mus. Nat. Hist.* **169**, 1–66.

49. Maisey JG. 1980 An evaluation of jaw suspension in sharks. *Am. Mus. Novit.* **2706**, 1–17.

50. Maisey JG. 1984 Higher elasmobranch phylogeny and biostratigraphy. *Zool. J. Linn. Soc.* **82**, 33–54.

51. Maisey JG. 1985 Cranial morphology of the fossil elasmobranch *Synechodus dubrisiensis*. *Am. Mus. Novit.* **2804**, 1–28.

52. Maisey JG. 2001 A primitive chondrichthyan braincase from the Middle Devonian of Bolivia. In *Major events in early vertebrate evolution* (ed. PE Ahlberg), *Systematics Association Special Volume Series* **61**, pp. 263–288, London, UK: Taylor & Francis.

53. Compagno LJV. 1990a Relationships of the megamouth shark, *Megachasma pelagios* (Lamniformes: Megachasmatidae), with comments on its feeding habits. *NOAA Tech. Rep. NMFS* **90**, 357–379.

54. Nishida K. 1990 Phylogeny of the suborder Myliobatidoidei. *Mem. Fac. Fish. Sci. Hokkaido Univ*. **37**, 1–108.

55. Shirai S. 1996 Phylogenetic interrelationships of neoselachians (Chondrichthyes: Euselachii). In *Interrelationships of Fishes* (eds MLJ Stiassny, LR Parenti, DG Jonhson), pp. 9–34. San Diego, CA: Academic Press.

56. Goto T. 2001 Comparative anatomy, phylogeny and cladistics classification of the order Orectolobiformes (Chondrichtyes, Elasmobranchii). *Mem. Grad. Sch. Fish. Sci. Hokkaido Univ.* **48**, 1–100.

57. Madisson WP, Madisson DR. 2023 Mesquite: a modular system for evolutionary analysis. Version 3.81. http://mesquiteproject.org.

58 Vullo R, Villalobos-Segura E, Amadori M, Kriwet J, Frey E, González González MA, Padilla Gutiérrez JM, Ifrim C, Stinnesbeck ES, Stinnesbeck W. 2024 Data from: Exceptionally preserved shark fossils from Mexico elucidate the long-standing enigma of the Cretaceous elasmobranch *Ptychodus*. Dryad Digital Repository. (doi:10.5061/dryad.12jm63z5n)

59. Goloboff PA, Morales ME. 2023 TNT version 1.6, with a graphical interface for MacOS and Linus, including new routines in parallel. *Cladistics* **39**, 144–153.

60. Goloboff P, De Laet J, Ríos-Tamayo D, Szumik CA. 2021 A reconsideration of inapplicable characters, and an approximation with step-matrix recoding. *Cladistics* **37**, 596–629.

61. Compagno LJV. 1984a Sharks of the world. An annotated and illustrated catalogue of shark species known to date. Volume 4, Part 1. Hexanchiformes to Lamniformes. *FAO Fish. Synop.* **125**, 1–249.

62. Compagno LJV. 1984b Sharks of the world. An annotated and illustrated catalogue of shark species known to date. Volume 4, Part 2. Carcharhiniformes. *FAO Fish. Synop.* **125**, 251–655.

63. Compagno LJV. 2001 Sharks of the world. An annotated and illustrated catalogue of shark species known to date. Volume 2. Bullhead, mackerel and carpet sharks (Heterodontiformes, Lamniformes and Orectolobiformes). *FAO Species Cat. Fish. Purp.* **1**, 1–269.

64. Ebert DA. 2014 *On board guide for the identification of pelagic sharks and rays of the Western Indian Ocean*. Roma, Italy: FAO.

65. Sternes PC, Shimada K. 2020 Body forms in sharks (Chondrichthyes: Elasmobranchii) and their functional, ecological, and evolutionary implications. *Zoology* **140**, 125799.

66. Compagno LJV. 1990b Alternative life-history styles of cartilaginous fishes in time and space. *Environ. Biol. Fishes* **28**, 33–75.

67. Hammer Ø, Harper DAT, Ryan PD. 2001 PAST: Paleontological statistics software package for education and data analysis. *Palaeontolol. Electron.* **4**, 1–9.

68. Taylor LR, Compagno LJV, Struhsaker PJ. 1983 Megamouth – A new species, genus, and family of lamnoid shark (*Megachasma pelagios*, family Megachasmidae) from the Hawaiian Islands. *Proc. Calif. Acad. Sci.* **43**, 87–110.

69. Compagno LJV. 1977 Phyletic relationships of living sharks and rays. *Amer. Zool.* **17**, 303–322.

70. Wilga CD. 2005 Morphology and evolution of the jaw suspension in lamniform sharks. *J. Morphol.* **265**, 102–119.

71. Newbrey MG, Siversson M, Cook TD, Fotheringham AM, Sanchez RL. 2015 Vertebral morphology, dentition, age, growth, and ecology of the large lamniform shark *Cardabiodon ricki*. *Acta. Palaeontol. Pol.* **60**, 877–897.

72. Motani R, Shimada K. 2023 Skeletal convergence in thunniform sharks, ichthyosaurs, whales, and tunas, and its possible ecological links through the marine ecosystem evolution. *Sci. Rep.* **13**, 16664.

73. Jambura PL, Kriwet J. 2020 Articulated remains of the extinct shark *Ptychodus* (Elasmobranchii, Ptychodontidae) from the Upper Cretaceous of Spain provide insights into gigantism, growth rates and life history of ptychodontid sharks. *PLoS ONE* **15**, e0231544.

74. Shimada K. 2005 Phylogeny of lamniform sharks (Chondrichthyes: Elasmobranchii) and the contribution of dental characters to lamniform systematics. *Paleontol. Res.* **9**, 55–72.

75. Kim SH, Shimada K, Rigsby CK. 2013 Anatomy and evolution of heterocercal tail in lamniform sharks. *Anat. Rec.* **296**, 433–442.

76. Tomita T, Toda M, Miyamoto K, Oka S-I, Ueda K, Sato K. 2018 Development of the lunate-shaped caudal fin in white shark embryos. *Anat. Rec.* **301**, 1068–1073.

77. Ahnelt H, Sauberer M, Ramler D, Koch L, Pogoreutz C. 2020 Negative allometric growth during ontogeny in the large pelagic filter-feeding basking shark. *Zoomorphology* **139**, 71–83.

78. Pfeil FH. 2021 The new family Mesiteiidae (Chondrichthyes, Orectolobiformes), based on *Mesiteia emiliae* Kramberger, 1884. A contribution to the Upper Cretaceous (early Cenomanian) shark fauna from Lebanon. In *Ancient fishes and their living relatives: a*

tribute to John Maisey (eds A Pradel, JSS Denton, P Janvier), pp. 102–182. München, Germany: Pfeil.

79. Reif W-E. 1985 Squamation and ecology of sharks. *Cour. Forsch.-Inst. Senckenberg* **78**, 1 – 255.

80. Reif W-E. 1973 Morphologie und Ultrastruktur des Hai-"Schmelzes". *Zool. Scr.* **2**, 231–250.

81. Maisey JG. 2008 The postorbital palatoquadrate articulation in elasmobranchs. *J. Morphol.* **269**, 1022–1040.

82 Pilgrim BL, Franz-Odendaal TA. 2009 A comparative study of the ocular skeleton of fossil and modern chondrichthyans. *J. Anat.* **214**, 848–858.

83. Maisey JG, Springer VG. 2013 Chondrocranial morphology of the salmon shark, *Lamna ditropis*, and the porbeagle, *L. nasus* (Lamnidae). *Copeia* **2013**, 378–389.

84. Condamine FL, Romieu J, Guinot G. 2019 Climate cooling and clade competition likely drove the decline of lamniform sharks. *Proc. Natl. Acad. Sci. U.S.A.* **116**, 20584–20590.

85. Shimada K, Popov EV, Siversson M, Welton BJ, Long DJ. 2015 A new clade of putative plankton-feeding sharks from the Upper Cretaceous of Russia and the United States. *J. Vert. Paleontol.* **35**, e981335.

86. Vullo R, Guinot G, Barbe G. 2016 The first articulated specimen of the Cretaceous mackerel shark *Haimirichia amonensis* gen. nov. (Haimirichiidae fam. nov.) reveals a novel ecomorphological adaptation within the Lamniformes (Elasmobranchii). *J. Syst. Palaeontol.* **14**, 1003–1024.

87. Vullo R, Frey E, Ifrim C, González González MA, Stinnesbeck ES, Stinnesbeck W. 2021 Manta-like planktivorous sharks in Late Cretaceous oceans. *Science* **371**, 1253–1256.

88. Longrich NR, Jalil N-E, Khaldoune F, Yazami OK, Pereda-Suberbiola X, Bardet N. 2022 *Thalassotitan atrox*, a giant predatory mosasaurid (Squamata) from the upper Maastrichtian phosphates of Morocco. *Cret. Res.* **140**, 105315.

89. Vullo R *et al.* 2024 Exceptionally preserved shark fossils from Mexico elucidate the long-standing enigma of the Cretaceous elasmobranch *Ptychodus*. *Figshare*.

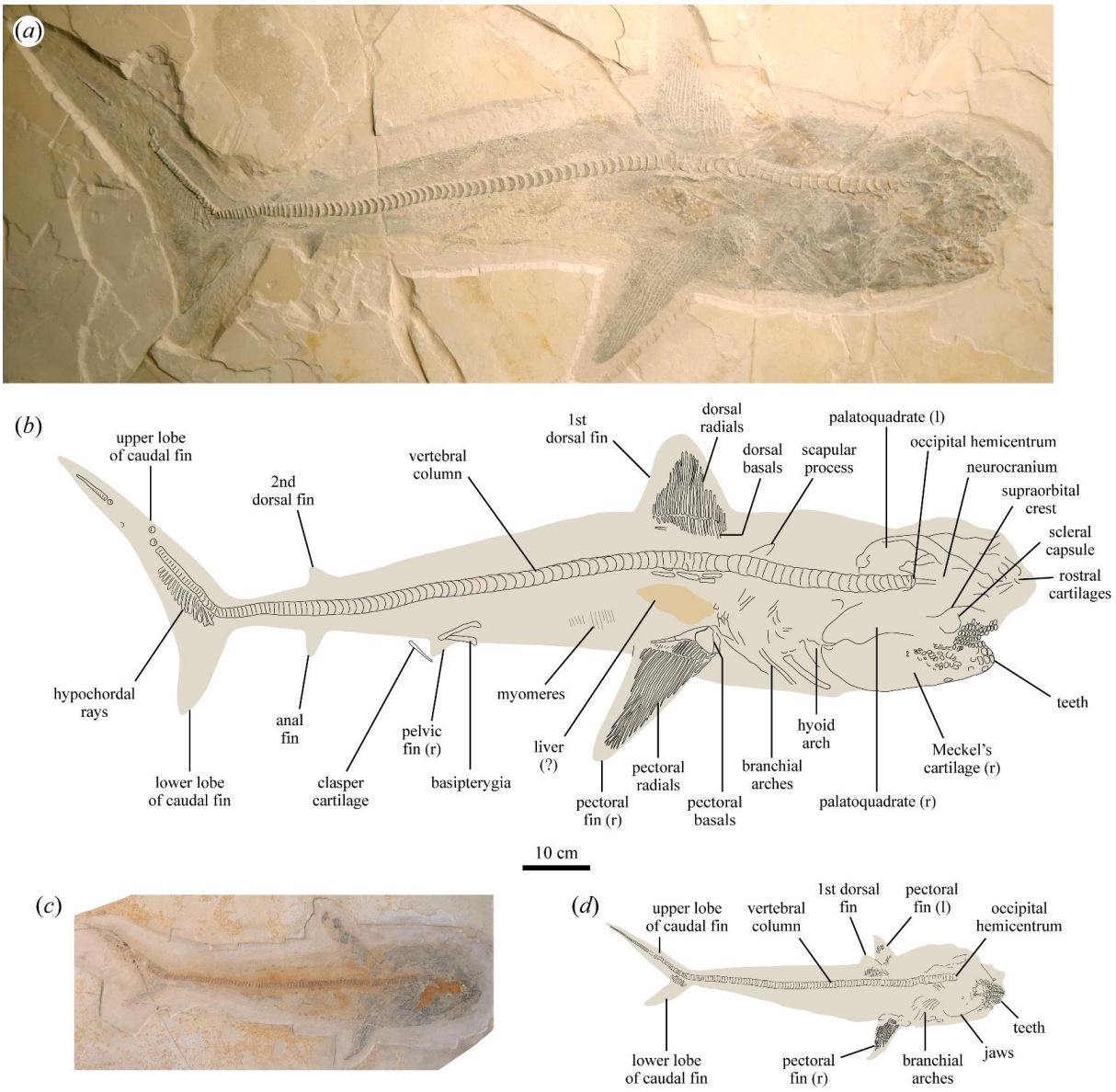

Figure 1. Fully articulated *Ptychodus* specimens from the early Late Cretaceous (Turonian) of Vallecillo showing the general morphology and anatomy of the genus. (*a*,*b*) Photograph (*a*) and interpretative line drawing (*b*) of MMSP CPC 3063, adult specimen of *Ptychodus* sp. (*c*,*d*) Photograph (*c*) and interpretative line drawing (*d*) of MMSP CPC 3064, juvenile specimen of *Ptychodus* sp. All to the same scale.

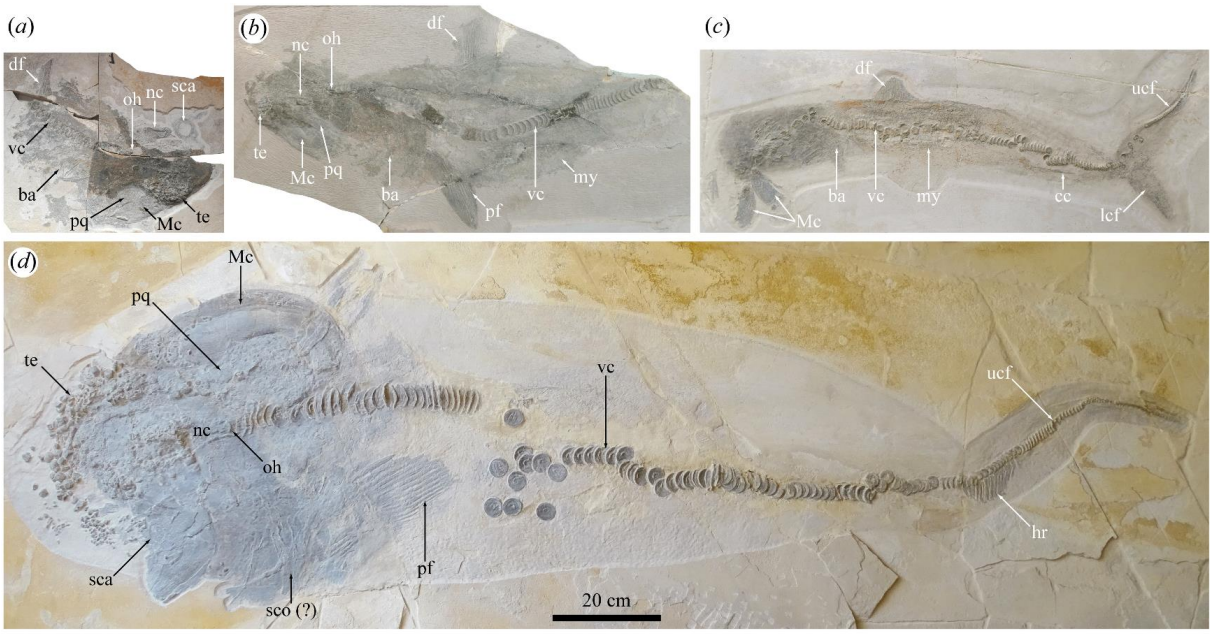

Figure 2. Additional, partially disarticulated *Ptychodus* specimens from the early Late Cretaceous (Turonian) of Vallecillo. (*a*) MUDE CPC 3065, *Ptychodus* sp., incomplete specimen mostly preserving the head. (*b*) MMSP CPC 3066, *Ptychodus* sp., incomplete specimen missing the tail. (*c*) MMSP CPC 3067, *Ptychodus* sp., nearly complete specimen. (*d*) MMSP CPC 3068, *Ptychodus decurrens*, nearly complete specimen. All to the same scale. Abbreviations: ba, branchial arches; df, dorsal fin; hr, hypochordal rays; lcf, lower lobe of caudal fin; Mc, Meckel's cartilage; my, myomeres; nc, neurocranium, oh, occipital hemicentrum; pq, palatoquadrate; sca, scleral capsule; sco, scapulocoracoid; te, teeth; ucf, upper lobe of caudal fin; vc, vertebral column.

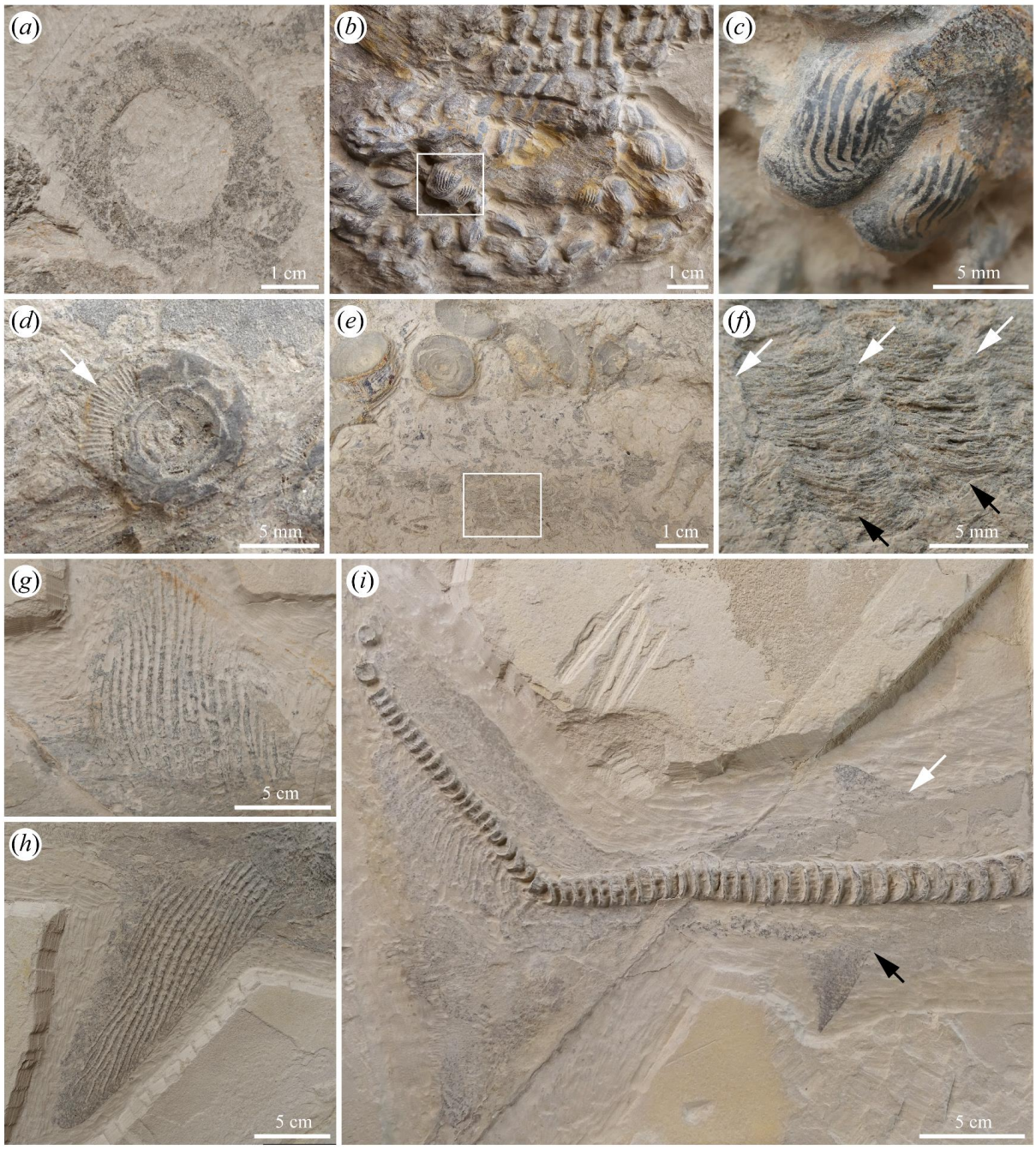

Figure 3. Anatomical details of *Ptychodus*. (*a*) Scleral capsule showing tesserae, specimen MUDE CPC 3065. (*b*) Portion of articulated dentition, specimen MMSP CPC 3063. (*c*) Close-up on two teeth of the lower dentition (box in (*b*)), specimen MMSP CPC 3063. (*d*) Precaudal vertebral centrum showing parallel lamellae (white arrow), specimen MMSP CPC 3067. (e) precaudal vertebral centra and muscle remains (well-preserved myomeres plus scattered isolated myofibers), specimen MMSP CPC 3067. (*f*) Close-up on muscle tissues (box in (*e*)) showing myospeta (white arrows) and myomeres composed of myofibers (black arrows), specimen MMSP CPC 3067. (*g*) First dorsal fin, specimen MMSP CPC 3063. (*h*) Pectoral fin, specimen MMSP CPC 3063. (*i*) Tail portion showing second dorsal fin (white arrow indicating its origin), anal fin (black arrow indicating its origin), and proximal caudal fin skeleton, specimen MMSP CPC 3063.

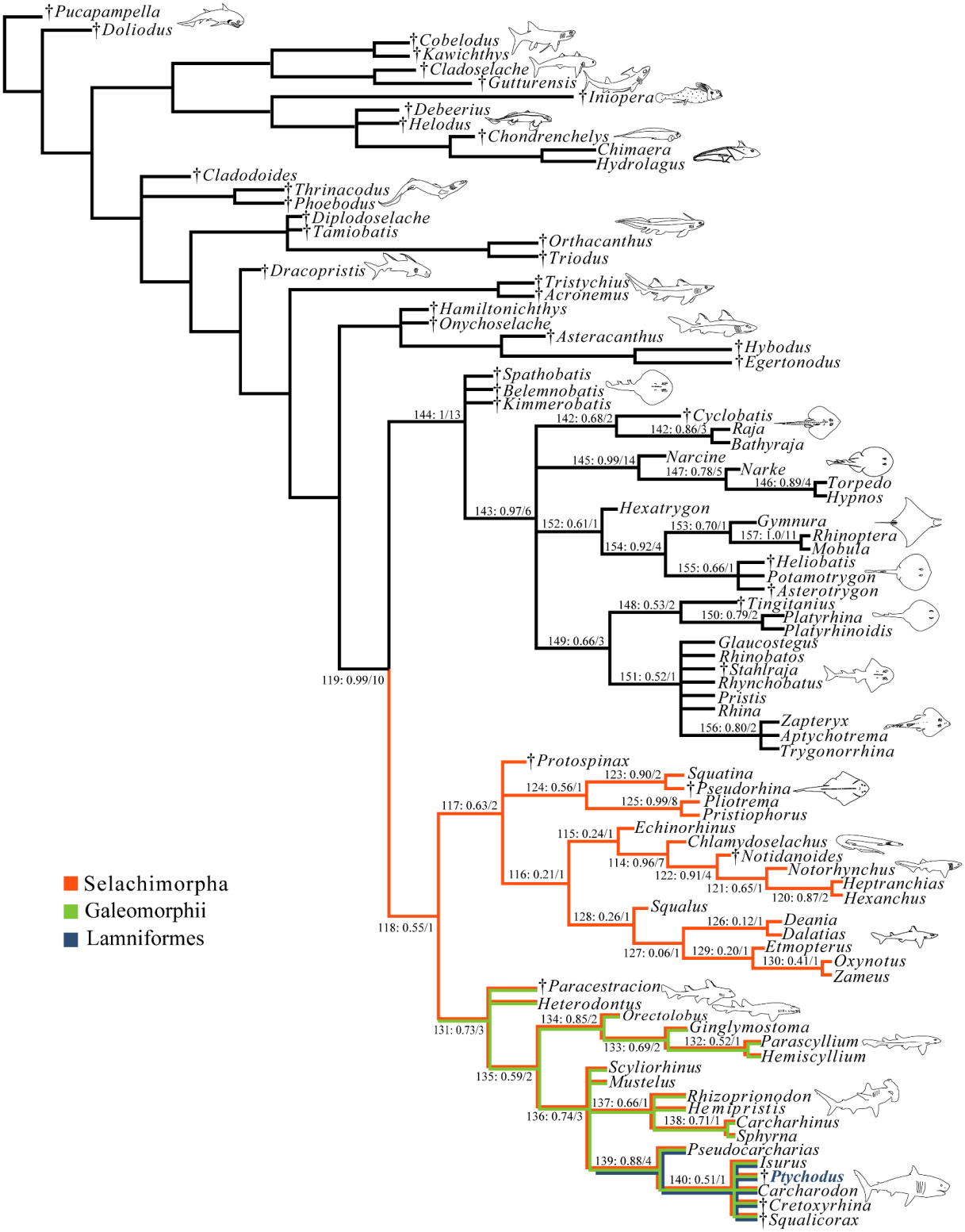

Figure 4. Cladogram (strict consensus tree estimated from the 6349 most parsimonious trees) showing the placement of *Ptychodus* within Elasmobranchii. Numbers in nodes follow the arrangement "Node number: Jackknife support/Bremer support". Clades of interest for the relations of *Ptychodus* are color coded.

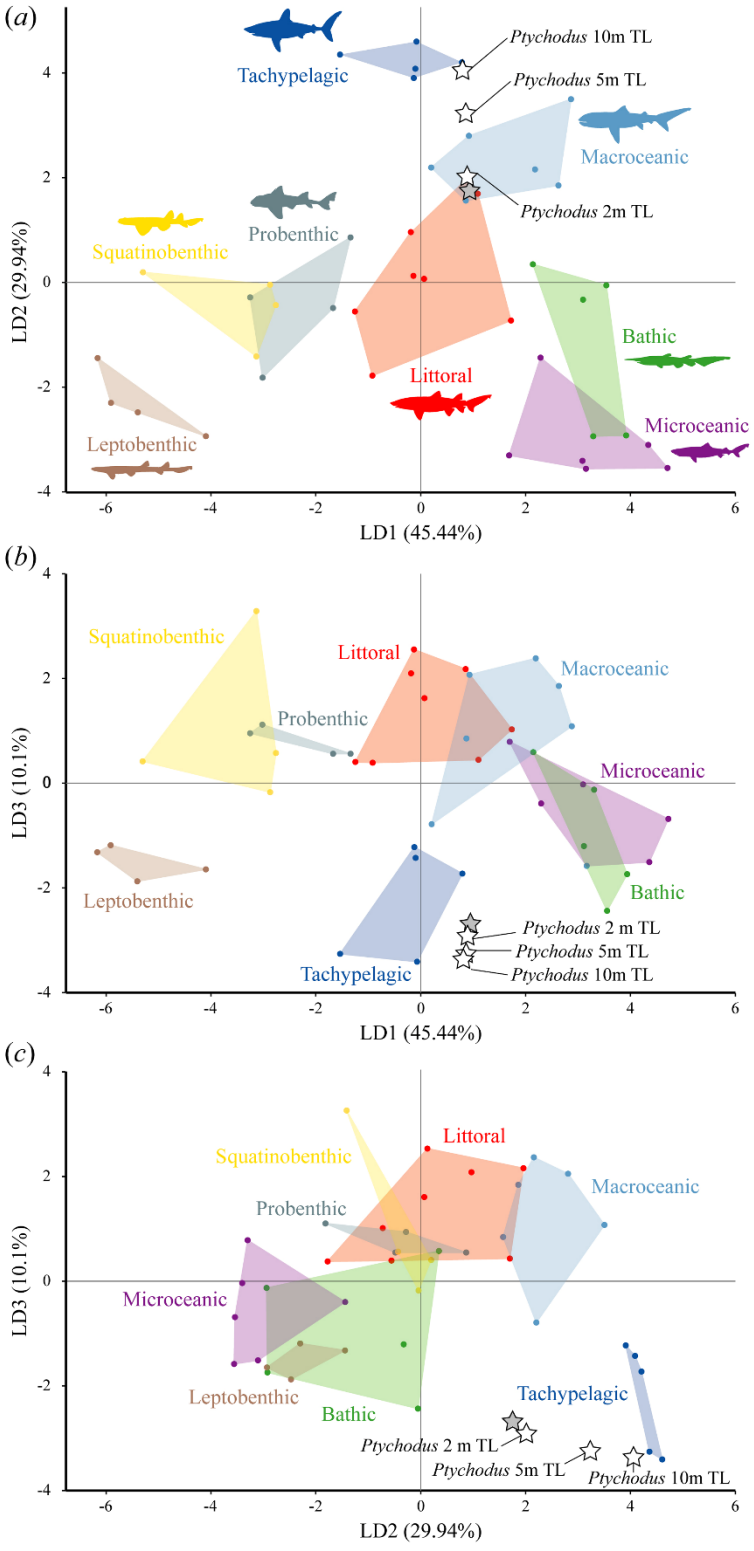

Figure 5. Plots of Linear Discriminant Analysis based on 11 log-transformed measurements for 42 living shark species belonging to eight ecomorphotypes, with *Ptychodus* specimen MMSP CPC 3063 (*P.* sp.) (grey star) and medium-, large- and giant-sized *Ptychodus* sp. (with the same proportions as MMSP CPC 3063) added (white stars). (*a*) LD1 vs. LD2. (*b*) LD1 vs. LD3. (*c*) LD2 vs. LD3. See electronic supplementary material, table S8 for LDA scores.

Figure 6. Life reconstruction of the tachypelagic lamniform shark *Ptychodus* in the early Turonian open marine environment of Vallecillo. Two individuals are shown preying on nektonic shelled organisms (i.e. an ammonite and a sea turtle) in a trophic hotspot. Artwork by Frederik Spindler.

ELECTRONIC SUPPLEMENTARY MATERIAL

Exceptionally preserved shark fossils from Mexico elucidate the long-standing enigma of the Cretaceous elasmobranch *Ptychodus*

Romain Vullo, Eduardo Villalobos-Segura, Manuel Amadori, Jürgen Kriwet, Eberhard Frey, Margarito A. González González, José M. Padilla Gutiérrez, Christina Ifrim, Eva S. Stinnesbeck and Wolfgang Stinnesbeck

DOI: 10.1098/rspb.2024.0262

Table of contents:

Part A. The Vallecillo Member and its fossil assemblage

In the Vallecillo area, the uppermost Cenomanian to basal middle Turonian (lower Upper Cretaceous) strata of the Vallecillo Member are exposed in small quarries. The Vallecillo Member is a distinct unit of pinkish platy limestone in the Agua Nueva Formation, a monotonous series of black marls and thick-bedded limestone (Ifrim, 2006) (figure S1).

At Vallecillo, lower Turonian platy limestone (plattenkalk) has yielded many open marine vertebrate fossils, which are generally articulated and often show exquisite soft tissue preservation. The vertebrate assemblage includes elasmobranchs such as *Aquilolamna milarcae* and *Cretodus* sp. (previously identified as *Cretoxyrhina* sp.), actinopterygians (*Araripichthys* sp., *Tselfatia formosa*, *Vallecillichthys multivertebratum*, *Robertichthys riograndensis*, *Rhynchodercetis regio*, Pachycormidae indet., Pachyrhizodontidae indet.), actinistians, protostegid sea turtles, polycotylid plesiosaurs (*Mauriciosaurus fernandezi*) and mosasauroids (*Vallecillosaurus donrobertoi*) (e.g. Blanco *et al.*, 2002; Blanco and Cavin, 2003; Ifrim *et al.*, 2007; Smith and Buchy, 2008; Schultze *et al.*, 2010; Frey *et al.*, 2017; Vullo *et al.*, 2021). Planktic foraminifers and invertebrate macrofossils, comprising ammonites and inoceramids, allow for a high-resolution biostratigraphical zonation and palaeoecological reconstructions (Ifrim and Stinnesbeck, 2008; Ifrim *et al.*, 2011; Ifrim, 2013, 2015).

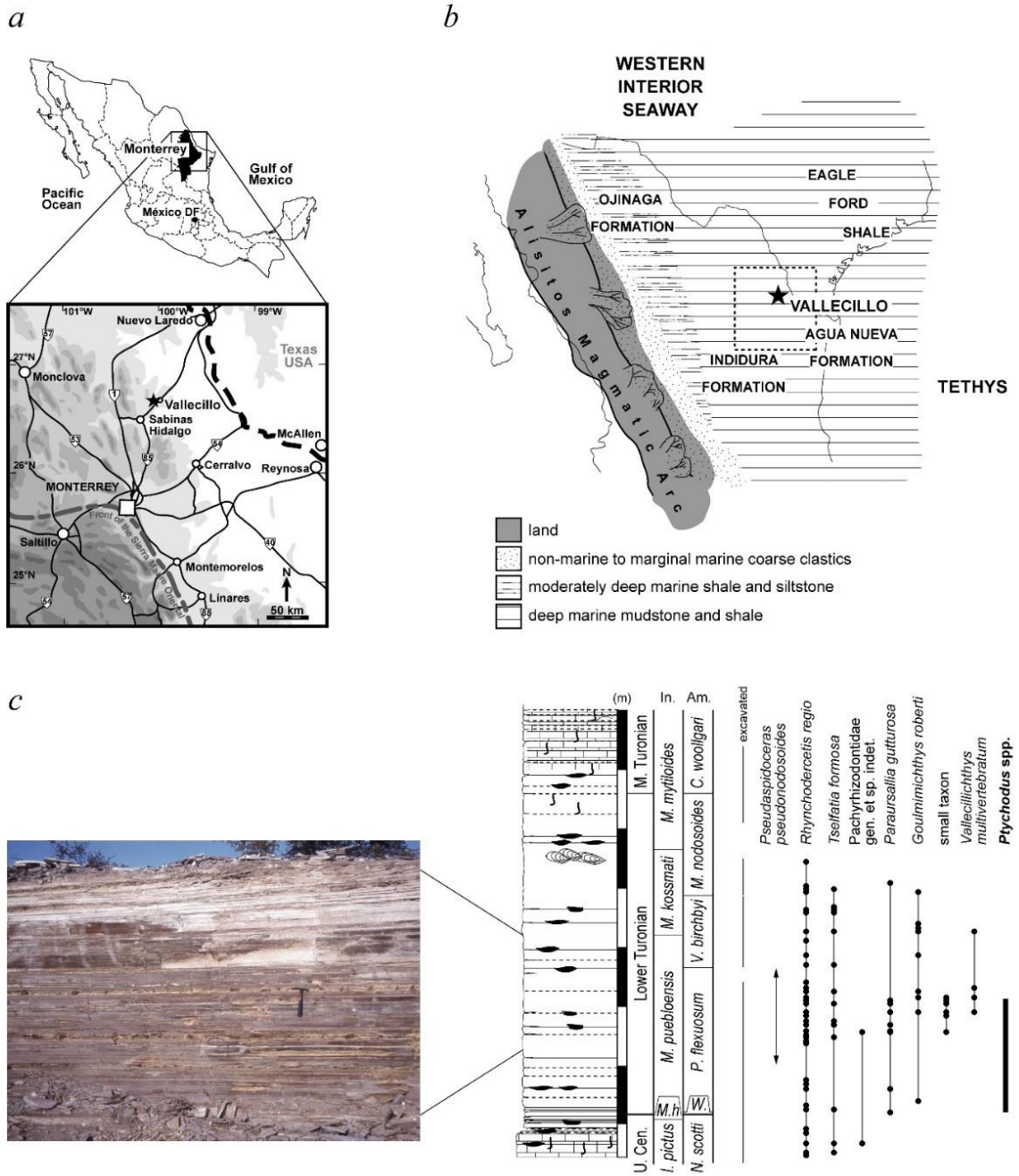

Figure S1. Location, palaeogeographic map, and stratigraphic column. (*a*) Location of the Vallecillo Lagerstätte, Nuevo León State, Mexico. (*b*) Palaeogeographic map and palaeoenvironments of northern Mexico during the early Turonian (ca. 93 million years ago); the dashed square marks the area of the zoomed map in *a*. (*c*) Vallecillo composite section showing the biostratigraphic zonation based on inoceramids (In.) (*I.*, *Inoceramus*; *M.*, *Mytiloides*; *M.h.*, *Mytiloides hattini*) and ammonites (Am.) (*C.*, *Collignoniceras*; *M.*, *Mammites*; *N.*, *Nigericeras*; *P.*, *Pseudaspidoceras*; *V.*, *Vascoceras*; *W.*, *Watinoceras* sp.), the stratigraphic range of *Pseudaspidoceras pseudonodosoides*, the distribution of main fish taxa, including *Ptychodus* spp.; the photograph on the left shows a portion of the lower Turonian platy limestone. U. Cen., upper Cenomanian; M. Turonian, middle Turonian.

Part B. Additional anatomical information

MMSP CPC 3063: *Ptychodus* sp., complete well-preserved specimen (1420 mm total length (TL); see table S1 for other measurements) exposed in right lateral view, showing almost all skeletal elements, dentition, phosphatized muscle remains, and body outline displaying all fins (figures 1*a*,*b* and S2). There are 90 precaudal vertebral centra. The largest centra are 23 mm in diameter. This specimen shows some portions of skin with well-preserved squamation (figure S8). The presence of clasper cartilages indicates that the specimen is a male. The degree of development of the claspers (i.e., elongated and calcified claspers) indicates that MMSP CPC 3063 represents a mature individual (Jensen *et al.*, 2002; Stehmann, 2002).

MMSP CPC 3064: *Ptychodus* sp., almost complete juvenile specimen (565 mm TL; see table S1 for other measurements) exposed in right laterodorsal view, showing jaws, dentition, vertebral column, pectoral, first dorsal and caudal fins, and most of the body outline (except second dorsal, pelvic and anal fins) (figures 1*c*,*d* and S3). There are 89 precaudal and ~70 caudal vertebral centra, respectively. The largest centra are 9 mm in diameter. The dentition is poorly preserved, consisting of low-crowned teeth that seem to be similar to those of *P. decurrens* (figure S9*a*); however, we prefer to assign this specimen to *P.* sp. No clasper cartilages can be observed, suggesting that the specimen may be a female.

MUDE CPC 3065: *Ptychodus* sp., a partial skeleton (head region) exposed in right lateral view, showing part of the neurocranium, scleral capsule, jaws, dentition, branchial elements, anterior vertebral column, and some dorsal fin radials (figures 2*a* and S4). The dentition is poorly preserved, consisting of high-crowned teeth that seem to be similar to those of *P. anonymus* (figure S9*b*); however, we prefer to assign this specimen to *P.* sp.

MMSP CPC 3066: *Ptychodus* sp., incomplete skeleton missing tail in left lateral view, showing neurocranium remains, scleral capsule, jaws, teeth, vertebral column, branchial elements, pectoral and first dorsal fins, phosphatized muscle remains and most of the body outline (figures 2*b* and S5). The largest vertebral centra are 22 mm in diameter. No clasper cartilages can be observed, suggesting that the specimen may be a female.

MMSP CPC 3067: *Ptychodus* sp., slightly disarticulated almost complete skeleton (~890 mm TL; see table S1 for other measurements) exposed in left lateral view, showing some jaw

elements (Meckel's cartilages), teeth, most of the vertebral column, first dorsal and caudal fins, phosphatized muscle remains and most of the body outline (figures 2*c* and S6). There are 92 precaudal vertebral centra. The largest centra are 13 mm in diameter. The presence of clasper cartilages indicates that the specimen is a male. The degree of development of the claspers (i.e., elongated and calcified claspers) indicates that MMSP CPC 3067 represents a mature individual (Jensen *et al.*, 2002; Stehmann, 2002).

MMSP CPC 3068: *Ptychodus decurrens*, almost complete skeleton (~2030 mm TL; see table S1 for other measurements) in dorsal view, showing neurocranium remains, jaws, dentition, pectoral and caudal fins, and vertebral column (figures 2*d* and S7). There are 92 precaudal and ~75 caudal caudal vertebral centra, respectively. The largest centra are 35 mm in diameter. The dentition is disarticulated, but some teeth are relatively well preserved (figure S9*c*). They show the typical crown morphology of *Ptychodus decurrens* (e.g. Hamm, 2020; Amadori *et al.*, 2022b), and this specimen can be confidently assigned to this widespread species. No clasper cartilages can be observed, suggesting that the specimen may be a female.

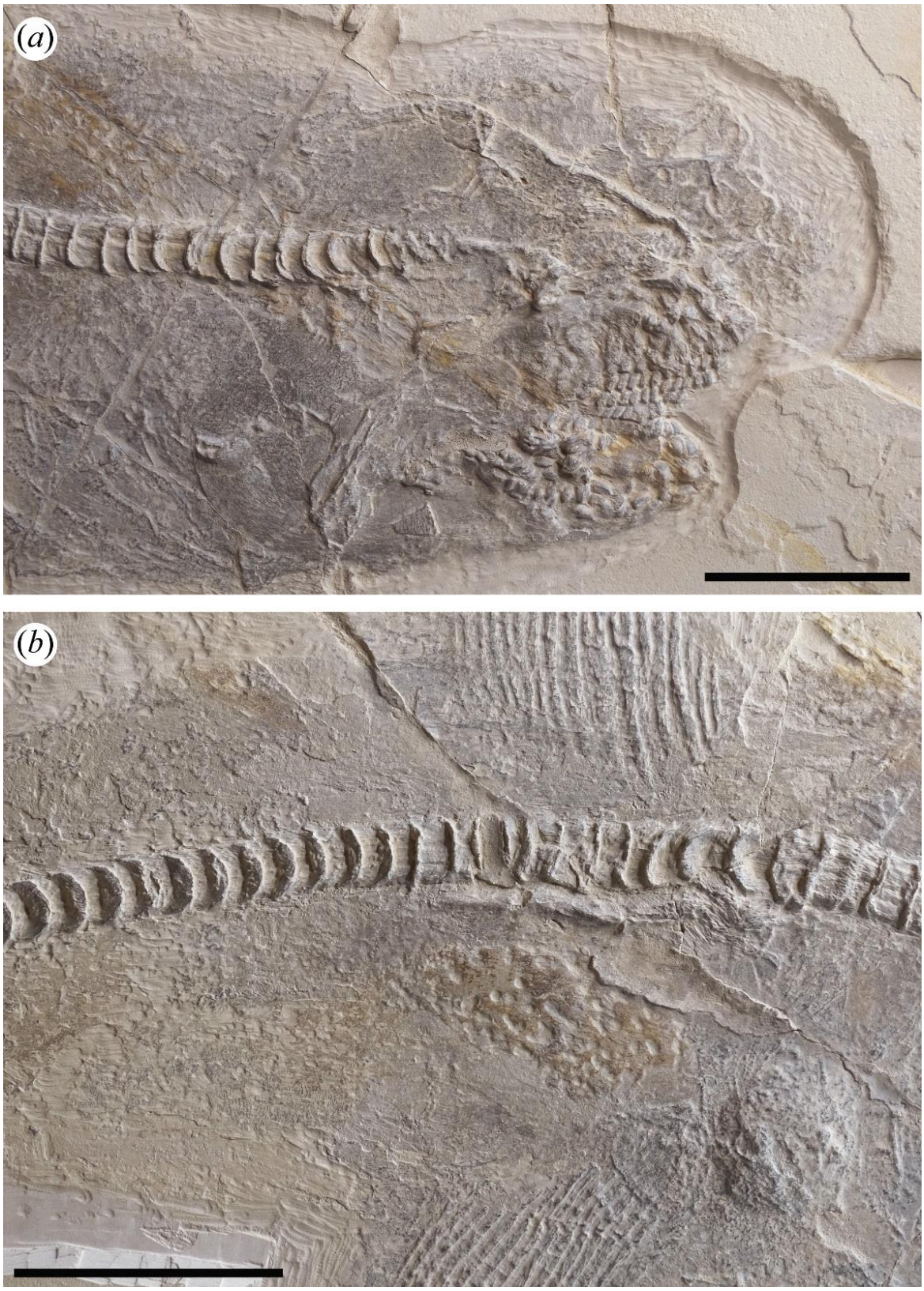

Figure S2. Close-up views of *Ptychodus* specimen MMSP CPC 3063. (*a*) Head region. (*b*) Trunk region, including the base of the dorsal (top) and pectoral (bottom) fins. Scale bars: 10 cm.

Figure S3. *Ptychodus* specimen MMSP CPC 3064. Scale bar: 10 cm.

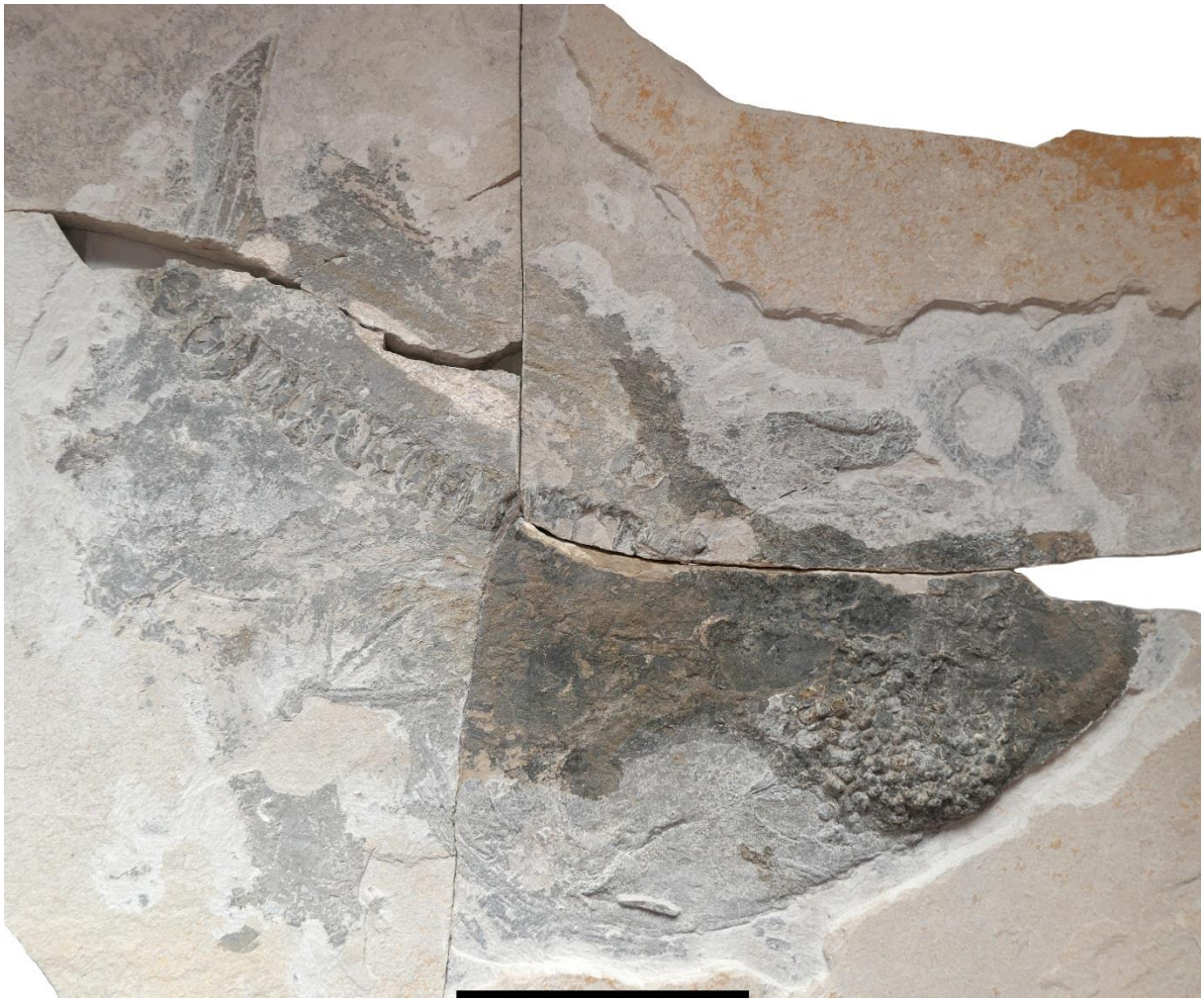

Figure S4. *Ptychodus* specimen MUDE CPC 3065. Scale bar: 10 cm.

Figure S5. *Ptychodus* specimen MMSP CPC 3066. Scale bar: 10 cm.

Figure S6. *Ptychodus* specimen MMSP CPC 3067. Scale bar: 10 cm.

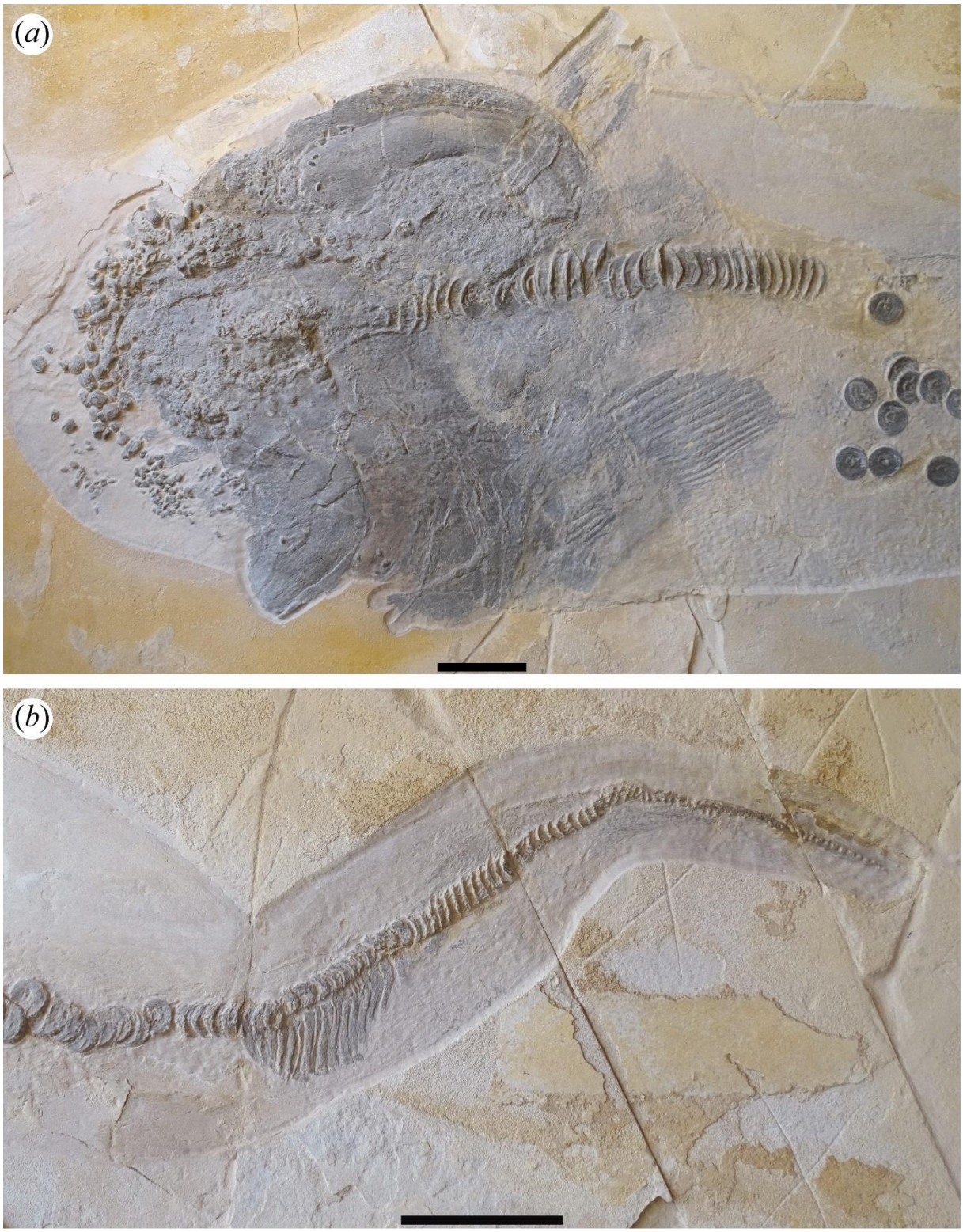

Figure S7. Close-up views of *Ptychodus* specimen MMSP CPC 3068. (*a*) Head region. (*b*) Tail region. Scale bars: 10 cm.

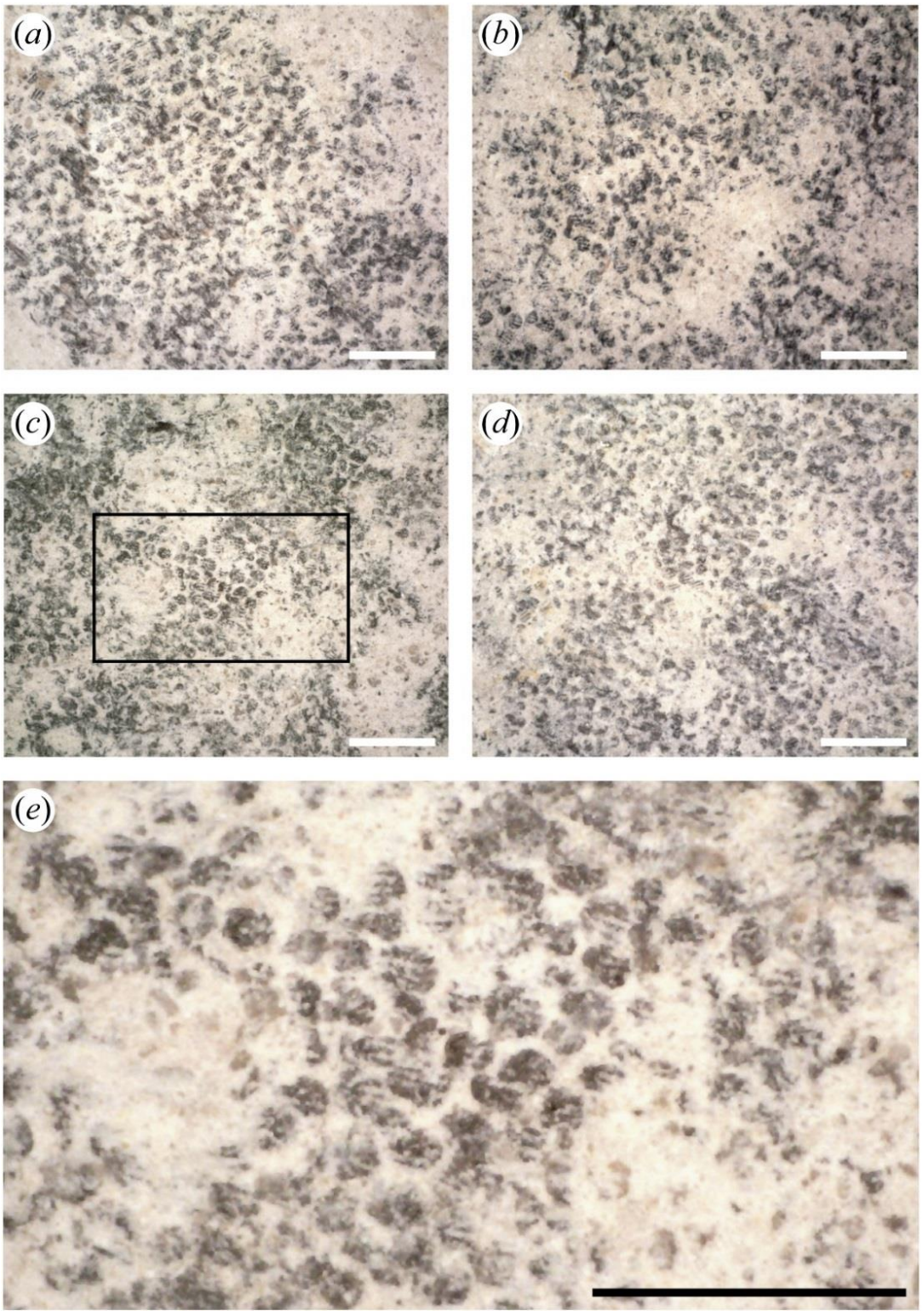

Figure S8. Skin portions showing the squamation of *Ptychodus* specimen MMSP CPC 3063. (*a*) Posterior margin of the pectoral fin. (*b*) Distal end of the posterior margin of the pectoral fin. (*c*) Second dorsal fin. (*d*) Anal fin. (e) Close-up on the leaf-shaped, five-ridged placoid scales (box in (*c*)). Scale bars: 1 mm.

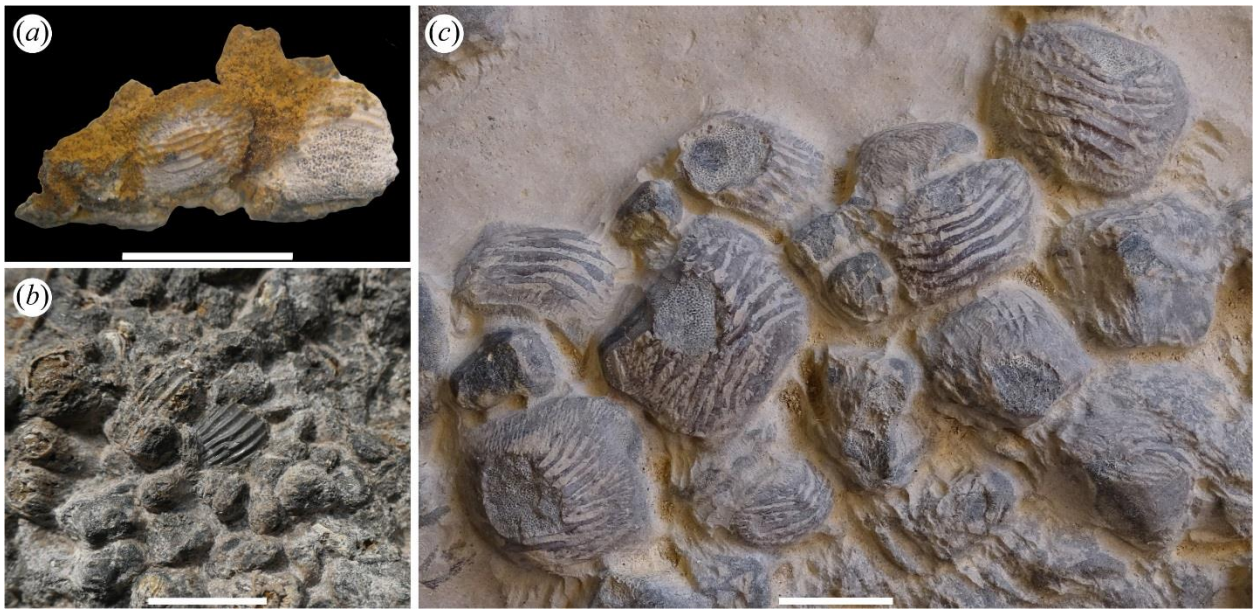

Figure S9. Tooth morphology of *Ptychodus* specimens MMSP CPC 3064, MMSP CPC 3065 and MMSP CPC 3068. (*a*) Two teeth extracted from specimen MMSP CPC 3064). (*b*) Portion of the dentition of specimen MUDE CPC 3065. (*c*) Portion of the dentition of specimen MMSP CPC 3068. Scale bars: 1 cm (*b*,*c*) and 5 mm (*a*).

Table S1. Main measurements (after Compagno, 2001) of the four most complete *Ptychodus* specimens studied here (in mm).

Measurements	**MMSP CPC 3063**	**MMSP CPC 3064**	**MMSP CPC 3067**	**MMSP CPC 3068**
Total Length (TL)	1420	565	890	2030
Fork Length (FL)	1245	470	n/a	1795
Precaudal Fin Length (PCL)	1155	440	n/a	1685
Pre-2nd Dorsal Fin Length (PD2)	995	n/a	n/a	n/a
Pre-1st Dorsal Fin Length (PD1)	475	165	n/a	n/a
Head Length (HL)	450	145	n/a	n/a
Prebranchial Length (PG1)	295	n/a	n/a	n/a
Prepectoral Fin Length (PP1)	440	145	n/a	n/a
Prepelvic Fin Length (PP2)	845	n/a	n/a	n/a
Preanal Length (PAL)	1020	n/a	n/a	n/a
Interdorsal Length (IDS)	460	n/a	n/a	n/a
1st Dorsal Caudal Fin Space (DCS1)	620	250	370	n/a
2nd Dorsal Caudal Fin Space (DCS2)	120	n/a	n/a	n/a
Pectoral–Pelvic Fin Space (PPS)	295	n/a	n/a	n/a
Pelvic–Anal Fin Space (PAS)	165	n/a	n/a	n/a
Anal–Caudal Fin Space (ACS)	110	n/a	n/a	n/a
Pelvic–Caudal Fin Space (PCA)	290	n/a	180	n/a
Pectoral Fin Height (P1H)	230	70	n/a	n/a
1st Dorsal fin height (D1H)	120	n/a	n/a	n/a
2nd Dorsal fin height (D2H)	25	n/a	n/a	n/a
Dorsal Caudal Fin Margin (CDM)	340	140	230	460
Preventral Caudal Fin Margin (CPV)	150	75	115	n/a

Part C. Size estimates of *Ptychodus*

Table S2. Size estimates of several *Ptychodus* specimens belonging to various species. The total length (TL) estimates are based on the proportion between lower symphysial tooth length and TL observed in specimen MMSP CPC 3063. µCl: average crown length of lower symphysial teeth.

References	Specimen	Material	Species	Tooth type	µCL (mm)	TL (mm)
This study	MMSP CPC 3063	Associated teeth	*Ptychodus* sp.	UC (?)	8.20	1420
Woodward (1904)	BMB 008524	Articulated teeth	*P. decurrens*	UC	6.91	1197
Woodward (1887)	NHMUK P. 40056	Articulated teeth	*P. decurrens*	UC	20.91	3621
Woodward (1887)	NHMUK P. 12830	Articulated teeth	*P. decurrens*	UC	24.36	4218
Woodward (1912)	MGL 2022	Associated teeth	*P. latissimus*	UC	37.50	6494
Amadori *et al.* (2020b)	MCSNV v.1612	Associated teeth	*P. latissimus*	UC	55.76	9656
Hamm and Shimada (2004)	KUVP 55277	Associated teeth	*P. martini*	UC	46.06	7976
Amadori *et al.* (2020a)	MSNUP I-17373	Articulated teeth	*P. mediterraneus*	UC	39.74	6882
Amadori *et al.* (2020a)	MPPSA IGVR 91031	Associated teeth	*P. mediterraneus*	UC	42.49	7358
Hamm (2020)	NHMUK P. 10464	Associated teeth	*P. marginalis*	UC	34.21	5924
Amadori *et al.* (2020a)	NHMUK PV P 10771	Associated teeth	*P. polygyrus*	UC	42.18	7304
Amadori *et al.* (2022a)	PIMUZ A/I 5056 (H)	Articulated teeth	*P. maghrebianus*	C	20.66	3578
Shimada (2012)	ROM 21705	Articulated teeth	*P. mortoni*	C	15.47	2679
Shimada (2012)	UNSM 1194	Articulated teeth	*P. mortoni*	C	24.19	4189
Shimada *et al.* (2010)	FHSM VP-17415	Associated teeth	*P. mortoni*	C	31.22	5406
Shimada *et al.* (2009)	UNSM 123607	Articulated teeth	*P. occidentalis*	C	8.10	1403
Hamm (2020)	AMNH 19553	Associated teeth	*P. rugosus*	C	9.12	1579
Hamm (2020)	SMU-SMP 69002	Associated teeth	*P. rugosus*	C	26.21	4539
Hamm (2020)	FHSM VP-2223	Associated teeth	*P. rugosus*	C	32.53	5633
Hamm (2020)	FHSM VP- 2073	Associated teeth	*P. rugosus*	C	34.18	5919
Average TL for the genus						**4849**
Average TL for uncuspidate (UC) species						**6063**
Average TL for cuspidate (C) species						**3880**

Part D. Ecomorphological analysis

The 11 measurements used for the Linear Discriminant Analysis (LDA) are indicated in figure S10, and measurement values for *Ptychodus* sp. and the 42 selected modern shark species are provided in table S3.

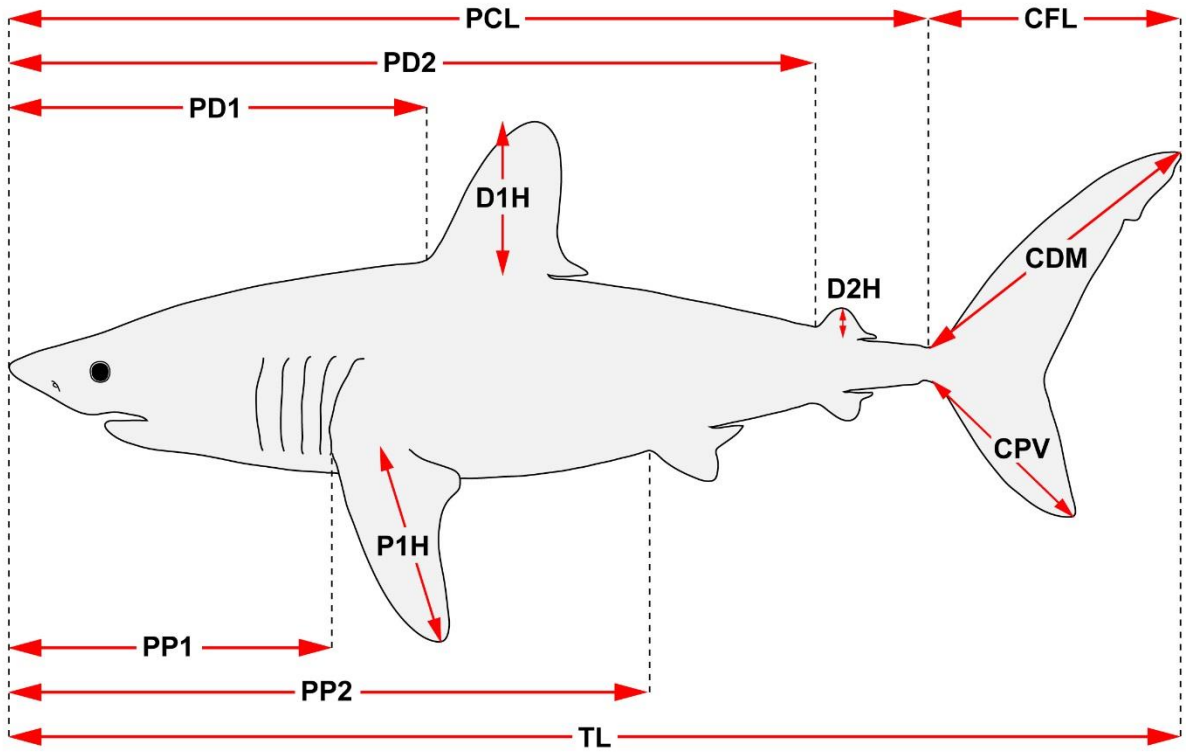

Figure S10. Measurements used for the Linear Discriminant Analysis (LDA) (modified after Compagno, 2001). Abbreviations: CDM, dorsal caudal fin margin; CFL, caudal fin length; CPV, preventral caudal fin margin; D1H, first dorsal fin height; D2H, second dorsal fin height; P1H, pectoral fin height; PCL, precaudal length; PD1, pre-first dorsal fin length; PD2, pre-second dorsal fin length; PP1, prepectoral fin length; PP2, prepelvic fin length; TL, total length (not included in the LDA as it equals PCL + CFL).

Table S3. Measurement values for *Ptychodus* sp. and 42 selected modern shark species belonging to the eight main ecomorphotypes (i.e. probenthic, leptobenthic, squatinobenthic, littoral, bathic, microceanic, macroceanic, tachypelagic) defined by Compagno (1990a).

Taxon	TL (max) (cm)	PCL (cm)	P1H (cm)	D1H (cm)	D2H (cm)	CFL (cm)	PD1 (cm)	PD2 (cm)	PP1 (cm)	PP2 (cm)	CDM (cm)	CPV (cm)	Ecomorphotype (Compagno, 1990a)	Reference
Somniosus antarcticus	456	383	40	12	9	73	188	316	113	291	77	64	Bathic	Ebert, 2014
Centroscymnus coelolepis	114	95	11	3	3	19	42	77	23	74	21	12	Bathic	Compagno, 1984a
Odontaspis noronhai	427	309	53	30	17	118	131	261	84	223	129	46	Bathic	Ebert, 2014
Mitsukurina owstoni	384	254	21	12	10	130	137	208	110	177	130	37	Bathic	Compagno, 2001
Pseudotriakis microdon	295	234	24	11	19	61	74	185	57	160	62	26	Bathic	Compagno, 1984b
Isurus paucus	430	343	116	41	5	87	159	298	104	300	99	66	Macroceanic	Ebert, 2014
Megachasma pelagios	550	379	96	34	17	171	174	302	142	280	174	79	Macroceanic	Ebert, 2014
Alopias pelagicus	375	173	56	24	2	202	83	152	46	129	211	27	Macroceanic	Ebert, 2014
Prionace glauca	380	286	77	32	10	94	138	253	79	205	102	44	Macroceanic	Ebert, 2014
Carcharhinus falciformis	330	252	63	27	6	78	108	219	70	169	89	39	Macroceanic	Ebert, 2014
Carcharhinus longimanus	350	247	85	45	10	103	107	215	72	178	115	55	Macroceanic	Ebert, 2014
Isurus oxyrinchus	400	329	71	43	6	71	149	291	106	231	95	72	Tachypelagic	Ebert, 2014
Carcharodon carcharias	640	523	113	60	10	117	234	448	164	380	141	96	Tachypelagic	Ebert, 2014
Lamna nasus	350	274	60	43	7	76	124	240	95	187	93	57	Tachypelagic	Ebert, 2014
Rhincodon typus	1200	932	218	88	28	268	533	783	250	576	336	162	Tachypelagic	Ebert, 2014
Cetorhinus maximus	1000	795	164	112	41	205	377	671	236	538	250	149	Tachypelagic	Ebert, 2014
Euprotomicrus bispinatus	27	23	3	1	1	4	14	18	6	16	4	3	Microceanic	Ebert, 2014
Heteroscymnoides marleyi	37	30	2	1	1	7	12	23	10	22	7	5	Microceanic	Ebert, 2014
Isistius brasiliensis	50	42	3	1	1	8	30	35	10	31	8	6	Microceanic	Ebert, 2014
Pseudocarcharias kamoharai	122	96	13	6	3	26	48	81	29	72	28	9	Microceanic	Ebert, 2014
Scymnodalatias albicauda	110	90	18	3	4	20	49	74	24	71	21	9	Microceanic	Ebert, 2014
Zameus squamulosus	84	69	7	2	2	15	35	57	19	55	16	10	Microceanic	Ebert, 2014
Squatina africana	108	91	19	4	4	17	68	80	22	44	12	14	Squatinobenthic	Compagno, 1984a
Squatina nebulosa	163	142	32	7	7	21	100	123	36	61	17	22	Squatinobenthic	Compagno, 1984a
Eucrossorhinus dasypogon	125	103	18	12	10	22	68	82	25	59	24	8	Squatinobenthic	Compagno, 2001
Orectolobus maculatus	320	259	32	24	21	61	162	203	67	139	62	15	Squatinobenthic	Compagno, 2001
Galeocerdo cuvier	550	389	101	46	15	161	170	366	111	275	175	73	Littoral	Ebert, 2014
Carcharhinus plumbeus	300	227	65	43	10	73	83	197	62	161	80	36	Littoral	Ebert, 2014
Carcharias taurus	318	239	37	18	18	79	123	195	74	168	81	28	Littoral	Compagno, 2001
Triakis semifasciata	180	142	21	13	10	38	52	107	30	75	39	16	Littoral	Compagno, 1984b
Mustelus dorsalis	64	51	5	5	3	13	20	40	14	28	13	4	Littoral	Compagno, 1984b
Nebrius ferrugineus	320	213	40	25	21	107	127	176	55	132	106	33	Littoral	Compagno, 2001
Stegostoma fasciatum	354	189	41	14	9	165	94	129	39	106	168	24	Littoral	Compagno, 2001
Sphyrna tiburo	150	109	19	19	5	41	48	93	32	69	42	14	Littoral	Compagno, 1984b
Chiloscyllium plagiosum	95	77	10	6	5	18	35	55	15	31	18	2	Leptobenthic	Compagno, 2001
Hemiscyllium ocellatum	107	89	10	7	6	18	41	63	14	34	18	4	Leptobenthic	Compagno, 2001
Parascyllium variolatum	91	73	8	5	5	18	44	62	13	31	18	4	Leptobenthic	Compagno, 2001
Halaelurus natalensis	47	38	5	2	2	9	21	31	7	17	9	3	Leptobenthic	Compagno, 1984b

Heterodontus portusjacksoni	165	131	31	15	13	34	40	90	31	68	38	25	Probenthic	Compagno, 2001
Brachaelurus waddi	122	93	14	10	9	29	52	71	21	45	29	11	Probenthic	Compagno, 2001
Heteroscyllium colcloughi	75	60	10	6	4	15	34	47	14	32	15	3	Probenthic	Compagno, 2001
Poroderma africanum	101	79	12	6	3	22	54	70	19	45	21	11	Probenthic	Compagno, 1984b
Ptychodus sp. (MMSP CPC 3063)	142	115.5	23	12	2.5	26.5	47.5	99.5	44	84.5	34	15	?	This study
Ptychodus sp. (2 m TL)	200	163	32	17	4	37	67	140	62	119	48	21	?	This study
Ptychodus sp. (5 m TL)	500	407	81	42	9	93	167	350	155	298	120	53	?	This study
Ptychodus sp. (10 m TL)	1000	813	162	85	18	187	335	701	310	595	239	106	?	This study

Table S4. One-way ANOSIM pairwise group comparisons of the measurement data for the 42 extant shark species included in the analysis. Hotelling's p-values of post-hoc pairwise test between ecomorphotype categories. Significant values ($p < 0.05$) are indicated in bold.

	Bathic	Macroceanic	Tachypelagic	Microceanic	Squatinobenthic	Littoral	Leptobenthic	Probenthic
Bathic		**0,0101**	**0,007**	**0,0102**	0,1331	0,6177	**0,0153**	**0,0405**
Macroceanic	**0,0101**		0,0808	**0,0025**	**0,0056**	0,1163	**0,0045**	**0,0057**
Tachypelagic	**0,007**	0,0808		**0,0026**	**0,0075**	**0,0287**	**0,007**	**0,0082**
Microceanic	**0,0102**	**0,0025**	**0,0026**		**0,0414**	**0,0026**	0,2059	0,0863
Squatinobenthic	0,1331	**0,0056**	**0,0075**	**0,0414**		0,1868	**0,0274**	0,3426
Littoral	0,6177	0,1163	**0,0287**	**0,0026**	0,1868		**0,0126**	0,1034
Leptobenthic	**0,0153**	**0,0045**	**0,007**	0,2059	**0,0274**	**0,0126**		0,1427
Probenthic	**0,0405**	**0,0057**	**0,0082**	0,0863	0,3426	0,1034	0,1427	

Table S5. One-way PERMANOVA pairwise group comparisons of the measurement data for the 42 extant shark species included in the analysis. Hotelling's p-values of post-hoc pairwise test between ecomorphotype categories. Significant values ($p < 0.05$) are indicated in bold.

	Bathic	Macroceanic	Tachypelagic	Microceanic	Squatinobenthic	Littoral	Leptobenthic	Probenthic
Bathic		**0,0095**	**0,0163**	**0,0078**	0,1332	0,4649	**0,0155**	**0,0421**
Macroceanic	**0,0095**		**0,0489**	**0,0024**	**0,0043**	**0,0464**	**0,0056**	**0,0057**
Tachypelagic	**0,0163**	**0,0489**		**0,002**	**0,0085**	**0,01**	**0,0079**	**0,008**
Microceanic	**0,0078**	**0,0024**	**0,002**		**0,0235**	**0,0038**	0,1771	0,0613
Squatinobenthic	0,1332	**0,0043**	**0,0085**	**0,0235**		0,226	**0,0275**	0,2939
Littoral	0,4649	**0,0464**	**0,01**	**0,0038**	0,226		**0,0163**	0,0928
Leptobenthic	**0,0155**	**0,0056**	**0,0079**	0,1771	**0,0275**	**0,0163**		0,1151
Probenthic	**0,0421**	**0,0057**	**0,008**	0,0613	0,2939	0,0928	0,1151	

Table S6. LDA confusion matrix showing the prediction accuracy of the LDA (total correct classification = 90.48%). This matrix provides for each given ecomorphotype (rows) the number of correctly (in bold) and incorrectly (in red) predicted ecomorphotypes (columns).

	Bathic	Macroceanic	Tachypelagic	Microceanic	Squatinobenthic	Littoral	Leptobenthic	Probenthic	Total
Bathic	**3**	**0**	**0**	1	**0**	1	**0**	**0**	3/5
Macroceanic	**0**	**6**	**0**	**0**	**0**	**0**	**0**	**0**	6/6
Tachypelagic	**0**	**0**	**5**	**0**	**0**	**0**	**0**	**0**	5/5
Microceanic	**0**	**0**	**0**	**6**	**0**	**0**	**0**	**0**	6/6
Squatinobenthic	**0**	**0**	**0**	**0**	**3**	**0**	**0**	1	3/4
Littoral	**0**	1	**0**	**0**	**0**	**7**	**0**	**0**	7/8
Leptobenthic	**0**	**0**	**0**	**0**	**0**	**0**	**4**	**0**	4/4
Probenthic	**0**	**0**	**0**	**0**	**0**	**0**	**0**	**4**	4/4
Total	3	7	5	7	3	8	4	5	38/42

Table S7. LDA classifier.

Species	Given group	Classification
Somniosus antarcticus	Bathic	Bathic
Centroscymnus coelolepis	Bathic	Microceanic
Odontaspis noronhai	Bathic	Littoral
Mitsukurina owstoni	Bathic	Bathic
Pseudotriakis microdon	Bathic	Bathic
Isurus paucus	Macroceanic	Macroceanic
Megachasma pelagios	Macroceanic	Macroceanic
Alopias pelagicus	Macroceanic	Macroceanic
Prionace glauca	Macroceanic	Macroceanic
Carcharhinus falciformis	Macroceanic	Macroceanic
Carcharhinus longimanus	Macroceanic	Macroceanic
Isurus oxyrinchus	Tachypelagic	Tachypelagic
Carcharodon carcharias	Tachypelagic	Tachypelagic
Lamna nasus	Tachypelagic	Tachypelagic
Rhincodon typus	Tachypelagic	Tachypelagic
Cetorhinus maximus	Tachypelagic	Tachypelagic
Euprotomicrus bispinatus	Microceanic	Microceanic
Heteroscymnoides marleyi	Microceanic	Microceanic
Isistius brasiliensis	Microceanic	Microceanic
Pseudocarcharias kamoharai	Microceanic	Microceanic
Scymnodalatias albicauda	Microceanic	Microceanic
Zameus squamulosus	Microceanic	Microceanic
Squatina africana	Squatinobenthic	Squatinobenthic
Squatina nebulosa	Squatinobenthic	Squatinobenthic
Eucrossorhinus dasypogon	Squatinobenthic	Probenthic
Orectolobus maculatus	Squatinobenthic	Squatinobenthic
Galeocerdo cuvier	Littoral	Littoral
Carcharhinus plumbeus	Littoral	Macroceanic
Carcharias taurus	Littoral	Littoral
Triakis semifasciata	Littoral	Littoral
Mustelus dorsalis	Littoral	Littoral
Nebrius ferrugineus	Littoral	Littoral
Stegostoma fasciatum	Littoral	Littoral
Sphyrna tiburo	Littoral	Littoral
Chiloscyllium plagiosum	Leptobenthic	Leptobenthic
Hemiscyllium ocellatum	Leptobenthic	Leptobenthic
Parascyllium variolatum	Leptobenthic	Leptobenthic
Halaelurus natalensis	Leptobenthic	Leptobenthic
Heterodontus portusjacksoni	Probenthic	Probenthic
Brachaelurus waddi	Probenthic	Probenthic
Heteroscyllium colcloughi	Probenthic	Probenthic
Poroderma africanum	Probenthic	Probenthic
***Ptychodus* sp.**	?	Tachypelagic
***Ptychodus* sp. (2 m TL)**	?	Tachypelagic
***Ptychodus* sp. (5 m TL)**	?	Tachypelagic
***Ptychodus* sp. (10 m TL)**	?	Tachypelagic

Table S8. LDA scores.

Species	Axis 1	Axis 2	Axis 3
Somniosus antarcticus	3,5376	-0,055605	-2,4338
Centroscymnus coelolepis	3,9178	-2,9249	-1,7367
Odontaspis noronhai	2,1334	0,34085	0,58362
Mitsukurina owstoni	3,0963	-0,33032	-1,2027
Pseudotriakis microdon	3,2907	-2,9427	-0,1236
Isurus paucus	2,8617	3,494	1,0826
Megachasma pelagios	2,6219	1,85	1,8476
Alopias pelagicus	2,1791	2,1533	2,3734
Prionace glauca	0,85774	1,5637	0,85084
Carcharhinus falciformis	0,19473	2,1937	-0,78315
Carcharhinus longimanus	0,91854	2,8015	2,0627
Isurus oxyrinchus	-0,081036	4,5968	-3,4034
Carcharodon carcharias	0,78377	4,1994	-1,7252
Lamna nasus	-0,10511	4,0785	-1,4258
Rhincodon typus	-1,543	4,3525	-3,2534
Cetorhinus maximus	-0,13097	3,9016	-1,2209
Euprotomicrus bispinatus	1,681	-3,3055	0,78741
Heteroscymnoides marleyi	4,7035	-3,5466	-0,68344
Isistius brasiliensis	3,1504	-3,5607	-1,5782
Pseudocarcharias kamoharai	2,2817	-1,4451	-0,38954
Scymnodalatias albicauda	3,0822	-3,4085	-0,030454
Zameus squamulosus	4,3386	-3,1069	-1,5074
Squatina africana	-3,139	-1,4186	3,2726
Squatina nebulosa	-5,3004	0,1929	0,41159
Eucrossorhinus dasypogon	-2,765	-0,43628	0,57209
Orectolobus maculatus	-2,8787	-0,045381	-0,17223
Galeocerdo cuvier	1,0852	1,6909	0,44246
Carcharhinus plumbeus	0,83803	1,9512	2,1697
Carcharias taurus	1,7207	-0,73095	1,0212
Triakis semifasciata	-1,2568	-0,55871	0,39931
Mustelus dorsalis	-0,92409	-1,7819	0,38575
Nebrius ferrugineus	-0,14027	0,1223	2,5436
Stegostoma fasciatum	0,061984	0,065642	1,6166
Sphyrna tiburo	-0,19515	0,95836	2,0887
Chiloscyllium plagiosum	-5,912	-2,3021	-1,1857
Hemiscyllium ocellatum	-6,1656	-1,4495	-1,3168
Parascyllium variolatum	-5,4029	-2,4803	-1,8732
Halaelurus natalensis	-4,1001	-2,9381	-1,6426
Heterodontus portusjacksoni	-1,3427	0,85849	0,55904
Brachaelurus waddi	-3,2556	-0,28869	0,94822
Heteroscyllium colcloughi	-3,022	-1,8186	1,1119
Poroderma africanum	-1,6761	-0,48961	0,55737
***Ptychodus* sp.**	0,93242	1,7441	-2,6881
***Ptychodus* sp. (2 m TL)**	0,87319	2,0089	-2,916
***Ptychodus* sp. (5 m TL)**	0,85473	3,224	-3,2598
***Ptychodus* sp. (10 m TL)**	0,80167	4,0505	-3,3662

Part E. Phylogenetic analysis

Additional supplementary material is downloadable from the Dryad Digital Repository: https://doi.org/10.5061/dryad.12jm63z5n. The strict consensus cladogram with all Jackknife and Bremer support values is provided in figure S11.

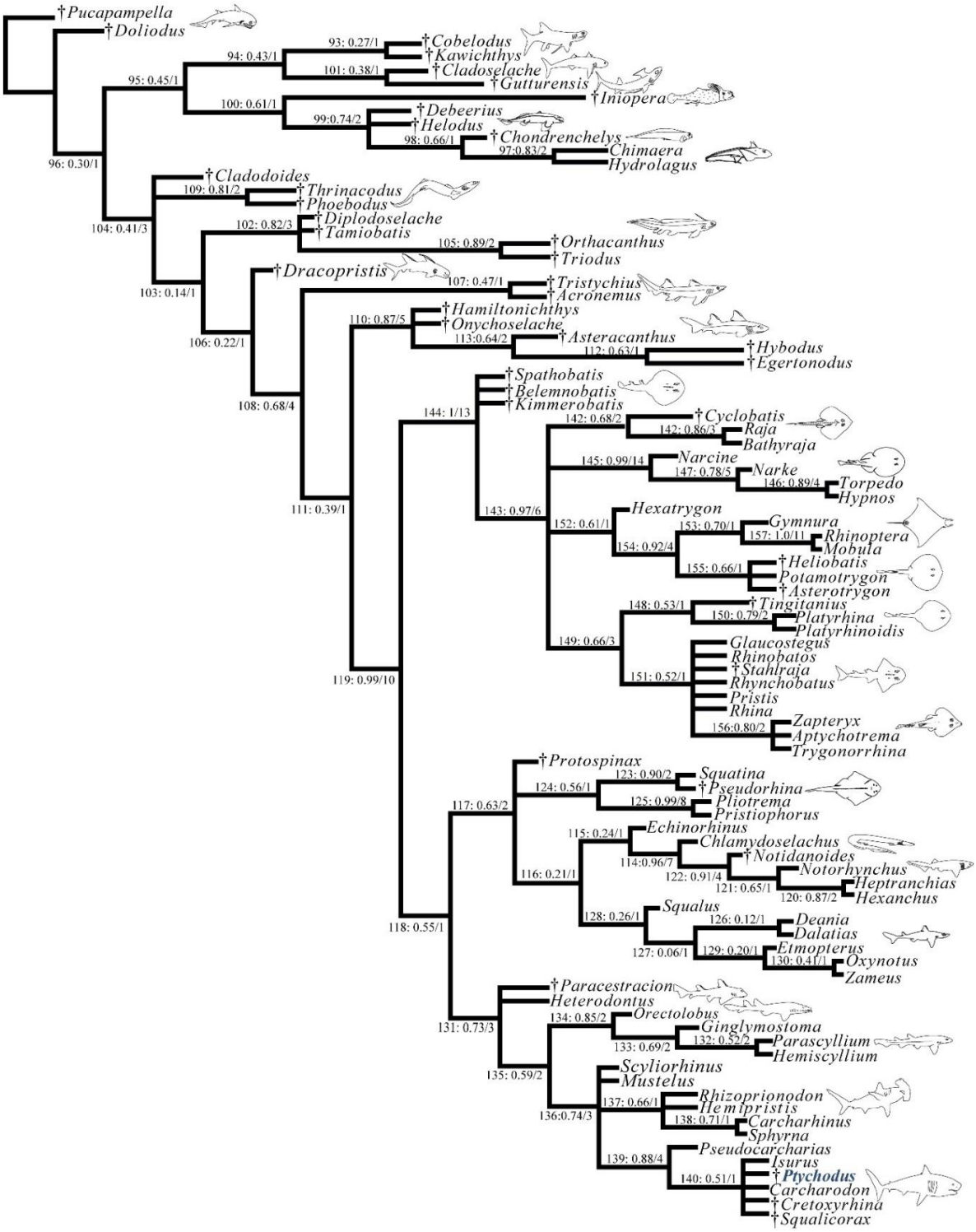

Figure S11. Strict consensus tree recovered from the parsimony analysis in TNT using step matrices. Numbers in nodes follow the format: node number: Jackknife support/Bremer support. *Ptychodus* is indicated in blue.

Node 93, Char: 46[0]->[1].
Node 94, Chars: 20[0]->[1], 122[0]->[1], 132[0]->[1], 135[1][3][5]->[0], 140[0]->[1], 144[1]->[0].
Node 95, Chars: 48[0]->[1], 54[0]->[1], 57[1]->[0].
Node 96, Char: 75[0]->[1].
Node 97, Chars: 121[1]->[0], 135[1]->[2].
Node 98, Char: 152[0]->[1][2].
Node 99, Chars: 36[0]->[1], 52[0]->[1], 53[0]->[1], 132[0]->[2], 221[0]->[1].
Node 100: Chars: 22[1]->[0], 47[0]->[2], 50[1]->[0], 56[1]->[0], 81[0]->[1], 91[1]->[0].
Node 101, Chars: 41[0]->[1], 217[0]->[1].
Node 102, Chars: 11[2]-> [4], 30[0]->[1].
Node 103, Chars: 83[0]->[1].
Node 104, Chars: 41[0]->[1], 76[0]->[1].
Node 105, Chars: 172[0]->[1], 203[0]->[1].
Node 106, Chars: 50[1]->[0], 176[2]->[0].
Node 107, Chars: 27[0]->[1], 58[0]->[1].
Node 108, Chars: 43[0]->[1], 84[1]->[0], 94[0]->[1], 101[1]->[0], 118[0]->[1], 178[1]->[0].
Node 109, Char: 8[0]->[1], 219[0]->[1].
Node 110, Char: 84[0]->[2], 138[1]->[2], 172[0]->[1], 195[0]->[1][3][4][7][8].
Node 111, Char: 41[1]->[0], 56[1]->[0], 82[1]->[0], 83[1]->[0], 179[1]->[0].
Node 112, Char: 217[0]->[1].
Node 113, Char: 33[3]->[4], 78[5]->[7], 195[3]->[8].
Node 114, Chars: 23[0]->[1], 46[0]->[1], 55[1]->[0], 83[0]->[1], 84[0]->[1], 114[1]->[0], 158[5]->[1], 174[1]->[0].
Node 115, Chars: 121[0]->[1], 169[1]->[0], 202[9]->[0].
Node 116, Char: 213[0]->[2].
Node 117, Chars: 31[1]->[2], 78[5]->[6], 168[0]->[1].
Node 118, Chars: 134[1]->[2], 135[5]->[7].
Node 119, Chars: 1[0]->[1], 4[1]->[0], 36[0]->[3], 62[0]->[1], 68[2]->[1], 72[0]->[1], 121[1]->[0], 142[0]->[1], 149[0]->[1][2], 154[0]->[1]. 155[0]->[1], 158[0]->[5][6][8][9][A][C], 164[0]->[2], 171[0]->[1], 175[0]->[1], 202[3][7]->[9], 209[0]->[1][2].
Node 120, Chars: 24[0]->[1], 40[0]->[1], 154[1]->[2].
Node 121, Char: 164[2]->[1].
Node 122, Chars: 82[0]->[2], 133[4]->[5], 214[0]->[2].
Node 123, Chars: 15[0]->[2], 146[0]->[1].
Node 124, Char: 176[1]->[3], 202[9]->[0].
Node 125, Chars: 10[0]->[1], 13[1]->[2], 39[0]->[1], 103[1]->[3], 154[1]->[2], 169[1]->[2], 201[0]->[1].
Node 126, Chars: 132[3]->[4], 135[7]->[0].
Node 127, Char: 169[1]->[0].
Node 128, Chars: 24[0]->[1], 36[4]->[2], 216[0]->[1].
Node 129, Chars: 158[5]->[1], 213[2]->[0].
Node 130, Chars: 99[1]->[0], 110[0]->[1].
Node 131, Chars: 1[1]->[3], 28[1]->[2], 169[1]->[0].
Node 132, Chars: 55[1]->[0], 70[1]->[2].
Node 133, Chars: 25[0]->[2], 132[3]->[5], 135[7]->[0].
Node 134, Chars: 95[2]->[3], 112[0]->[1], 139[0]->[1].
Node 135, Chars: 11[0]->[1], 13[1]->[0], 166[0]->[1][2], 176[1]->[2], 202[9]->[0].
Node 136, Chars: 1[3]->[2], 138[1]->[0], 158[5]->[1].
Node 137, Chars: 19[0]->[1], 28[2]->[0].
Node 138, Chars: 133[4]->[6].
Node 139, Char: 83[0]->[1], 84[0]->[1], 213[0]->[1].
Node 140, Chars: 175[0]->[1].
Node 141, Char: 7[0]->[1], 140[0]->[1].
Node 142, Chars: 143[0]->[1], 200[0]->[1].
Node 143, Chars: 25[0]->[1], 127[0]->[2][3][4], 133[4]->[6], 134[1]->[3], 135[5]->[9], 162[0]->[1], 169[1]->[2].
Node 144, Chars: 23[0]->[2], 31[1]->[0], 55[1]->[0], 78[5]->[0], 94[1]->[2], 95[2]->[0], 113[0]->[1], 122[0]->[1], 139[0]->[1], 154[1]->[3], 166[0]->[3], 177[1]->[2].
Node 145, Chars: 23[2]->[3][5], 28[1]->[0], 33[1][3]->[0], 100[0]->[1], 115[0]->[1], 116[1]->[0], 121[0]->[1], 125[0]->[1], 127[2][3][4]->[1], 133[6]->[7], 143[0]->[1], 162[1]->[2], 194[0]->[1].
Node 146, Chars: 23[3][5]->[4], 25[1][2]->[0].
Node 147, Chars: 15[0]->[1], 70[1]->[2], 103[4][5]->[0], 185[0]->[1], 186[0]->[1].
Node 148, Char: 13[1]->[3].
Node 149, Chars: 36[3]->[5], 127[2][3][4]->[6], 212[0]->[1].
Node 150, Char: 162[1]->[2].
Node 151, Chars: 7[0]->[1], 18[0]->[1].
Node 152, Chars: 13[1]->[0], 36[3]->[5], 127[2][3][4]->[C], 155[1]->[2], 208[0]->[1].
Node 153, Chars: 68[1]->[0], 140[0]->[1], 141[0]->[1].
Node 154, Chars: 15[0]->[1], 109[0]->[2], 155[2]->[4], 174[1]->[2].
Node 155, Char: 7[0]->[1].
Node 156, Char: 23[6][7]->[2], 70[1]->[2], 88[0][1]->[1], 103[4]->[2], 118[0][1]->[0], 173[0]->[1], 177[1][2]->[1], 191[1]->[2].
Node 157, Chars: 1[4]->[7], 18[0]->[1], 33[3]->[4], 77[0]->[1], 86[0]->[1], 103[2][4][5]->[0], 126[0]->[1], 162[1]->[3], 174[2]->[0], 182[0] ->[1].

Notes: In bold is the previous publication where the original description on the characters is carried. Marked with an asterix (*) are publication that further describe or provide further description on the characters. The suffix Sup (superior) and Sub (subordinate) in front of some the characters refers to the nomenclature implemented in TNT for the analysis of step matrices (see Goloboff *et al*., 2021). States present in †*Ptychodus* Agassiz, 1834 are in bold.

Neurocranium (Skeleton)

1. Sup Rostral cartilages: [0] arise from the medial area of the trabecula only, **[1]** medial area of the trabecula + lamina orbitonasalis. †*Ptychodus***[?]**.**Villalobos-Segura *et al*. (2022, Char. 3).**

2. Sub Rostral cartilage: [0] well-developed rostral plate with various degrees of contribution from the lamina orbitonasalis, [1] reaches the tip of the snout (carried by the growth of the pectoral fin, [2] reaches the tip of the snout (growth of lamina orbitonasalis to support the cephalic fins). †*Ptychodus***[?]**. **Villalobos-Segura *et al*. (2022, Char. 4).**

3. Sub Rostral cartilage "rostrum": [0] trough-like rostrum, [1] tripodal rostrum, [2] greatly reduced to medial bar. †*Ptychodus***[?].** Landemaine *et al*. (2018, Char. 1), Klug (2010, Char. 1), Goto (2001, Char. 21), de Carvalho (1996, Char. 1), **Shirai (1996, Char. 1)**

4. Internasal plate separating the two palatoquadrates absent: [0] absent, [1] present. **Pradel (2011, Char. 4**).

5. Sup Rostral processes: [0] absent, [1] present. †*Ptychodus***[?]**. Villalobos-Segura *et al*. (2022, Char. 7), Villalobos-Segura *et al*. (2019, Char. 32), **Aschliman *et al*. (2012, Char. 29)**.

6. Sub Rostral processes (proximal articulation): [0] articulated with nasal capsules, [1] continuous with chondrocranium, [2] articulated with ventral aspect of rostral cartilage. †*Ptychodus***[?]**. **Villalobos-Segura *et al*. (2022, Char. 8)**.

7. Rostral appendix: [0] absent, [1] present. †*Ptychodus***[?]**. **Aschliman *et al*. (2012, Char. 25)**.

8. Elongate, tooth-bearing, pre-nasal ethmo-rostral region: [0] absent, [1] present. †*Ptychodus***[?]**. **Frey *et al*. (2020, Char. 106)**.

9. Ethmoidal region of neurocranium (down-curved): [0] absent, [1] present. †*Ptychodus***[?]**. Landemaine *et al*. (2018, Char. 3), Klug (2010, Char. 3), Goto (2001, Char. 9a), **de Carvalho (1996, Char. 4)**, **Shirai (1996, Char. 2)**.

10. Rostral passage of superficial ophthalmic nerve: [0] covered, [1] open. †*Ptychodus***[?]**. **Villalobos-Segura *et al*. (2022, Char. 11)**.

11. Trigeminofacial complex: [0] exits neurocranium through prootic foramen, [1] separate foramen for superficial ophthalmic nerve, [2] emerged from the braincase via a single

foramen and then branched to form separate dorsal (superficial ophthalmic) and ventral (buccomaxillary) complexes. The superficial ophthalmic complex passed through a short canal in the dorsal part of the postorbital arcade and merged below the roof of the orbit. The prootic foramen and the foramen for the hyomandibular branch of facialis (hmVII) in anteromedial position, [3] separate foramen for superficial ophthalmic nerve with prootic foramen and foramen for hmVII going through the subocular shelf, [4] The superficial ophthalmic complex passed through a short canal in the dorsal part of the postorbital arcade and merged below the roof of the orbit. The prootic foramen and the foramen for hmVII in posteromedial position, [5] three separate foramina, foramen for hmVII in anteromedial position, [6] single foramina for the whole complex, [7] three separate foramina, foramen for hmVII in posteromedial position. †*Ptychodus***[?]**. (Modified from Landemaine *et al*. (2018, Char. 6), Klug (2010, Char. 6), de Carvalho (1996, Char. 7), Shirai (1996, Char. 9), **Shirai (1992, Char. 5)**.

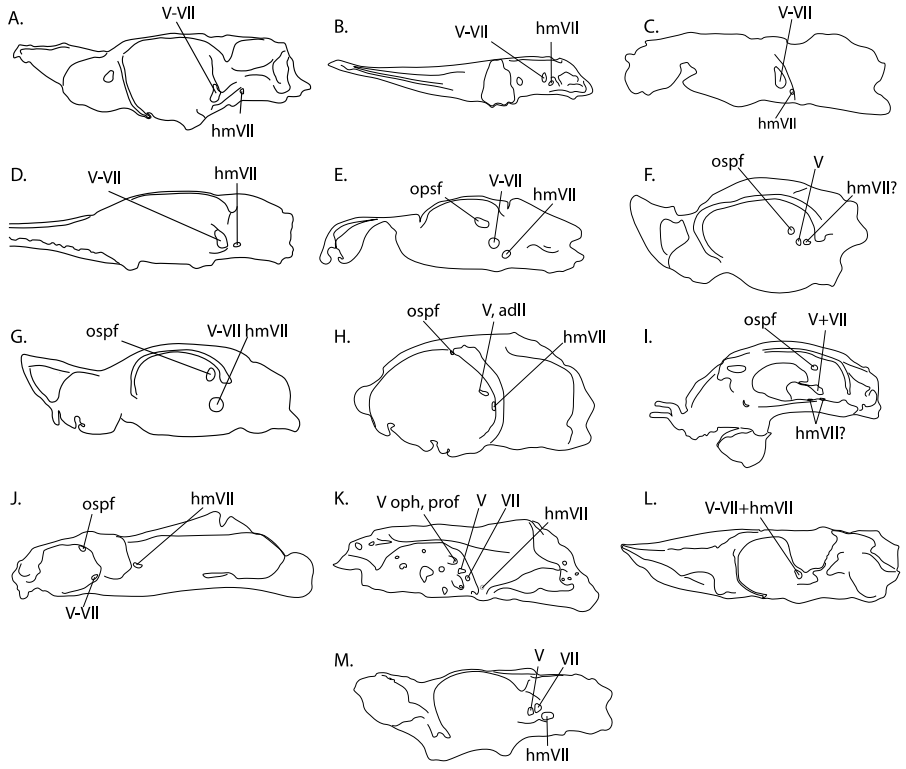

Figure S12. Lateral view of various chondrocrania displaying the arrangement of some of the foramina involved with the trigeminofacial nerve complex. A. *Squalus acanthias* Linnaeus, 1758 (redrawn and modified from Shirai, 1992: plate 8c). B. *Rhinobatos schlegelii* Müller and Henle, 1841 (redrawn and modified from Holmgren, 1941: text-fig. 46). C. *Squatina japonica* Bleeker, 1858 (HUMZ 91670) (redrawn and modified from Shirai, 1992: plate 13c). D. *Pristiophorus nudipinnis* Günther, 1870 (FSFL-EA 735) (redrawn and modified from Shirai, 1992: plate 14c). E. *Eucrossorhinus dasypogon* (Bleeker, 1867) (CSIRO CA 4051) (redrawn and modified from Goto, 2001: text-fig. 2b). F. *Lamna nasus* (Bonnaterre, 1788) (LJVC-880127), G. *Triakis semifasciata* Girard, 1855 (HUMZ 119338), H. Idealized symmoriiform (mainly based on ‘‘†*Cobelodus’’,* but with ethmoid region after †*Stethacanthus* Newberry, 1889 and †*Falcatus* Lund, 1985 (redrawn from Maisey, 2007: text-fig. 2a). I. *Callorhynchus* Lacepède, 1798 (redrawn from de Beer and Moy-Thomas, 1935: text-fig. 1). J. †*Xenacanthus* sp. (MCZ 13388) (redrawn and modified from the composite restoration of Schaeffer, 1981: text-figs. 5). K. †*Egertonodus* Maisey, 1987 (NHM P60110). L. *Echinorhinus brucus* (Bonnaterre, 1788) (HUMZ 113400)

(redrawn and modified from Shirai, 1992: plate 3c). M. *Zameus squamulosus* (Günther, 1877) (HUMZ 75872) (redrawn and modified from Shirai, 1992: plate 6c). **State [0]**: A-D. **State [1]**: E-G. **State [2]**: H. **State [3]**: I. **State [4]**: J. **State [5]**: K. **State [6]**: [L]. **State [7]**: M. **Abbreviations:** adll: foramen for anterodorsal lateral line ramus, hmVII: hyomandibular ramus of facial nerve, opsf: foramen for ophthalmicus superficialis, prof: profundus nerve, V oph+prof: foramen for trigeminal nerve component of superficial ophthalmic complex and profundus nerve, V: foramen for trigeminal nerve VII: foramen for facial nerve, V-VII: trigeminofacial foramen.

Remarks: A modification to previous scorings is proposed in the present work, because several taxa have a separate foramen for the superficial ophthalmic nerve (Maisey, 1985), and simple coding as separate can lead to confusion. Modern holocephalians (FigI), †*Cobelodus* Zangerl, 1973 (figure S12H) and †*Xenacanthus* Beyrich, 1848 (figure S12J), Orectolobiformes, Carcharhiniformes, and Lamniformes (figure S12E-G) all present a separate foramen for the superficial ophthalmic nerve. However, the arrangement of foramina associated with the trigeminofacial complex varies. In holocephalians, the foramen for the hyomandibular branch of the facialis (hmVII) is located on the subocular shelf, whereas in Orectolobiformes, when a separate foramen for the (hmVII) is present, is located anteriorly and slightly dorsal to the hyomandibular facet. Initially, a different pattern was identified for Carcharhiniformes and Lamniformes by Goodrich (1930, p. 259), Holmgren (1940, 1941) and Goto (2001) based on the absence of the prefacial commissure, resulting in the hyomandibular branch of the facialis exiting the chondrocranium through the foramen for the trigeminal nerve (V-VII) (also referred to as the trigeminal foramen (Sewertzoff, 1897; Mori, 1924; de Beer, 1937), trigemino-facialis foramen (Holmgren, 1941; El-Toubi, 1949), prootic foramen (Goodrich, 1930), or orbital fissure (Daniel, 1934; Nishida, 1990)) (figure S12F-G). However, Maisey and Springer (2013) recently questioned this pattern for Lamniformes, because *Lamna nasus* (Bonnaterre, 1788) (figure S12F) shows a separate foramen next to the trigeminal foramen, possibly for the exit of hmVII. A similar arrangement is observed in *Isurus oxyrhinchus* Rafinesque, 1810, *Carcharodon carcharias* (Linnaeus, 1758), but not in *Pseudocarcharias kamoharai* (Matsubara, 1936) (https://sharksrays.org/).

While the arrangement of hmVII appears to vary within Lamniformes, the presence of a separate foramen of the superficial ophthalmic nerve is a shared feature among some Orectolobiformes, Carcharhiniformes, and some Lamniformes. Among Squaliformes and Batomorphii, there appear to be differences in the arrangement of the foramina depending on the presence and extent of the lateral commissure. However, typically, these foramina merge into a single foramen (figure S12A-D, L-M; V-VII), separated from the foramen for the hyomandibular branch of the facialis (figure S12A-D, L-M; hmVII). There are exceptions to this pattern: *Echinorhinus* Blainville, 1816 has a single foramen (figure S12L; V-VII+hmVII) and *Zameus* Jordan and Fowler, 1903 has three separate foramina (figure S12M).

The ancestral status for Elasmobranchii remains inconclusive because †*Egertonodus* Maisey, 1987 and †*Tribodus* Brito and Ferreira, 1989 (figure S12K) present three separate foramina, one for the trigeminal nerve and superficial ophthalmic nerve (figure S12K; V), and two separate foramina one for the facial nerve and one for the hyomandibular branch of the facial nerve (figure S12K; VII, hmVII) located ventral to the postorbital (anteromedial) process (Lane, 2010), unlike in *Zameus* Jordan and Fowler, 1903, which also presents three foramina but one more posteromedial (hmVII), whereas †*Xenacanthus* Beyrich, 1848 appears to present a single foramen for the trigeminofacial (figure S12J; V-VII) and a separate foramen for the hyomandibular branch of the facial nerve (figure S12J; hm VII), resembling the condition in *Heterodontus* de Blainville, 1816.

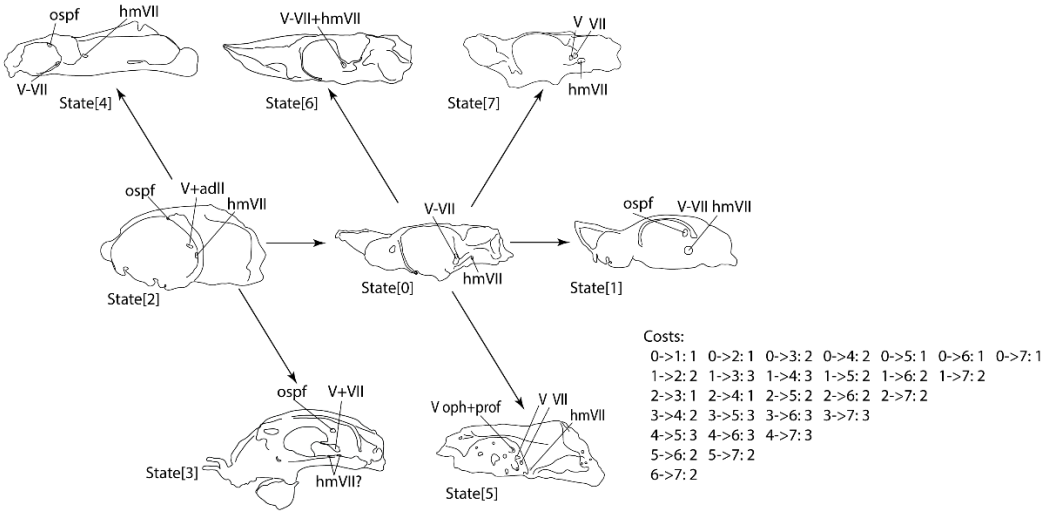

Figure S13. Enforced path using the "cstree" command on TNT for state evolution on character 11. Arrows indicate the allowed transformation path initiating for the states, each stop on a state increases one step. The transformation path begins in the state [2]. For abbreviation and genus see figure S12 caption.

Scoring: The ancestral state hypothesized in the present work for chondrichthyans is the one found in †*Cobelodus* Zangerl, 1973 after considering the observations of Goodrich (1930), from which the states of the remaining groups of chondrichthyans would have evolved (figure S13).

12. Precerebral fontanelle: [0] absent, **[1]** present. Villalobos-Segura *et al*. (2022, Char. 142), Landemaine *et al*. (2018, Char. 23), Klug (2010, Char. 23(17)), de Carvalho and Maisey (1996, Char. 4), **Shirai (1992, Char. 13)**.

13. Sup precerebral fossa: [0] absent, [1] present. †*Ptychodus***[?]**. Landemaine *et al*. (2018, Char. 2 & 43), Klug (2010, Char. 2(2) & 43(31)), de Carvalho (1996, Char. 3), de Carvalho and Maisey (1996, Char. 5)*, Shirai (1996, Char. 3), **Shirai (1992, Char. 14)**.

14. Sub precerebral fossa: [0] circular or ovoid concavity, [1] extending anteriorly and roofed to form a tube. †*Ptychodus***[?]**. Landemaine *et al*. (2018, Char. 2 & 43), Klug (2010, Char. 2(2) & 43(31)), **Shirai (1996, Char. 3)**.

Remarks: Following Jambura *et al*. (2023) observations, character 14 is considered a subordinate of character 13 as a modification to the original coding proposed by Shirai (1992, Chars. 21–22). This character is present twice in Klug (2010) and Landemaine *et al*. (2018).

15. Nasal capsules: [0] laterally expanded, [1] ventrolaterally expanded, [2] anteriorly expanded, [3] trumpet-like. (Villalobos-Segura *et al*. (2022, Char. 34)*, Villalobos-Segura *et al*. (2019, Char. 34)*, Landemaine *et al*. (2018, Char. 44), Claeson *et al*. (2013, Char. 10), Aschliman *et al*. (2012, Char. 31), McEachran and Aschliman (2004, Char. 27), Klug (2010, Char. 44(32)), McEachran *et al*. (1996, Char. 23), Shirai (1996, Char. 4), **Nishida (1990, Char. 37)**.

16. Nasal capsule margin (anterior process "horn like process"): [0] absent, [1] present. Villalobos-Segura *et al*. (2022, Char. 35), Villalobos-Segura *et al*. (2019, Char. 83), Claeson *et al*. (2013, Char. 9), **Brito and Seret (1996, Char. 5)**.

17. Nasal capsules separated from orbits: [0] absent, [1] present. †*Ptychodus***[?]**. New

Remarks: Derived from Villalobos-Segura *et al*. (2022; Char. 34), the present character is proposed based on the presence of the "trumpet"-shaped nasal capsules in some galeomorphs (orectolobids and heterodontids) (Shirai, 1992; Char. 2). However, the present character reflects the lack of direct immediacy between the posterior wall of the nasal capsules and the anterior wall of the orbits, which was also observed by Shirai (1992) and coded as part of his character two.

18. Anterior preorbital foramen: [0] located dorsally, [1] located anteriorly. †*Ptychodus***[?]**. Villalobos-Segura *et al*. (2022, Char. 12), Villalobos-Segura *et al*. (2019, Char. 37), Aschliman *et al*. (2012, Char. 35), McEachran *et al*. (1996, Char. 27), **Nishida (1990, Char. 85).**

19. Preorbital process (nasal capsule): [0] absent, [1] present. †*Ptychodus***[?]**. Modified from Villalobos-Segura *et al*. (2022, Char. 13), Aschliman *et al*. (2012, Char. 33), **de Carvalho and Maisey (1996, Char. 16)**, McEachran *et al*. (1996, Char. 25), Shirai (1992, Char. 33 & 34 & 35), Nishida (1990, Char. 17).

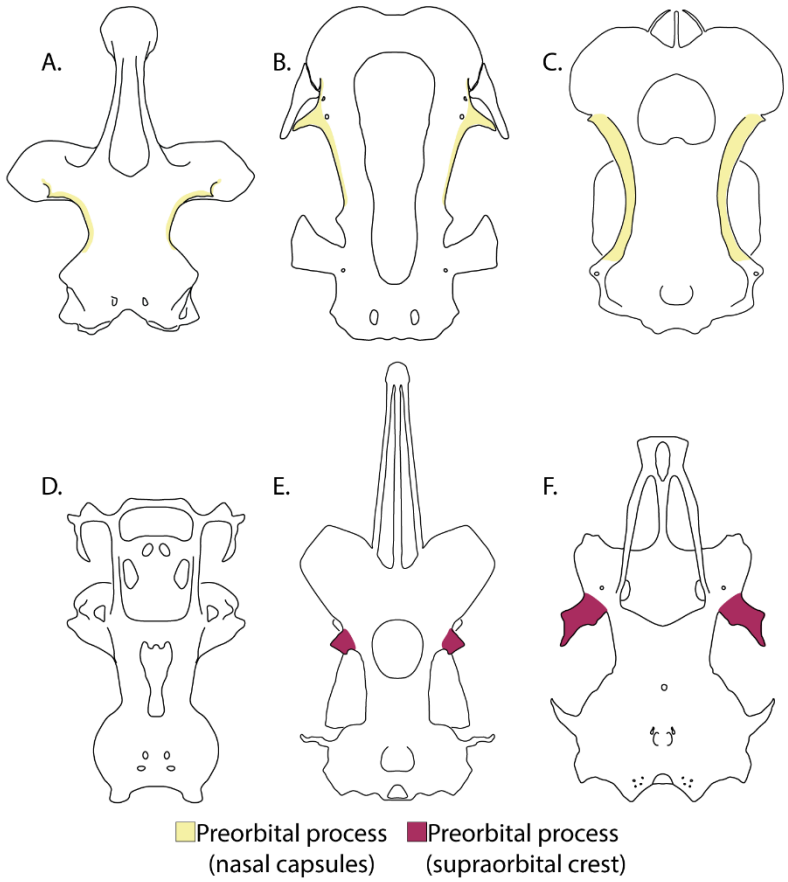

Figure S14. Line drawings of the character states recognized for character 19. A. *Trygonorrhina fasciata* Müller and Henle, 1841 (MCZ 982S) (redrawn from McEachran *et al*., 1996: text-fig. 7). B. *Potamotrygon yepezi* Castex and Castello, 1970 (redrawn from Nishida, 1990: text-fig. 13a). C. *Scyliorhinus haeckelii* (de Miranda-Ribeiro, 1907) (AC.UERJ 1690) (redrawn from Soares *et al*., 2016: text-fig. 17a). D. *Diplobatis picta* Palmer, 1950 (NSMT-P 40560) (redrawn from Nishida, 1990: text-fig. 7d). E. *Apristurus longicephalus* Nakaya, 1975 (HUMZ 170382) (redrawn from Soares and de Carvalho, 2020: text-fig. 13g). F. *Carcharhinus falciformis* (Bibron in Müller and Henle, 1841) (AC.UERJ 1456) (redrawn from de Olivera Lana *et al*., 2021 text-fig 1A). **State [0]**: A-D. **State [1]**. E.-F.

Remarks: The preorbital process has been embryonically related to the lamina orbitonasalis. This process is initially present as a lateral outgrowth from the lamina in dorsally position in relation to the orbit and orbitonasal canal (Figure S14E-F). This process seems to be developed without the supraorbital crest, considering that the taxa presenting it lack a supraorbital crest. Another possible postorbital process can be recognized in other neoselachians (crown elasmobranchs), conjoined with the supraorbital crest (Figure S14A-C). Because of this, these two processes were recognized as two separate characters in the present analysis (Char. 19 and Char. 28).

20. Scleral (= sclerotic) ring: [0] absent, [1] present. Giles *et al*. (2015, Char. 52), Qiao *et al*. (2016, Char. 277), Zhu *et al*. (2016, Char. 275); Burrow *et al*. (2016); Coates *et al*. (2018), **Frey *et al*. (2020, Char. 22)**.

Remarks: Recent analyses have increasingly focused on scoring scleral rings in early chondrichthyans (Coates *et al.*, 2018; Frey *et al.*, 2020). However, in the case of these ancient taxa, such as *Damocles* Lund, 1986, the scleral ring is composed of plates exhibiting continuous calcifications or ossifications without prismatic calcified cartilage (Lund, 1986). This observation is also supported by the coding proposed by Coates *et al.* (2018) for their characters 22 and 23. As a result, we have opted to differentiate this feature from the scleral capsule present in *Ptychodus* and other modern taxa, such as *Lamna nasus* (Bonnaterre, 1788) (Pilgrim and Franz-Odendaal, 2009; Maisey and Springer, 2013), which contains tessellated calcified cartilage.

21. Interorbital space: [0] broad, [1] narrow. Brazeau (2009), Davis *et al*. (2012), Zhu *et al*. (2013), Coates *et al*. (2017), **Frey *et al*. (2020, Char. 110)**.

22. Optic pedicel: [0] absent, **[1]** present. Dupret *et al.* (2014), Zhu *et al*. (2009, 2013), Coates *et al*. (2017), **Frey *et al*. (2020, Char. 111)**.

23. Antorbital process: [0] membranous, [1] mineralization of the antorbital process in the presence of the ectethmoid process, [2] mineralized in absence of an ectethmoid process (antorbital cartilages, triangular shaped with regular outline, lateral articulation), [3] antorbital cartilages, variously shaped and with an irregular outline, lateral articulation, [4] antorbital cartilages, variously shaped and with an irregular outline, anterolateral articulation, [5] antorbital cartilages, triangular-shaped with regular outline, anterolateral articulation, [6] antorbital cartilages, triangular-shaped with regular outline, posterolateral articulation, [7] antorbital cartilages, triangular-shaped with regular outline, posterolateral articulation, anterior process. †*Ptychodus***[?]**. Landemaine *et al*. (2018, Char. 7), Klug (2010, Char. 7), Shirai (1996, Char. 10), de Carvalho (1996, Char. 8)*****, de Carvalho (2004, Char. 2), Villalobos-Segura *et al*. (2022, Char. 23; Char. 24; Char. 26; Char. 110)., Villalobos-Segura *et al*. (2019, Char. 8; Char. 9), Claeson *et al*. (2013, Char. 5), Aschliman *et al*. (2012, Char. 8), Brito and Seret (1996, Char. 2), **Nishida (1990, Char. 3)**.

Remarks: Previous works have proposed polymorphic and ordered scorings for this character, in which the antorbital process developed at early development stages among several elasmobranchs groups and becomes calcified in some (Holmgren 1940; 1941). This antorbital process can be in close relation to the ectethmoid process (e.g., *Heptranchias* Rafinesque, 1810), separated from it (e.g., *Chlamydoselachus anguineus* Garman, 1884) or be developed and mineralized in the absence of an ectethmoid process (batomorphs). Consequently, the mineralization of the antorbital process in the presence of the ectethmoid process and the development of the antorbital cartilages via the antorbital process in the absence of an

ectethmoid process are coded as a single character. The phylogenetic separation between the groups with a mineralized antorbital process (Hexanchiformes and Batomorphii) suggests independent gains for the calcification of the antorbital processes and antorbital cartilages. Characters associated with the antorbital cartilages are included as subsequent steps after the addition of the antorbital cartilages.

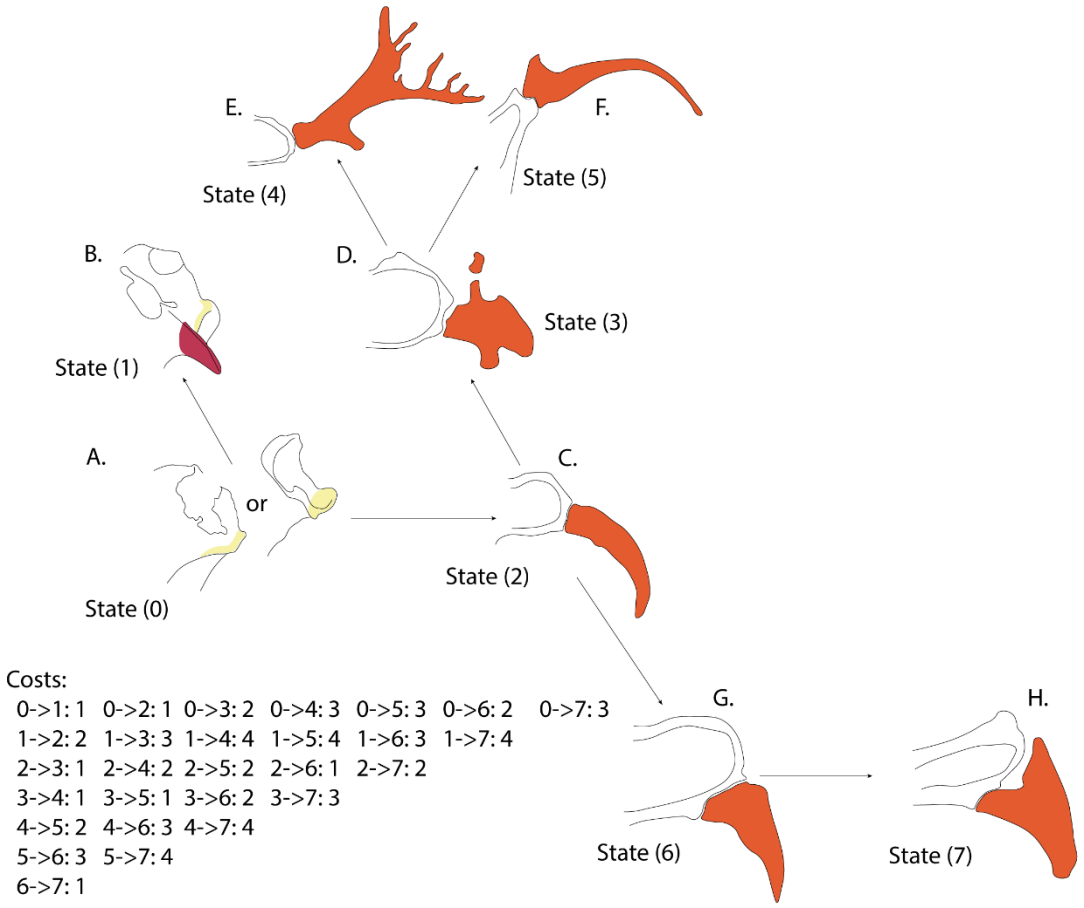

Figure S15. Enforced path using the "cstree" command on TNT for state evolution on character 23. Arrows indicate the allowed transformation path initiating for the state [0], each stop on a state increases one step. A. *Dalatias licha* (Bonnaterre, 1788) (HUMZ 74603) (redrawn and modified from Shirai, 1992: plate 8c). A'. *Lamna nasus* (Bonnaterre, 1788) (AMNH FF 20426) (redrawn and modified from Maisey and Springer, 2013: text-fig. 2b); B. *Chlamydoselachus anguineus* Garman, 1884 (redrawn and modified from Allis, 1923: plate 9, fig. 11); C. *Aptychotrema vincentiana* (Haacke, 1885) (CSIRO 101, https://sharksrays.org/, accessed on 20 Oct. 2023); D. *Platyrhinoidis triseriata* (Jordan and Gilbert, 1880) (MNHN 3211); E. *Narcine brasiliensis* (Olfers, 1831) (AMNH 77069, https://sharksrays.org/, accessed on 20 Oct. 2023); F. *Torpedo fuscomaculata* Peters, 1855 (USNM, https://sharksrays.org/, accessed on 20 Oct. 2023); G. *Rhinobatos productus* (Ayres, 1854) (CNPE-IBUNAM 17829); H. *Rhynchobatus springeri* Compagno and Last, 2010 (HO 180) (https://sharksrays.org/, accessed on 20 Oct. 2023).

Scoring: The scoring of character 23 (Figure S15) follows the homologies proposed by Holmgren (1940, 1941) and de Carvalho and Maisey (1996) considering the ectethmoid process of *Chlamydoselachus anguineus* Garman, 1884 (indicated by Allis, 1923: plate 7, fig. 7) equivalent to the antorbital cartilage (antorbital process) of *Heptranchias perlo* (Bonnaterre,

1788) (Holmgren, 1941: text-fig. 4) and the membranous "antorbital cartilage" of squaloid sharks. However, the "ectethmoid process" of squaloid sharks is not homologous to the "ectethmoid process" in the same sense as that of *Chlamydoselachus anguineus* Garman, 1884 but corresponds to that ventral part of the antorbital frame from which the "ectethmoid process" originates. Therefore, the ectethmoid process is the process-like ventral border of the antorbital ridge (Holmgren, 1941: p. 7). The revision of fossil material from the Late Jurassic revealed that some batoids genera lack antorbital cartilages (e.g., †*Belemnobatis* Thiollière, 1852), while some possess them (e.g., †*Asterodermus* Agassiz, 1836). This seems to support that the absence of mineralization antorbital cartilages is the primitive state for neoselachians (crown elasmobranchs) and the mineralization of the structures is derived state. However, the putative homology between the denser antorbital process of *Pristiophorus* Müller and Henle, 1837 and the antorbital cartilage of Rajiformes inferred by de Carvalho and Maisey (1996) (by coding both within the same character state: Char. 16, state 2) as well as the differentiated state recognized by de Carvalho (1996) for *Pristiophorus* (Char. 8, state 2) are not recognized in the present work, because in the end it indicates a lack of mineralization of the antorbital process, which is the same process observed in other squalid sharks (Holmgren, 1941: p. 113, text-fig. 68) "The triangular process has two high longitudinal ridges, the ventral connecting it with the infraorbital sensory line, the lateral, with the eyebrow area. A third short anterior dorsal ridge connects with the sclera of the eye. In future development, the process becomes ligamentous and thus disappears as a skeletal element in *Squalus* Linnaeus, 1758. In the rays, as will be shown later, it becomes the so-called antorbital cartilage or fin-supporting cartilage, which is thus not a part of the ectethmoid process in *Squalus*". For the present work, the presence of a dense connective tissue process connecting the posterior part of the nasal capsule and the border of the rostrum is interpreted as a shared feature of sawsharks (*Pristiophorus* and *Pliotrema* Regan, 1906), possibly related to the support of the elongated rostrum, rather than indicative of a close common ancestry with batomorphs (i.e., hypnosqualean hypothesis).

24. Subnasal fenestra: [0] absent, [1] present. †*Ptychodus***[?]**. Klug (2010, Char. 5), de Carvalho (1996, Char. 6), de Carvalho and Maisey (1996, Char. 6), Shirai (1996, Char. 7), **Shirai (1992, Char. 15)**.

25. Sup_Epiphyseal foramen: [0] absent, [1] present. †*Ptychodus***[?]**. Goto (2001, Char. 10)**, Jambura *et al*., (2023, Char. 26)**.

26. Sub_Epiphyseal foramen: [0] isolated, [1] fused with prefrontal fontanelle. †*Ptychodus***[?]**. Goto (2001, Char. 10), **Jambura *et al*. (2023, Char. 27**).

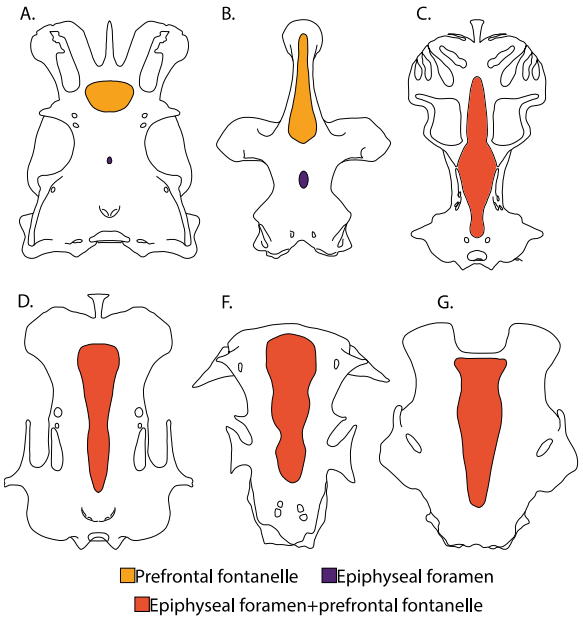

Figure S16. Line drawings of the character states recognized for character 26. A. *Orectolobus ornatus* (De Vis, 1883) (AMS 114236) (redrawn from Goto, 2001: text-fig. 9c). B. *Trygonorrhina fasciata* Müller and Henle, 1841 (MCZ 982S) (redrawn from McEachran *et al*. 1996: text-fig. 7). C. *Parascyllium ferrugineum* McCulloch, 1911 (HUMZ 131588) (redrawn from Goto, 2001: text-fig. 11c). D. *Ginglymostoma cirratum* (Bonnaterre, 1788) (ZMUC P0629) F. *Gymnura japonica* (Temminck and Schlegel, 1850) (HUMZ 4830) (redrawn from Nishida, 1990, text-fig 15A), G. *Rhinoptera javanica* Müller and Henle, 1841 (HUMZ 97698) (redrawn from Nishida, 1990, text-fig 17A). **State [0]:** A-B. **State [1]:** C-G.

Remarks: Following Jambura *et al*. (2023, Chars. 28–29) observations, character 29 is considered a subordinate of character 28. The expanded state of the epiphyseal foramen refers to the fusion of the prefrontal fontanelle and the epiphyseal foramen (figure S16 A-B and D-F); this fusion is also referred to as fontanelle by Nishida (1990) and occurs in several myliobatiform groups.

27. Supraotic shelf: [0] narrow, [1] broad. †*Ptychodus***[?]**. Frey *et al*. (2020, Char. 161)

28. Sup_Supraorbital crest: [0] absent, [1] present. †*Ptychodus***[?]**. Villalobos-Segura *et al*. (2022, Char. 20), Achliman *et al*. (2012, Char. 34), McEachran *et al*. (1996, Char. 26), **Nishida (1990, Char. 32)**.

29. Sub_Preorbital process (supraorbital crest): [0] absent, [1] present. †*Ptychodus***[?]**. (Modified from Villalobos-Segura *et al*. (2022, Char. 13), Aschliman *et al*. (2012, Char. 33), de Carvalho and Maisey (1996, Char. 16), McEachran *et al*. (1996, Char. 25), Shirai (1992, Char. 33 & 34 & 35), Nishida (1990, Char. 17).

Remarks: See character 19 (figure S14A-C).

30. Occipital crest: [0] absent, [1] present separated from the brain cavity by the otic occipital fissure, **[2]** present but with otic occipital fissure absent. New.

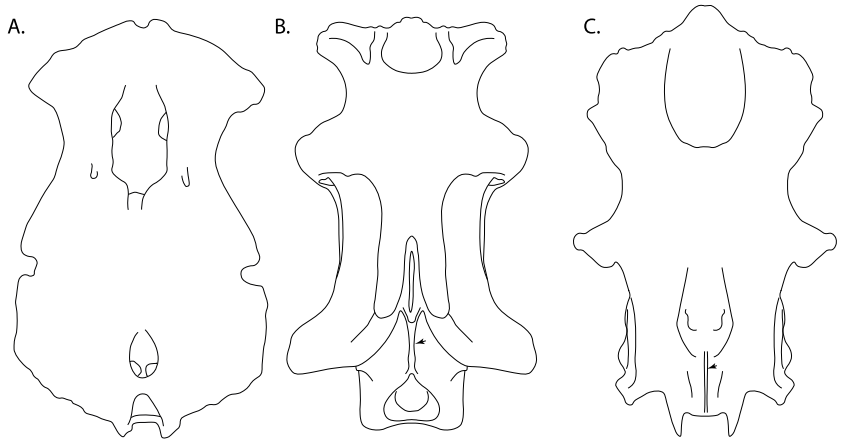

Figure S17. Line drawings of the character states recognized for character 30. A. *Heterodontus francisci* (Girard, 1855) (AMNH 217862) (redrawn from de Carvalho, 1996: text-fig. 6a). B. †*Xenacanthus* sp. (MCZ 13388) (redrawn and modified from the composite restoration of Schaeffer, 1981: text-figs. 3, 5-6). C. *Notorynchus cepedianus* (Péron, 1807) (drawn from Maisey, 2004: text-fig. 3). **State [0]**: A. **State [1]**: B. **State [2]**. C. Arrows indicate the occipital crest.

Remarks: Based on Schaeffer (1981) observations on Xenacanthiformes, which present an occipital crest posterior to the dorsal otic foramen and the otico occipital fissure [1] (figure S17B). An occipital crest is also present in some modern shark groups [2] (figure S17C) (e.g., *Hexanchus* Rafinesque, 1810, *Heptranchias* Rafinesque, 1810, *Notorhynchus* Ayres, 1855, *Pseudocarcharias* Cadenat, 1963, *Isurus* Rafinesque, 1810 and *Carcharodon* Smith in Müller and Henle, 1838).

31. Sup_Basicranial processes: [0] absent, [1] present. †*Ptychodus***[?]**. Modified from Villalobos-Segura *et al*. (2022, Chars. 40–41), de Carvalho and Maisey (1996, Char. 3), Shirai (1992, Char. 44). See figure S18.

32. Sub_Basicranial processes (position): [0] trabecular, [1] polar. †*Ptychodus***[?]**. Villalobos-Segura *et al*. (2022, Chars. 40–41), de Carvalho and Maisey (1996, Char. 3), Shirai (1992, Char. 44). See figure S18.

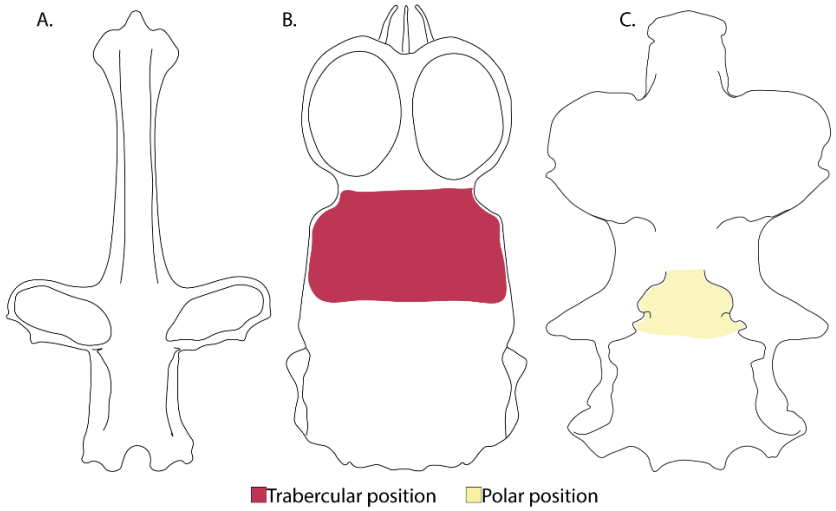

Figure S18. Line drawings of the character states recognized for characters 31-32. A. *Rhinobatos glaucostigma* Jordan and Gilbert, 1883 (CNPE-IBUNAM 17810). B. *Scyliorhinus cabofriensis* Soares *et al*., 2016 (AC.UERJ 2231.4) (redrawn from Soares *et al*. 2016: text-fig. 7b). C. *Squalus acanthias Linnaeus*, 1758 (redrawn from Shirai, 1992: text-fig. 5.1b). **Character 31: State [0]**: A. **State [1]**: B-C. **Character 32 State [0]**: B. **State [1]**: C.

33. Sup_Postorbital process: [0] present, **[1]** absent. Modified from Villalobos-Segura *et al*. (2022, Char. 27)**,** Claeson *et al*. (2013, Char. 12), McEachran and Aschliman (2004, Char. 32), Brito and Seret (1996, Char. 7), **Nishida (1990, Char. 35)**.

34. Sub: Postorbital process: [0] separated from triangular, **[1]** fused with triangular process. Villalobos-Segura *et al*. (2022, Char. 29)*, Aschliman *et al*. (2012, Char. 37), **McEachran *et al*. (1996, Char. 29)**.

35. Sub: Postorbital process: [0] projects laterally, [1] projects ventrolaterally. (Villalobos-Segura *et al*. (2022, Char. 30), Aschliman *et al*. (2012, Char. 38), **McEachran *et al*. (1996, Char. 30)**.

36. Lateral commissure: [0] Forms part of the postorbital arcade, [1] absent, due to the lack of spiracular cartilages and hyoid arch with not supporting connection with the mandibular arch, [2] lateral commissure is not fully chondrified not enclosing the foramen prooticum, **[3]** reduced, [4] continuous and strong enclosing the foramen prooticum, [5] narrow and situated behind the foramen prooticum in close relation to the hyomandibular fossa. †*Ptychodus***[?]**. New. See figure S19.

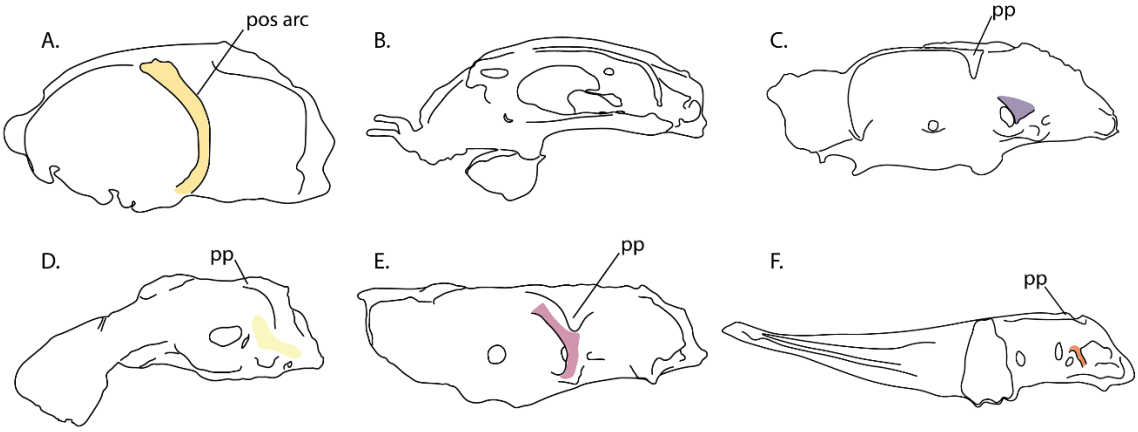

Figure S19. Line drawings of the character states recognized for character 36. A. Idealized symmoriiform (mainly based on ‘‘*Cobelodus*’’, but with ethmoid region after †*Stethacanthus* Newberry, 1889 and †*Falcatus* Lund, 1985, (redrawn from Maisey, 2007: text-fig. 2a) postorbital arcade marked in yellow. B. *Callorhynchus* Lacepède, 1798 (redrawn from de Beer and Moy-Thomas, 1935: text-fig.1). C. *Dalatias licha* (Bonnaterre, 1788) (HUMZ 74603) (redrawn from Shirai, 1992: plate 8c), lateral commissure marked in purple. D. *Heterodontus zebra* (Gray, 1831) (HUMZ 37666) (redrawn from Shirai, 1992: plate 16c) lateral commissure area marked in yellow. E. *Oxynotus bruniensis* (Ogilby, 1893) (HUMZ 91383) (redrawn from Shirai, 1992: plate 7c), lateral commissure marked in purple. F. *Rhinobatos lentiginosus* (Garman, 1880) (redrawn from https://sharksrays.org/), lateral commissure marked in purple. **State [0]**: A. **State [1]**: B. **State [2]**: C. **State [3]**: D. **State [4]**: E. **State [5]:** F.

37. Jugular canal diameter: [0] small, [1] large, [2] canal absent**.** †*Ptychodus***[?]**. Pradel *et al*. (2011), **Frey (2020, Char. 126)**.

38. Hyomandibular fossa: [0] posterior part of the otic region, [1] anteriorly situated in the otic region. †*Ptychodus***[?]**. (de Carvalho (1996, Char. 13), Goto (2001, Char. 7a), Shirai (1996, Char. 17), **Shirai (1996, Char. 1).**

39. Hyomandibular fossa: [0] not composed of two horizontally divided cavities, [1] fossa with cavities as such. †*Ptychodus***[?]**. Landemaine *et al*. (2018, Char. 13), Klug (2010, Char. 13), Char. 18 Shirai (1996), **Char. 14 de Carvalho (1996)**, de Carvalho and Maisey (1996, Char. 29), Shirai (1996, Char. 54).

40. Concavity ventral to hyomandibular fossa: [0] absent, [1] present. †*Ptychodus***[?]**. Landemaine *et al*. (2018, Char. 14), Klug (2010, Char. 14), **de Carvalho (1996, Char. 15)**, de Carvalho and Maisey (1996, Char. 26), Shirai (1996, Char. 19), Shirai (1996, Char. 51).

41. Dorsal otic ridge: [0] absent, [1] present. **Frey *et al*. (2020, Char. 162)**.

42. Lateral otic process: [0] absent, [1] present. Schaeffer (1981); Coates and Sequeira (1998), Brazeau (2009); Davis *et al*. (2012); Zhu *et al*. (2013), **Frey *et al*. (2020, Char. 138)**.

43. Postotic process: [0] absent, **[1]** present. **Frey *et al*. (2020, Char. 141)**.

44. Jugal arch: [0] absent, [1] present. †*Ptychodus***[?]**. Villalobos-Segura *et al*. (2022, Char. 22), Aschliman *et al*. (2012, Char. 39), **McEachran *et al*. (1996, Char. 31)**.

45. Stapedial arch: [0] absent, [1] present. †*Ptychodus***[?]**. Shimada (2005, Char. 22). Originally, Shimada (2005) coded the stapedial foramina. We instead coded the process

surrounding the foramina because it might be easier to be observed in fossil taxa. See figure S20.

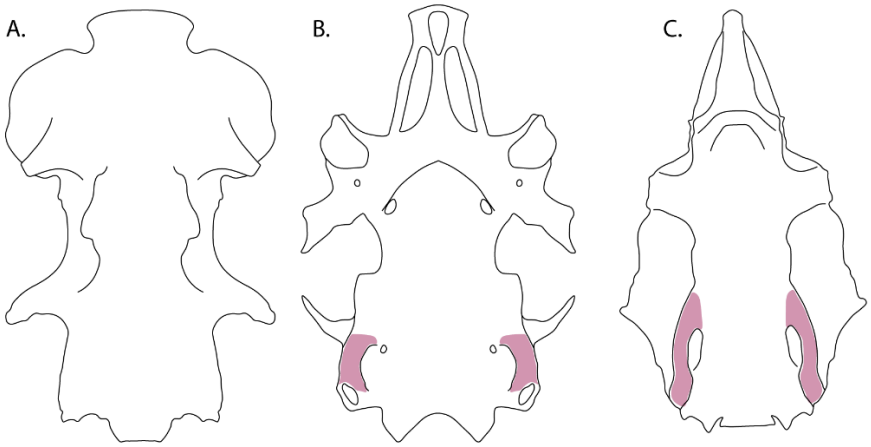

Figure S20. Line drawings of the character states recognized for character 45. A. *Chlamydoselachus anguineus* Garman, 1884 (MSM-88-40), (redrawn and modified from Shirai, 1992: plate 1b). B. *Carcharhinus falciformis* (Bibron in Müller and Henle, 1841) (AC.UERJ 1456), (redrawn from de Oliveira Lana, 2021: text-fig.1b). C. *Isurus oxyrhinchus* Rafinesque, 1810 (LJVC-0216), (redrawn from Compagno, 1990b: plate 6k). State [0]: A. State [1]: B-C. Stapedial arch marked in purple.

46. Entrance of internal carotids: [0] through a common opening at the central midline of the basicranium, [1] through separate openings flanking the hypophyseal opening or recess. †*Ptychodus***[?]**. Modified from Frey *et al*. (2020, Char 116).

Remarks: This character is simplified, because in modern elasmobranch groups the hypophyseal foramen is missing or not separated from the openings for the internal carotids.

47. Canal for dorsal aorta and/or lateral dorsal aortae: [0] runs inside the neurocranium, **[1]** runs external, no groove and enters brain, [2] runs externally and does not enter the brain directly, [3] runs external, has a groove, and enters brain. Coates *et al*., (2017, Char. 117), a subsequent character was included to add variation observed in some hybodonts**)**.

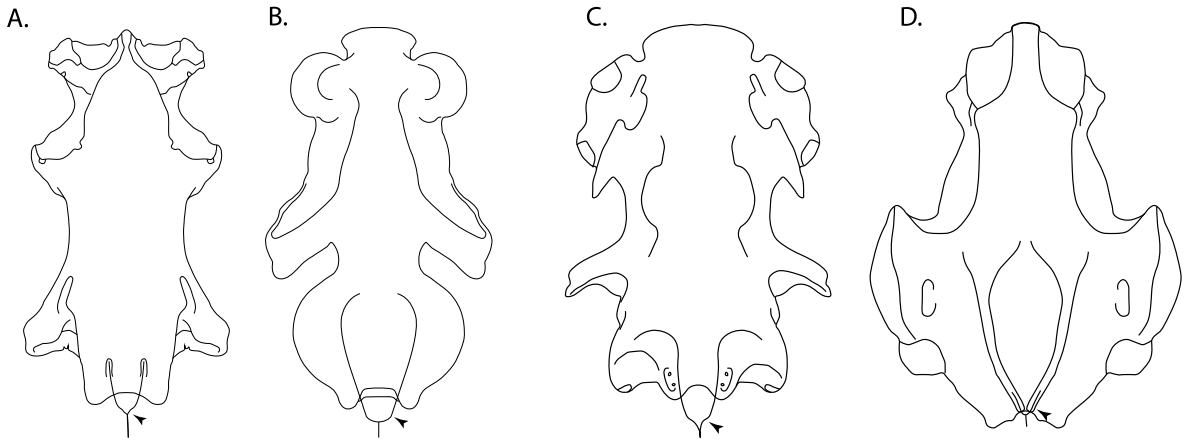

Figure S21. Line drawings of the character states recognized for character 47. A. †*Xenacanthus* Beyrich, 1848 (redrawn from Schaeffer, 1981: text-fig. 12a). B. †*Cobelodus aculeatus* (Cope, 1894) (FMNH 7472), (redrawn from Schaeffer, 1981: text-fig. 13b). C. *Chlamydoselachus anguineus* Garman, 1884 (redrawn from Schaeffer, 1981: text-fig. 13c). **State [0]**: A. **State [1]**: B-C. Arrows indicate the dorsal aorta.

Remarks: These characters are based on Coates *et al*. (2017, Char. 117), with a subsequent character, included adding the variation observed in some fossil taxa, where the lateral dorsal aorta are fitted in a deep groove (see Maisey, 1987: text-figs. 5 and 7) (figure S21D).

48. Dorsal aorta divides into lateral dorsal aorta: [0] posterior to occipital level, [1] anterior to level of the occiput. †*Ptychodus***[?].** Pradel *et al*. (2011), Giles *et al*. (2015), Coates *et al*. (2017), Frey *et al*. (2020, Char 176)

49. Basal angle of the neurocranium: [0] absent, [1] present. †*Ptychodus***[?]**. Landemaine *et al*. (2018, Char. 35), Klug (2010, Char. 35(24)), Goto (2001, Char. 4a), de Carvalho and Maisey (1996, Char. 22), Shirai (1992, Char. 47).

50. Metotic (otic-occipital) fissure: [0] absent, [1] present. **Frey *et al*. (2020, Char. 169)**.

51. Space for forebrain and at least proximal portion of olfactory tracts narrow and elongate extending between orbits: [0] absent, [1] present. **Frey *et al*. (2020, Char. 169)**.

52. Orbitonasal lamina expanded: [0] absent, [1] present. **Frey *et al*. (2020, Char. 105)** also see Patterson (1965).

53. Ophthalmic foramen in anterodorsal extremity of orbit communicates with enclosed cranial space: [0] absent, [1] present. **Frey *et al*. (2020, Char. 113)**.

54. Orbit vs otic capsule: [0] orbit smaller than otic capsule, [1] obit larger than otic capsule. **Frey *et al*. (2020, Char. 122)**.

55. Orbital artery foramen: [0] absent, [1] present. †*Ptychodus***[?]**

56. Canal, likely for trigeminal nerve (V) mandibular ramus, passes through the postorbital process from proximal dorsal entry to distal and ventral exit: [0] absent, [1] present**. Frey *et al*. (2020, Char. 127)**. See figure S22.

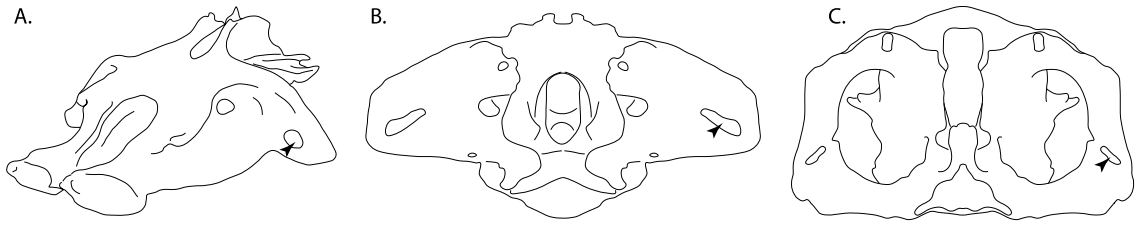

Figure S22. Line drawings of the "present" state recognized in character 56. A. †*Tristychius arcuatus* Agassiz, 1837 (redrawn from Coates and Tietjen, 2018: text-fig. 3e). B. †*Cladodoides* Jaekel, 1921 (redrawn from Maisey, 2005: text-fig. 8a). C. ''*Cobelodus''* (FMNH PF 13242), (redrawn from Maisey, 2007: text-fig. 10). **State [1]:** A-C. Arrows indicate the dorsal aorta the mandibular ramus of trigeminal nerve.

57. Trigemino-facial recess: [0] absent, [1] present. †*Ptychodus***[?]**. Goodrich (1930); Gardiner (1984); Pradel (2010); Pradel *et al*. (2011); Davis *et al*. (2012). **Frey *et al*. (2020, Char. 130).**

Remarks: The acustico-trigemino-facial recess was defined by Allis (1914, 1923) as an internal recess located immediately anterior to the otic capsule within the prefacial commissure and containing the roots of the trigeminal, facial and abducens nerves. The ganglia of the trigeminal and facial nerves lie partly in this recess and partly in the trigemino-pituitary fossa for the trigeminal one. The prootic foramen is situated in a depression in the internal wall of the endocranial cavity, which was probably housed at least part of the trigeminal ganglion. An acustico-trigemino-facial recess, or at least a trigemino-facial recess (containing only the facial and trigeminal foramina), is present in neoselachians and probably in some Palaeozoic elasmobranchs, such as †*Cladodoides* (Maisey 2005). In extant chimaeroids, it seems to be absent (Jollie 1962: fi gs 5-19D; Maisey *et al*., 2019) since there is no evidence of a prefacial commissure and the ganglia for trigeminal and facial nerves lie within the prootic foramen and the trigemino-pituitary fossa.

58. C-bout notch separates postorbital process from supraotic shelf: [0] absent, [1] present. **Frey *et al*. (2020, Char. 132).** See figure S23.

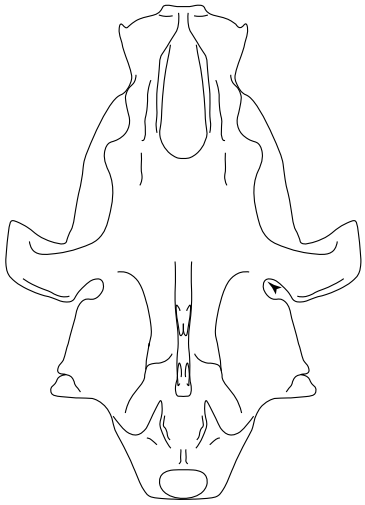

Figure S23. Line drawing of the "present" state recognized in character 58. A. †*Tristychius arcuatus* Agassiz, 1837 (redrawn from Coates and Tietjen, 2018: text-fig. 3a). **State [1]:** A. Arrows indicate the position of the C-bout notch.

59. Periotic process: [0] absent, [1] present. †*Ptychodus***[?].** Maisey (2007), Coates *et al*. (2017). **Frey *et al*. (2020, Char. 134).**

60. Hyomandibula articulates with neurocranium beneath otic shelf: [0] absent, [1] present. †*Ptychodus***[?]**. **Frey *et al*. (2020, Char. 139).**

61. Sub-otic occipital fossa: [0] absent, [1] present. †*Ptychodus***[?]. Frey *et al*. (2020, Char. 140).**

62. Otic capsule extends posterolaterally relative to occipital arch: [0] absent, **[1]** present. Maisey (1985). **Frey *et al*. (2020, Char. 144).**

63. Endocranial roof anterior to otic capsules domelike, smoothly convex dorsally and anteriorly: [0] absent, [1] present. **Frey *et al*. (2020, Char. 145).**

64. Roof of skeletal cavity for cerebellum and mesencephalon significantly higher than dorsal-most level of semicircular canals. [0] absent, [1] present**. Frey *et al*. (2020, Char. 146).**

65. Labyrinth cavity separated from the main neurocranial cavity: [0] by a cartilaginous or ossified capsular wall, [1] skeletal medial capsular wall absent. Pradel *et al*. (2011), Davis *et al*. (2012), Zhu *et al*. (2013). **Frey *et al*. (2020, Char. 148).**

66. Sinus superior: [0] absent or indistinguishable from union of anterior and posterior canals, [1] present, elongate and nearly vertical. †*Ptychodus***[?].** Davis *et al*. (2012), Zhu *et al*. (2013). **Frey *et al*. (2020, Char. 155).**

Remarks: Maisey (2005) noted several similarities of the otic region between †*Tribodus* Brito and Ferreira, 1989, †*Egertonodus* Maisey, 1987, and neoselachians, which include the absence of a crus commune and a sinus superior. Consequently, this state was generalized to all extant neoselachian species, while fossil species were scored as undetermined (?). Regardless, fossil species within neoselachians would be optimized as absent (0), considering that the most common state within the neoselachian clade is the absence of the sinus superior.

67. External opening for endolymphatic ducts: [0] posterior to crus commune, [1] anterior to crus commune. †*Ptychodus***[?].** Coates *et al*. (2017). **Frey *et al*. (2020, Char. 160).**

68. Sup Endolymphatic fossa: [0] absent, **[1]** present. **Frey *et al*. (2020, Char. 164).** See figure S24.

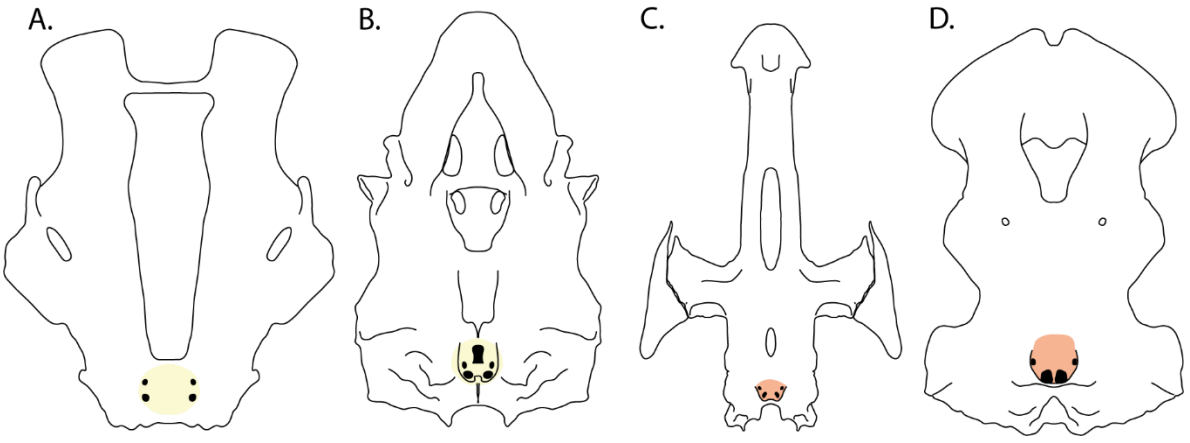

Figure S24. Line drawings of the character states recognized for characters 68. A. *Rhinoptera javanica* Müller and Henle, 1841 (HUMZ 97698), (redrawn from Nishida, 1990: text-fig. 17a), B. *Lamna nasus* (Bonnaterre, 1788) (AMNH FF 20426), (based on Maisey and Springer, 2013: text-fig. 1c). C. *Rhynchobatus djiddensis* (Forsskål in Niebuhr, 1775) (HUMZ 6135) (redrawn from Shirai, 1992: text-fig. 15a). D. *Heterodontus zebra* (Gray, 1831) (HUMZ 37666), (redrawn from Shirai, 1992: text-fig. 16a). **State [0]**: A absent, does not form a sunken endolymphatic fossa, marked in yellow. **State [1]**: C-D present, sunken endolymphatic fossa, marked in orange.

69. Sub Endolymphatic fossa elongate (slot-shaped), dividing dorsal otic ridge along midline: [0] absent, [1] present. **Frey *et al*. (2020, Char. 165).** See figure S25.

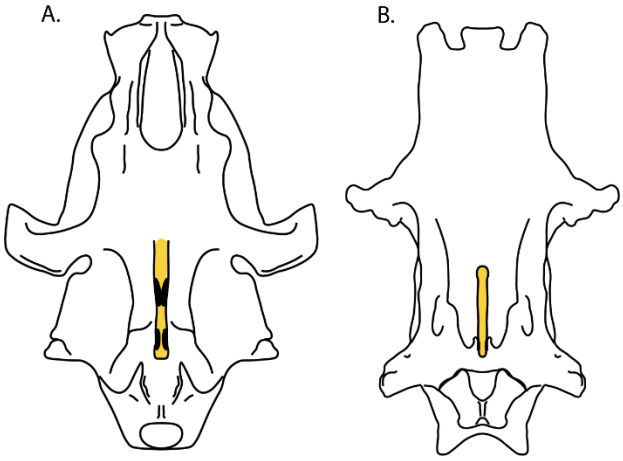

Figure S25. Line drawings of the "present" state recognized in character 69. A. †*Tristychius arcuatus* Agassiz, 1837 (redrawn from Coates and Tietjen, 2018: text-fig. 3a). B. †*Xenacanthus* Beyrich, 1848 (redrawn from Schaeffer, 1981: text-fig. 5). **State [1]**: A- B. Endolymphatic fossa marked in yellow.

70. Perilymphatic fenestra: [0] un-calcified, [1] separate opening form the endolypmphatic fenestra, [2] common opening with the endolypmphatic fenestra, [3] posterior to the anterior pair of small rounded endolymphatic foramina. †*Ptychodus***[?].** Pradel *et al*. (2011); Coates *et al*. (2017). **Frey *et al*. (2020, Char. 166).** See figure S26.

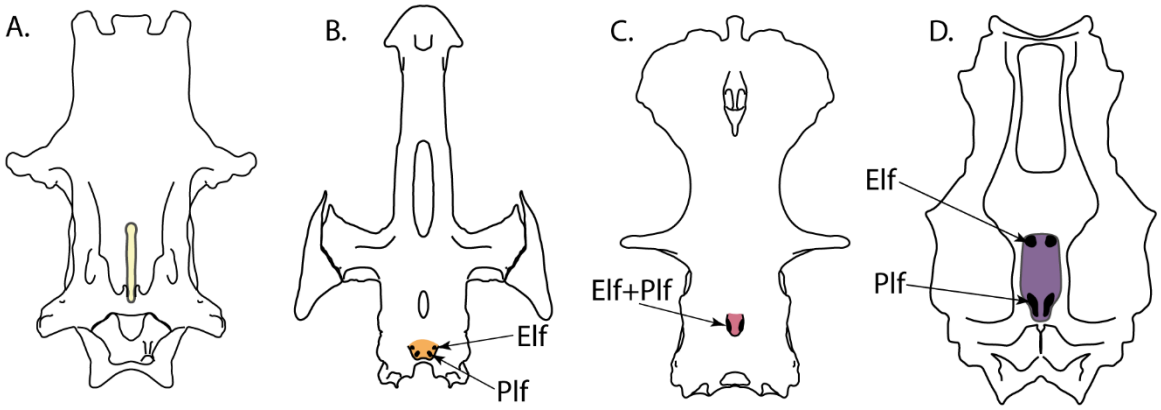

Figure S26. Line drawings of the states recognized in character 70. A. †*Xenacanthus* Beyrich, 1848 (redrawn from Schaeffer, 1981: text-fig. 5). B. *Rhynchobatus djiddensis* (Forsskål in Niebuhr, 1775) (HUMZ 6135) (redrawn from Shirai, 1992: text-fig. 15a). C. *Dalatias licha* (Bonnaterre, 1788) (HUMZ 74603). D. †*Egertonodus basanus* (Egerton, 1844) (NHM P. 60110) (redrawn from Maisey and Lane, 2010: text-fig. 8b). **State [0]**: A, endolymphatic fossa marked in yellow with no recognizable perilymphatic fossa. **State [1]**: B, endolymphatic fossa, marked in orange with the perilymphatic and edolymphatic fenestras. **State [2]**: C, endolymphatic fossa, marked in red with the perilymphatic+edolymphatic fenestra. **State [3]**: D, endolymphatic fossa, marked in purple with the perilymphatic fenestra behind the pair of small rounded endolymphatic foramina.

71. Hypotic lamina: [0] absent, **[1]** present. Schaeffer (1981); Maisey (1984, 2001); Brazeau (2009); Pradel *et al*. (2011, 2013); Davis *et al*. (2012); Zhu *et al*. (2013), Coates *et al*. (2017) and Maisey *et al*. (2019) **Frey *et al*. (2020, Char. 171)**.

72. Glossopharyngeal nerve path: [0] directed posteriorly and exits through metotic fissure or foramen in posteroventral wall of otic capsule, **[1]** exits laterally through a canal contained ventrally (floored) by the hypotic lamina, [2] exits through a foramen anterior to the posterior ampulla. **Coates *et al*. (2017, Char. 115).**

Remarks: One of the character states described by Coates *et al*. (2017: "directed laterally, across the floor of the saccular chamber and exits via foramen inside the wall of the otic capsule") was removed from the analysis as none of the terminals included in the present analysis presents it.

73. Glossopharyngeal and vagus nerves share common exit from neurocranium: [0] absent, [1] present. †*Ptychodus***[?]. Frey *et al*. (2020, Char. 173).**

74. Basicranial morphology: [0] platybasic, [1] tropibasic. †*Ptychodus***[?]. Frey *et al*. (2020, Char. 77).**

75. Ventral portion of occipital arch wedged between rear of otic capsules: [0] absent, **[1]** present. **Frey *et al*. (2020, Char. 174).**

76. Dorsal portion of occipital arch wedged between otic capsules: [0] absent, **[1]** present. **Frey *et al*. (2020, Char. 178).**

77. Antimeres of upper and lower jaws: [0] separated, [1] fused. Villalobos-Segura *et al*. (2022, Char. 78), Frey *et al*., (2020, Char. 99)**,** Aschliman *et al*. (2012, Char. 40), **McEachran *et al*. (1996, Char. 32)**.

78. Sup Craniopalatine articulation: [0] absent, **[1]** present. Landemaine *et al*. (2018, Char. 47), Klug (2010, Char. 47(35), **Shirai (1996, Char. 11)**.

79. Sub Craniopalatine articulation (Fusion): [0] fused, **[1]** articulated. **Frey *et al*. (2020, Char. 92).**

80. Sub Craniopalatine articulation (articulation): [0] ethmoidal, [1] orbitostylic, [2] palatine and ethmoidal, [3] grooved in ethmoidal region. Landemaine *et al*. (2018, Char. 47), Klug (2010, Char. 47(35)), Goto (2001, Char. 2a), de Carvalho and Maisey (1996, Char. 20), **Shirai (1996, Char. 11), Shirai (1996, Char. 43).**

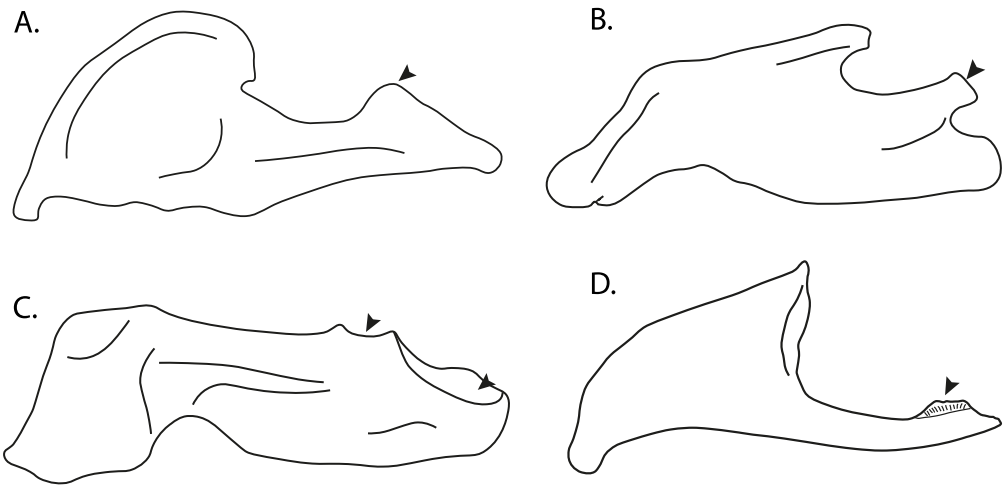

Figure S27. Line drawings of the states recognized in character 80. A. †*Dracopristis hoffmanorum* Hodnett *et al*. 2021 (NMMNH P-68537) (redrawn from Hodnett *et al*., 2021: text-fig. 4d). B. *Pristiophorus nudipinnis* Günther, 1870 (FSFL-EA 735) (redrawn from Shirai, 1992: plate 26f). C. †*Hybodus hauffianus* Fraas, 1896 (redrawn from Maisey, 1982, text-fig 7A). D. †*Cobelodus aculeatus* (Cope, 1894) (FMNH PF 7347) (redrawn from Hodnett *et al*., 2021: text-fig. 4d). **State [0]**: A. **State [1]**: B. **State [2]**: C. **State [3]**: D. Arrows indicate the articulation points with the cranium.

Remarks: Characters 79 and 80 are considered subordinates of 78. Character 79 includes two of the characters of Jambura *et al*., 2023 (Chars. 48 and 49). The placement of these two characters as states of a single character follows that the ethmoidal and orbitostylic are both types of craniopalatine articulations. Two additional states were included as hybodonts palatoquadrate articulation is much more complex than previously thought, with articulation points in the ethmoidal and orbital regions (including an orbital process). In Palaeozoic groups, the articulation seems grooved and occurs in the ethmoidal region (figure S27D). Previous scoring without step matrices created illogical character reconstructions for batomorphs, because they lack a craniopalatine articulation. A similar case is related to the fusion of the palatoquadrate and neurocranium in holocephalians. It is possible that some extinct batomorph could have presented a type of craniopalatine articulation. However, none of the recovered Jurassic remains shows evidence of this. Ultimately, the use of reductive coding for these and characters 78–80 is proposed to counter the reconstructions of an ancestral state for batomorphs that could be affected by the terminal composition of the analysis, in which the most distributed state is often considered the plesiomorphic state.

81. Jaw articulation located on rearmost extremity of mandible: [0] absent, [1] present. Davis *et al*. (2012), Zhu *et al*. (2013), **Frey *et al*. (2020, Char. 95)**.

82. Postorbital articulation: [0] absent, [1] lateral, [2] dorsal. **Villalobos-Segura *et al*. (2022, Char. 17)**, Klug (2010, Char. 11), de Carvalho (2004, Char. 12), **de Carvalho and Maisey (1996, Char. 15)***, Shirai (1996, Char. 14), **Shirai (1996, Char. 32).**

Remarks: An extra character state was included to incorporate Maisey (2008) observations on Palaeozoic cartilaginous fishes postorbital articulation.

83. Oblique ridge or groove along medial face of palatoquadrate: [0] absent, **[1]** present. **Frey *et al*. (2020, Char. 88).**

84. Large otic process of the palatoquadrate: [0] absent, **[1]** present, [2] present, forming a quadrate flange**. Villalobos-Segura *et al*. (2022, Char. 19)**.

Remarks: An additional character state was included following Maisey (2008) observations regarding the downturned postorbital process as part of the palatoquadrate observed in hybodonts.

85. Meckel's cartilage: [0] not expanded medially, [1] expanded medially. Villalobos-Segura *et al*. (2022, Char. 79), Aschliman *et al*. (2012, Char. 41), **McEachran *et al*. (1996, Char. 33).**

86. Winglike process on Meckel's cartilage: [0] absent, [1] present. Villalobos-Segura *et al*. (2022, Char. 80)**,** Aschliman *et al*. (2012, Char. 42)**,** McEachran *et al*. (1996, Char. 34), **Nishida (1990, Char. 86).**

87. Sustentaculum: [0] absent, [1] present. **Jambura *et al*. (2023, Char. 57)**.

Remarks: This character refers to the processes in the Meckel's cartilage in some Orectolobiformes and Torpediniformes.

88. Quadratomandibularis process: [0] absent, [1] present. New.

Remarks: This character is proposed to incorporate the presence of an articulation process in the quadrate portion for the constrictor dorsalis, constrictor hyoideous dorsalis and spiracularis muscle, present in several neoselachians (figure S28B-F), which seems to be less pronounced and occupying less of the palatoquadrate in comparison with the otic process (figure S28A) (see character matrix or character optimization).

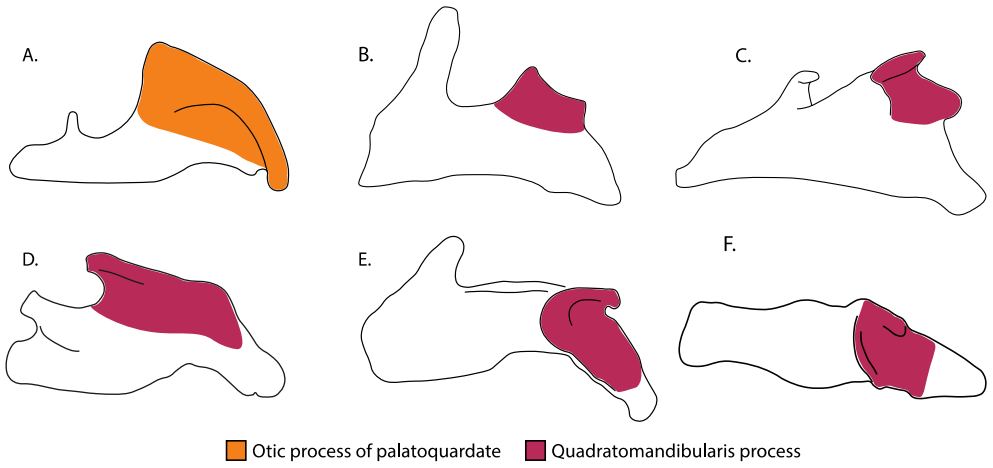

Figure S28. Line drawings of the states recognized in character 88. A. *Heptranchias perlo* (Bonnaterre, 1788) (AMNH YP Teaching Coll. no. AA 4-7) (redrawn from Maisey, 1986: text-fig. 4c). B. *Etmopterus granulosus* (Günther, 1880) (HUMZ 91316) (redrawn from Shirai, 1992: plate 4c), C. *Dalatias licha* (Bonnaterre, 1788) (HUMZ 74603) (redrawn from Shirai, 1992, plate 4D). D. *Pristiophorus nudipinnis* Günther, 1870 (FSFL-EA 735) (redrawn from Shirai, 1992: plate 4f). E. *Squalus acanthias* Linnaeus, 1758 (GMBL 7313) (redrawn from https://sharksrays.org/). F. *Orectolobus maculatus* (Bonnaterre, 1788) (USNM 50725) (redrawn from https://sharksrays.org/). State [0]: A. State [1]: B-F.

89. Dental trough adjacent to oral rim on Meckel's cartilage and palatoquadrate: [0] absent, [1] present. **Frey *et al*. (2020, Char. 97)**.

90. Dental trough divided, scalloped tooth-bearing margin on Meckel's cartilage and palatoquadrate: [0] absent, [1] present**.** †*Ptychodus***[?]**. **Frey *et al*. (2020, Char. 97)**.

91. Gill skeleton position: [0] posterior to the occipital region, **[1]** partly beneath otico-occipital regions. Villalobos-Segura *et al*. (2022, Char. 140), **Coates *et al*. (2017, Char. 29**).

92. Spiracularis: [0] undivided, [1] divided. †*Ptychodus***[?]**. **Villalobos-Segura *et al*. (2022, Char. 65),** Aschliman *et al*. (2012, Char. 85), McEachran *et al*. (1996, Char. 61).

93. Coracohyomandibularis: [0] single origin, [1] separate origins. †*Ptychodus***[?]**. Villalobos-Segura *et al*. (2022, Char. 68)**, Aschliman *et al*. (2012, Char. 88),** McEachran *et al*. (1996, Char. 64).

94. Hyoid arch: [0]: reduced, having no insertion of the dorsal constrictor muscle, hyoid arch well behind the jaw cartilages, **[1]** massive, holding the mandibular arch from behind, [2] composed of reduced ventral parts (ceratohyal missing) and developed hyomandibula, the latter suspending the lower jaw directly, [3] similar to State 2, but the articulation between the hyomandibula and mandible is interrupted by a ligament. [4] postorbital articulation non-suspensory, hyomadibula running dorsally to the palatoquadrate. [5] postorbital articulations present, hyomandibula suspensory (reduced) not protruding jaws.

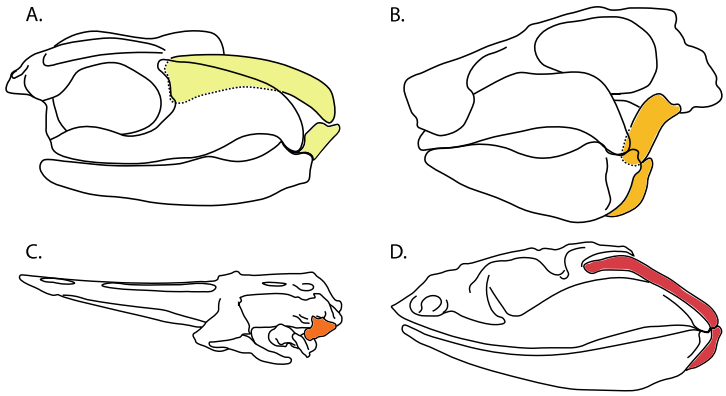

Figure S29. Line drawings of some of the states recognized in character 94. A. †*Cobelodus aculeatus* (Cope, 1894) (redrawn and modified from Zangerl and Case, 1976: text-fig. 14). B. *Heterodontus francisci* (Girard, 1855) (after Daniel, 1934; redrawn and modified from Maisey, 1980: text-fig. 6d). C. *Rhynchobatus springeri* Compagno and Last, 2010 (HO 180) (https://sharksrays.org/, accessed on 20 Oct. 2023). D. *Chlamydoselachus anguineus* Garman, 1884 (after Allis, 1923; redrawn and modified from Maisey, 1980: text-fig. 5a). **State [0]**: A. **State [1]**: B. **State [2]**: C. **State [4]**: D.

Remarks: Two extra states were added to Jambura's *et al*. 2023 scoring of Char. 62, following Compagno (1977) and Maisey (1980; 2008) observations. These two extra states are included to incorporate the variations of the jaw support in *Chlamydoselachus anguineus* Garman, 1884, *Pseudocarcharias* Cadenat, 1963 (figure S29D), †*Cobelodus* Zangerl, 1973 and Hexanchiformes (figure S29A).

95. Sup_Ceratohyal: [0] absent, **[1]** present. **Aschliman *et al*., (2012, Char. 49).**

96. Sub_Ceratohyal spatulate or bladed anteriorly: [0] absent, **[1]** present. **Frey *et al*. (2020, Char. 55).**

97. Sub Ceratohyal [0] resembling branchial arches, [1] with broad posteroventral flange or shelf projecting laterally into recess behind Meckel's cartilage, [2] expanded posteriorly with a flange projecting laterally and posteriorly fitting the posterior edge of the Meckel's cartilage. †*Ptychodus***[?]**. New. See figure S30.

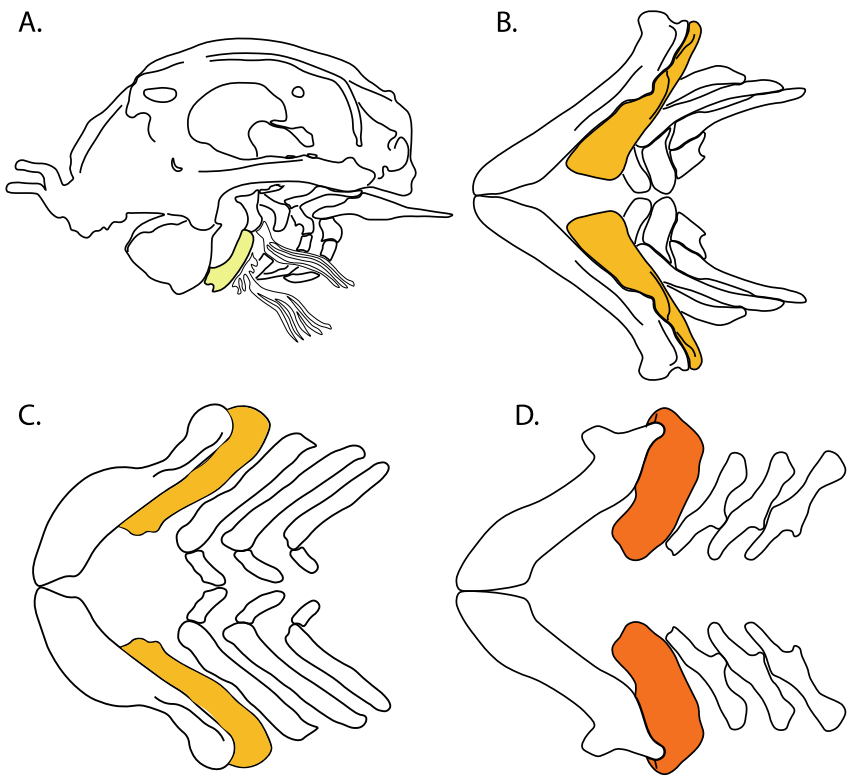

Figure S30. Line drawings of the states recognized in character 97. A. *Callorhynchus* Lacepède, 1798 (redrawn from de Beer and Moy-Thomas, 1935: text-fig. 1), ceratohyal marked in yellow. B. *Squatina nebulosa* Regan, 1906 (AMNH 258172) (redrawn from https://sharksrays.org/, accessed on 20 Oct. 2023). C. *Squalus acanthias* Linnaeus, 1758 (GMBL 7313) (redrawn from https://sharksrays.org/, accessed on 20 Oct. 2023). D. *Orectolobus maculatus* (Bonnaterre, 1788) (USNM 50725) (redrawn from https://sharksrays.org/, accessed on 20 Oct. 2023**). State [0]**: A. **State [1]**: B-C. **State [2]**: D.

98. Small cartilages associated with hyomandibular-Meckelian ligament: [0] absent, [1] present. Villalobos-Segura *et al*. (2022, Char. 75), Aschliman *et al*. (2012, Char. 47), **McEachran *et al*. (1996, Char. 38)**.

99. Hyomandibula articulates with neurocranium beneath the otic shelf: [0] absent, [1] present. †*Ptychodus***[?]**. **Frey *et al*. (2020, Char. 139)**.

100. Medial section of hyomandibula: [0] narrow, [1] expanded. Villalobos-Segura *et al*. (2022, Char. 73)**, Aschliman *et al*. (2012, Char. 44).**

101. Hypohyals: [0] absent, [1] present. **Frey *et al*. (2020, Char. 56)**.

102. Pseudohyal: [0] absent, [1] present. Villalobos-Segura *et al*. (2022, Char. 47)**, Aschliman *et al*. (2012, Char. 3)**.

103. Sup_Basihyal: [0] absent, [1] present. †*Ptychodus***[?]**. Modified from Villalobos-Segura *et al*. (2022, Char. 44)*, Villalobos-Segura *et al*. (2019, Char. 48), **Aschliman *et al*. (2012, Char. 48)**, Jambura *et al*., (2023, Char. 70).

104. Sub_Basihyal: [0] as long as broad, [1] elongated, [2] basihyal very thin (connected to ceratohyal), [3] basihyal very thin (no ceratohyal), [4] reduced. †*Ptychodus***[?]**. (Modified from

Landemaine *et al*. (2018, Char. 22 & 25), Klug (2010, Char. 22 & 25), de Carvalho (2004, Char. 65), **de Carvalho and Maisey (1996, Char. 8)**, Jambura *et al*., (2023, Char. 71)***.**

105. Sup_Segmented basibranchial: [0] absent, [1] present. †*Ptychodus***[?]**. Landemaine *et al*. (2018, Char. 131), Klug (2010, Char. 132(72)), de Carvalho (2004, Char. 22), de Carvalho and Maisey (1996, Char. 43), **Shirai (1996, Char. 32), Shirai (1996, Char. 90**).

106. Sub_Segemented basibranchial (Series): [0] anterior, [1] posterior, [2] both. †*Ptychodus***[?]**. New.

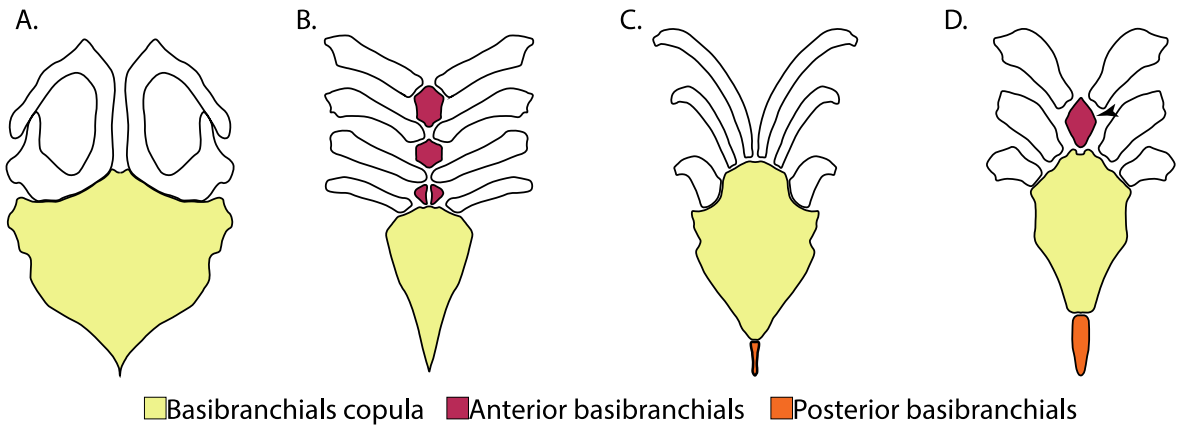

Figure S31. Line drawings of the states recognized in characters 105-106. A. *Rhinobatos hynnicephalus* Richardson, 1846 (redrawn from Nishida, 1990: text-fig. 28d). B. *Hexanchus griseus* (Bonnaterre, 1788) (HUMZ 95104) (redrawn from Shirai, 1992: plate 29c), C. *Pliotrema warreni* Regan, 1906 (RUSI 6225), (redrawn from Shirai, 1992: plate 31d), D. *Heterodontus zebra* (Gray, 1831) (HUMZ 37666) (redrawn from Shirai, 1992: plate 32d). **Character 105**: **State [0]**: A. **State [1]**: B-D. **Character 106**: **State [0]**: B; **State [1]**: C. **State [2]**: D.

Remarks: Character 106 is proposed as a subordinate of char. 105. Character 106 includes the information regarding the position of the segments of the basibranchial are located, which vary among sharks (figure S31B-D).

107. Second to last Hypobranchials direction: [0] not directed towards midline, **[1]** midline directed. **Villalobos-Segura *et al*. (2022, Char. 38)**.

Remarks: The first hypobranchial is always directed laterally, but the remaining hypobranchials can be directed towards the midline.

108. Hypobranchials-basibranchial (relation): [0] articulated, [1] fused. †*Ptychodus***[?]**. **Villalobos-Segura *et al*. (2022, Char. 42)**.

109. First hypobranchial-basihyal: [0] separated, [1] fused [2] segmented. †*Ptychodus***[?]**. **Villalobos-Segura *et al*. (2022, Char. 45)**.

110. Hypobranchial bar: [0] absent, [1] present. †*Ptychodus***[?]**. Landemaine *et al*. (2018, Char. 132), Klug (2010, Char. 133(73)), de Carvalho (2004, Char. 23), **Shirai (1996, Char. 33**).

111. Pharyngobranchial blade: [0] absent, [1] present. †*Ptychodus***[?].** Landemaine *et al*. (2018, Char. 134), Klug (2010, Char. 135(75)), Goto (2001, Char. 1a), de Carvalho (2004, Char. 67), **Shirai (1996, Char. 35)**.

112. Bifurcate ceratobranchials: [0] absent, [1] present. Goto (2001, Char. 29)

113. Last ceratobranchial: [0] free of scapulocoracoid, [1] articulates with scapulocoracoid. (Villalobos-Segura *et al*. (2022, Char. 43), Landemaine *et al*. (2018, Char. 174), Aschliman *et al*. (2012, Char. 4), Shirai (1996, Char. 29), Shirai (1996, Char. 86), **Nishida (1990, Char. 5)**.

114. Posterior most elements of dorsal gill arches: [0] not completely fused, [1] completely fused (gill "pickaxe"). †*Ptychodus***[?].** Landemaine *et al*. (2018, Char. 133), Klug (2010, Char. 134(74)), de Carvalho (2004, Char. 24), **Shirai (1996, Char. 34**).

115. Branchial electric organs: [0] absent, [1] present. Villalobos-Segura *et al*. (2022, Char. 21), **Aschliman *et al*. (2012, Char. 86**).

116. Sup_Coracohyoideus: [0] present, [1] absent. †*Ptychodus***[?]**. Villalobos-Segura *et al*. (2022, Char. 70), Aschliman *et al*. (2012, Char. 89), **McEachran *et al*. (1996, Char. 65)**.

117. Sub_Coracohyoides (if present): [0] parallel to body axis, [1] short, [2] diagonal, [3] fused. †*Ptychodus***[?].** Villalobos-Segura *et al*. (2022, Char. 71)**,** Aschliman *et al*. (2012, Char. 89), McEachran *et al*. (1996, Char. 65).

118. Labial cartilages: [0] absent, **[1]** present. Modified from Landemaine *et al*. (2018, Char. 138), **Klug (2010, Char. 139)**.

Girdles and paired fins

119. Fin base articulation on scapulocoracoid: [0] stenobasal, deeper than wide; **[1]** eurybasal wider than deep. Lu *et al*. (2016), **Frey *et al*. (2020, Char. 197).**

120. Biserial pectoral fin endoskeleton: [0] absent, [1] present. Lu *et al*. (2016), **Frey *et al*. (2020, Char. 201).**

121. Ventral antimeres of scapulocoracoid: [0] fused, [1] not coalescent. †*Ptychodus***[?]**. Villalobos-Segura *et al*. (Char. 105), de Carvalho and Maisey (1996, Char. 1), **Shirai (1992, Char. 3**).

122. Paired fin rays: [0] aplesodic, **[1]** plesodic. **Aschliman *et al*. (2012, char. 68)**, Villalobos–Segura *et al*., (2019, char. 66).

123. Radial calcification: [0] crustal, [1] catenated (two chains), [2] catenated (four chains). **Remarks:** Modified from **Marramà *et al*. (2018 char. 100)** to include the remaining variation observed by Schaefer and Summers (2005) regarding the number of chains**.**

124. Scapular process-scapula: [0] fused, [1] articulated. †*Ptychodus***[?]**. **Villalobos-Segura *et al*. (2022, Char. 98).**

125. Scapular process: [0] short and dorsally directed, [1] long, U-curved, posteriorly directed, [2] short posterodorsally directed. Villalobos-Segura *et al*. (2022, Char. 99)*, **Aschliman *et al*. (2012, Char. 86)**.

126. Scapular process: [0] without fossa, [1] with fossa. (**Villalobos-Segura *et al*. (2022, Char. 100)**.

127. Sup Suprascapulae: [0] absent, [1] present. **Villalobos-Segura *et al*. (2022, Char. 93)**, Goto (2001, Char. 30), Aschliman *et al*. (2012, Char. 6).

128. Suprascapular cartilages: [0] absent, [1] present. New.

Remarks: Unlike Villalobos-Segura *et al*. (2022, Char. 93), this feature is proposed here as a character. This is after considering that although the position of these paired cartilages and the suprascapular cartilage (biomorphs) are the same, their interaction with other skeletal elements and their development seems to differ. In batoids, the suprascapula develops medially as a single piece over the vertebral column. In contrast, the suprascapular cartilage in sharks has no interaction with the axial skeleton. Considering that the development of the suprascapula occurs over the vertebral column in batoids and not at the sides of the scapula, as in sharks, the homology of these structures is unlikely.

129. Sub Suprascapulae (articulation): [0] curved**,** [1] crenated, [2] ball socket**.** †*Ptychodus***[-]. Villalobos-Segura *et al*. (2022, Char. 96).**

Remarks: The previously recognized state for Torpediniformes is reconsidered as it is very similar to that observed in Rajiformes (*Raja* and *Bathyraja*).

130. Sub Suprascapulae Sup Interacts with axials skeleton: [0] absent (free of axial skeleton), [1] present. †*Ptychodus***[-]. Villalobos-Segura *et al*. (2022, Char. 94)**.

131. Sub Interacts with axials skeleton: [0] articulates with vertebral column, [1] fused medially to synarcual, [2] fused medially and laterally to synarcual. †*Ptychodus***[-]. Villalobos-Segura *et al*. (2022, Char. 95)**.

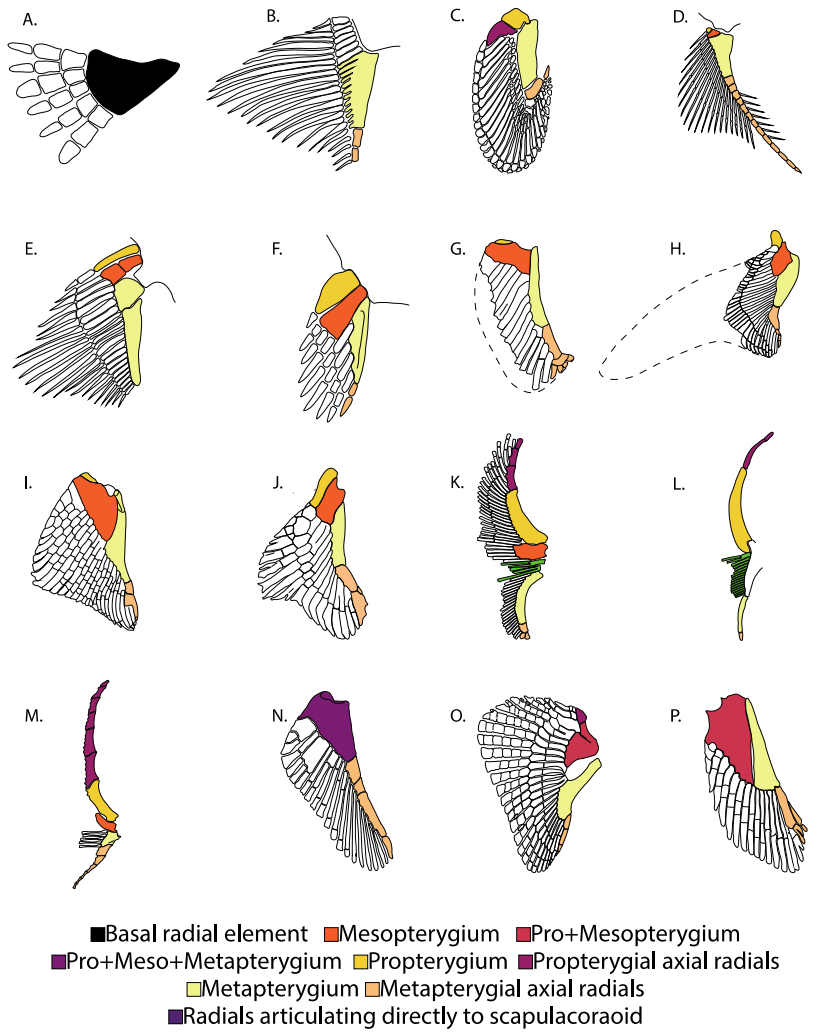

Figure S32. Line drawings of the states recognized in characters 132-137. A. †*Doliodus problematicus* (Woodward, 1892) (NBMG 10127) (redrawn and modified from Maisey *et al*., 2017: text-fig. 4a). B. †*Cobelodus aculeatus* (Cope, 1894) (after Zangerl and Case, 1976) (redrawn from Shirai, 1992: text-fig. 3.1b). C. *Callorhinchus milii* Bory de Saint-Vincent, 1823 (ANSP 174675) (redrawn from Riley *et al*., 2017: text-fig. 1h). D. †*Diplodoselache woodi* Dick, 1981 (RSM.GY.1972.27.447A) (redrawn from Dick, 1981: text-fig. 7a,c). E. †*Dracopristis hoffmanorum* Hodnett *et al*., 2021 (NMMNH P-68537) (redrawn from Hodnett *et al*., 2021: text-fig. 9b). F. *Lissodus cassangensis* (redrawn from Maisey, 1982: text-fig. 12a). G. *Chlamydoselachus anguineus* Garman, 1884 (MZUSP 110974) (redrawn from da Silva and de Carvalho, 2015: text-fig. 26g). H. *Isurus oxyrinchus* Rafinesque, 1810 (USNM 201733) (redrawn from da Silva and de Carvalho, 2015: text-fig. 28e). I. *Hexanchus griseus* (Bonnaterre, 1788) (CAS uncatalogued) (redrawn from da Silva and de Carvalho, 2015: text-fig. 32g). J. *Pseudocarcharias kamoharai* (Matsubara, 1936) (MZUSP 112028) (redrawn from da Silva and de Carvalho, 2015: text-fig. 27g). K. *Zapteryx brevirostris* (Müller and Henle, 1841) (MZUSP uncatalogued), (redrawn from da Silva and de Carvalho, 2015: text-fig. 21g). L. *Zanobatus schoenleinii* (Müller and Henle, 1841) (UF 176858), (redrawn from https://sharksrays.org/). M. *Tetronarce nobiliana* (Bonaparte, 1835) (AC.UERJ 1249), (redrawn from da Silva and de Carvalho, 2015: text-fig. 17h). N. *Echinorhinus brucus* (Bonnaterre, 1788) (HUMZ 113400), (redrawn from Shirai, 1992: plate 48c). O. *Ginglymostoma cirratum* (Bonnaterre, 1788) (CAS 232210) (redrawn from da Silva and de Carvalho, 2015: text-fig. 10f). P. *Zameus squamulosus* (Günther, 1877) (USNM 94520) (redrawn from da Silva and de Carvalho, 2015: text-fig. 4f). **Character 131:** State [0]: A; State [1]: B; State [2]: C; State [3] D-M; State [4]: N; State [5]: O-P. **Character 132:** State [0]: B; State [1]:C; State [2]: D; State [3]: E; State [4]: F-H, O-P; State [5]: I; State [6]: J, K-L; State [7] M. **Character 133:** State [0]: D, E; State [1]: F; State [2]: G-J, O-P; State [3]: K-M. **Character 134:** State [0]: A-B, N-P; State [1]: C-M. **Character 135:** State [0]: C; State [1]: D; State [2]: E-F; State [3]: G-J; State [4]: K-M. **Character 136:** State [0]: D-F, H, J-M; State [1]: C, G, I.

132. Pectoral basal elements: [0] large basal element, [1] multiple free radials articulating directly and a metapterygium, [2] two main cartilages (propterygium and metapterygium), **[3]** tribasal pectoral fin, [4] all three basal elements fused, [5] propterygium and mesopterygium fused. **Villalobos-Segura *et al*. (2022, Char. 141).** See figure S32.

Remarks: Modify from Villalobos-Segura et al. (2022, Char. 141). Additional character states were included to incorporate the variation observed in the cartilaginous fishes included in the present analysis (figure S33).

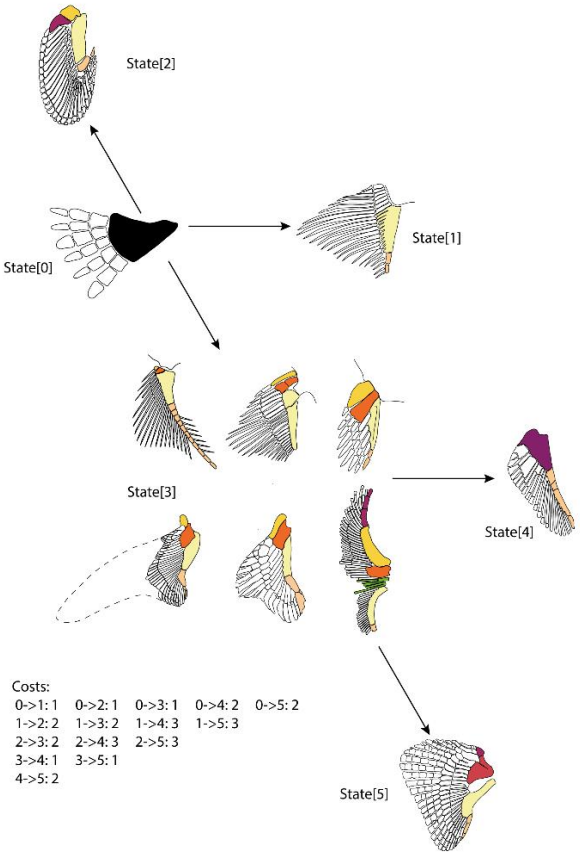

Figure S33. Enforced path using the "cstree" command on TNT for state evolution on character 132. Arrows indicate the allowed transformation path initiating for the state [0], each stop on a state increases one step. For genus and color code see figure S32 caption.

133. Metapterygium: [0] pectinated, [1] rectangular, [2] rectangular tampering distally, articulating with a sequence of multiple axial cartilages, [3] rectangular articulated to a massive axial cartilage, **[4]** elongated with a broad distal end to which the pectoral radials articulate, [5] proximally segmented, with a broad distal end to which the pectoral radials, [6] elongated with multiple radials articulating across its entire outer surface, [7] multiple segments. **Frey *et al*. (2020, Char. 199)**. See figure S32.

134. Mesopterygium: [0] reduced, [1] expanded of similar size as the propterygium, **[2]** enlarged broader and larger than the propterygium, [3] reduced, propterygium and metapterygium larger. New. See figure S32.

135. Sup Propterygium: [0] absent, **[1]** present. New. See figure S32.

136. Sub Propterygium: [0] rectangular and being the point of articulation for the rest of basal elements, [1] narrow and reduced, [2] enlarged, similar size as the mesopterygium, **[3]** broad and reduced, [4] anteriorly expanded. New. See figure S32.

137. Sub Propterygium: [0] articulating with radials, [1] not contacting radials. †*Ptychodus***[?]**. Landemaine *et al*. (2018, Char. 109), Klug (2010, 110(52)), Goto (2001, Char. 5a), de Carvalho (2004, Char. 40), Shirai (1996, Char. 63), **Shirai (1996, Char. 141**). See figure S32.

138. Pectoral articulation: [0] facets, [1] condyles, [2] facets and condyles. †*Ptychodus***[?]**

139. Independent metacondyle: [0] absent, [1] present. †*Ptychodus***[?]**

140. Pectoral fin radials: [0] all articulate to pterygia, [1] some articulate directly with scapulocoracoid. **Villalobos-Segura *et al*. (2022, Char. 114**). †*Ptychodus***[?]**

141. Pectoral fin with interradial connections ("cross-braces"): [0] absent, [1] present. Villalobos-Segura *et al*. (2022, Char. 111), Shirai (1996, Char. 67).

142. Pelvic girdle: [0] separated, [1] fused. †*Ptychodus***[?]**. Villalobos-Segura *et al*. (2022, Char. 124).

143. Lateral prepelvic process: [0] absent, [1] present. †*Ptychodus***[?]**. **Villalobos-Segura *et al*. (2022, Char. 117), McEachran and Dunn (1998, Char. 36**).

144. Pelvic basals: [0] multiple radials articulated directly to the pelvic girdle**,** the latest fussing into the baspterygium**,** [1] two large basal cartilages**,** [2] single large element. †*Ptychodus***[?]**. **Villalobos-Segura *et al*. (2022, Char. 60**).

145. Postpelvic processes: [0] absent, [1] present. †*Ptychodus***[?]**. **Villalobos-Segura *et al*. (2022, Char. 118), Claeson *et al*. (2013, Char. 37).**

146. Posterior margin of puboischiadic bar: [0] straight or anteriorly directed, [1] posteriorly directed. †*Ptychodus***[?]**. **Villalobos-Segura *et al*. (2022, Char. 119).**

147. Posterior process of the coracoid: [0] absent, [1] present. †*Ptychodus***[?]**. New.

Remarks: Follows da Silva and Datovo's (2020) observations on the variation of the pectoral girdle of neoselachians.

148. Metapterygial whip: [0] absent, [1] present. Coates *et al*. (2017), **Frey *et al*. (2020, Char. 200).**

149. Sup Reduced number of cartilages between pelvic basipterygium and clasper: [0] absent, **[1]** present. Villalobos-Segura *et al*. (2022, Char. 125).

150. Sub Reduced number of cartilages between pelvic basipterygium and clasper (T3): [0] not spinous, [1] spinous, [2] modified into the external mesorhipidion. †*Ptychodus***[?]**. New.

Remarks: The codification and homology of character 150 need to be evaluated because in several Rajiformes, the T-3 cartilage forms a shield-like structure that covers T2 and T1 (McEachran and Miyake 1988: text-fig. 11), which seems to be missing in sharks. This structure in Myliobatiformes seems to present more complex forms than a simply spinous (Aschliman *et al.*, 2012: text-fig. 3.5). Because of this, the codification of this character was kept dichotomic, and the spinous state for remaining batomorphs was changed to [?] if there was no information available regarding the morphology of this cartilage for the taxa (see also Moreira *et al.*, 2017; Moreira and de Carvalho, 2021).

151. Extended dorso and Ventral terminal cartilages [0] absent, [1] present. †*Ptychodus***[?]**. **(Deactivated)**.

Axial skeleton

152. Sup Chordacentra: [0] absent, [1] present. Stahl (1999), Coates and Sequeira (2001), Coates *et al*. (2017), Frey *et al*. (2020, Char. 182)

153. Sub Chordacentra polyspondylous and consist of narrow closely packed rings: [0] absent, [1] present. †*Ptychodus***[-].** Patterson (1965), Coates *et al*. (2017), Frey *et al*. (2020, Char. 183)

154. Occipital hemicentrum: [0] absent, **[1]** present, [2] secondary lost, [3] lost as a product of a synarcual. Villalobos-Segura *et al*. (2022, Char. 50), Landemaine *et al*. (2018, Char. 16), Klug (2010, Char. 16), de Carvalho (1996, Char. 17), de Carvalho and Maisey (1996, Char. 29), Shirai (1996, Char. 21), **Shirai (1992, Char. 53).**

Remarks: There is an uncertainty regarding the presence or absence of this structure in *Echinorhinus* de Blainville, 1816 and hexanchid sharks (*Notorynchus*, *Hexanchus* Rafinesque, 1810 and *Heptranchias* Rafinesque, 1810) (see Jambura *et al*., 2023), and regarding its absence in pristiphoroids (Maisey *et al*., 2019), where this structure seems to be present in juveniles (C. Underwood pers. com.). Considering the reduction in the calcification of the vertebral column in some modern groups like hexanchids and the presence of well-calcified vertebral centra in their older representatives (†*Notidanoides*), we coded this as a secondary loss. We consider that if this structure is lost in these taxa (as coded by de Carvalho 1996 and Shirai 1996), this loss is not homologous to the one in batoids, which present a fusion of basiventral cartilages and

displacement of areolar centrum cartilages caudally as the result of the development of the synarcual cartilage (K. Claeson pers. com.). Consequently, this character was ordered using the "cstree" command (see script in supplementary materials).

155. Sup Calcified thoracic and caudal vertebral centra: [0] absent, **[1]** present. **Frey *et al*. (2020, Char. 181).**

Remarks: Previously, the calcification of the vertebra centra was used as a single character (Frey *et al*. 2020, char. 181; Jambura *et al*., 2023, char. 133). For the present analysis, we divided this character into three (cervical, thoracic, and caudal).

156. Sub Calcified thoracic and caudal vertebral centra (Caudal vertebrae): [0] diplospondylus, [1] fused. Villalobos-Segura *et al*. (2022, Char. 89), **Aschliman *et al*. (2012, Char. 80**).

157. Sub Calcified thoracic and caudal vertebral centra (Second synarcual): [0] absent, [1] present. Villalobos-Segura *et al*. (2022, Char. 88), Aschliman *et al*. (2012, Char. 54), McEachran *et al*. (1996, Char. 43), **Nishida (1990, Char. 66**).

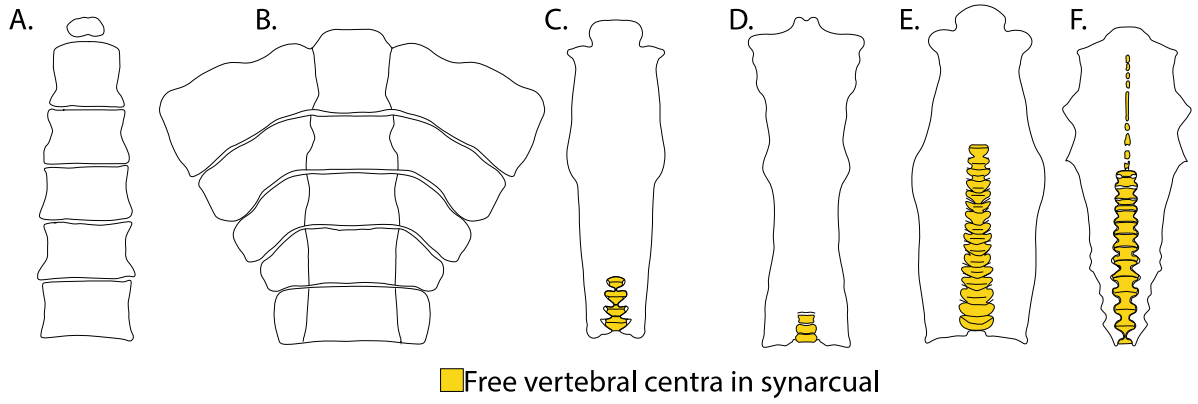

Figure S34. Line drawings of the states recognized in characters 158-161. A. Unmodified vertebra centra on cervical region, B. *Squatina guggenheim* Marini, 1936 (ZMB 33878) (redrawn from Claeson and Hilger, 2011: text-fig. 2a), C. *Okamejei kenojei* (Bürger, in Müller and Henle, 1841) (ZMB 15512) (redrawn from Claeson, 2011: text-fig. 4c), D. *Potamotrygon* Garman, 1877 (AMNH 38138), E. *Glaucostegus typus* (Bennett, 1830) (NHMUK 1967.2.11.3), F. *Platyrhinoidis triseriata* (Jordan and Gilbert, 1880). **Character 158**: State [1]: A-F. **Character 159**: State [0]: A; State [1]: B; State [2]: C-F. **Character 160:** State [0]: A-B; State [1]: C-F. **Character 161:** State [0]: F; State [1]: E; State [2]: C-D.

158. Sup Calcified Cervical vertebra: [0] absent**, [1]** present. New. See figure S34.

159. Sub Calcified Cervical vertebra (basiventral): [0] not expanded, [1] expanded and unfused, [2] fused. Villalobos-Segura *et al*. (2022, Char. 48), **Aschliman *et al*. (2012, Char. 5**). See figures S34 and S35.

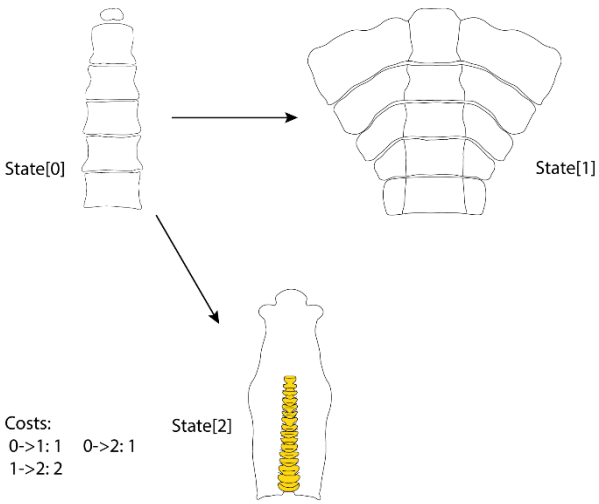

Figure S35. Enforced path using the "cstree" command on TNT for state evolution on character 159. Arrows indicate the allowed transformation path initiating for the state [0], each stop on a state increases one step. For genus and color code see figure S34 and its caption.

160. Sub_Calcified Cervical vertebra_Sup_Synarcual: [0] absent, [1] present. **Villalobos-Segura *et al*. (2022, Char. 49**). See figure S34.

161. Sub Synarcual (Vertebrae in synarcual): [0] present the entire length, [1] reaching rostral to suprascapula, [2] reaching caudal to suprascapula. †*Ptychodus***[-]. Villalobos-Segura *et al*. (2022, Char. 55), Marrama *et al*. (2018, Char. 78).** See figures S34 and S36.

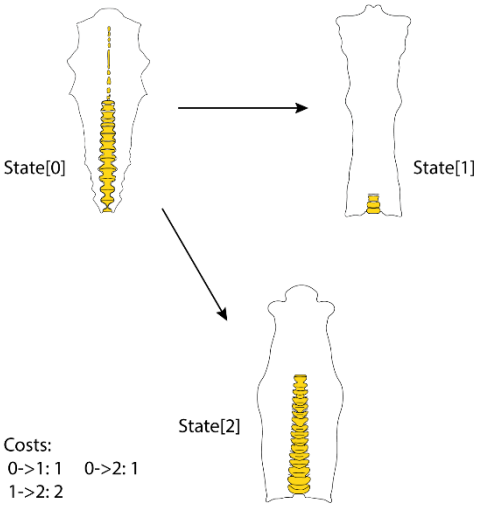

Figure S36. Enforced path using the "cstree" command on TNT for state evolution on character 161. Arrows indicate the allowed transformation path initiating for the state [0], each stop on a state increases one step. For genus and color code see figure S34 and its caption.

162. Sup Lateral stays: [0] absent, [1] present. (**Villalobos-Segura *et al*. (2022, Char. 51**).

163. Sub Lateral stays (if present): [0] dorsally directed and free of medial crest, [1] laterally directed and free of medial crest, [2] reduced. †*Ptychodus***[-].** Villalobos-Segura *et al*. (2022, Char. 52)*, **Villalobos-Segura *et al*. (2019, Char. 53).** See figure S37.

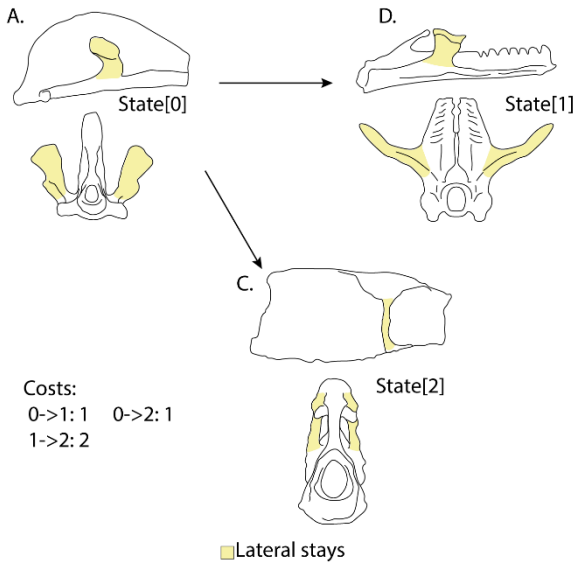

Figure S37. Enforced path using the "cstree" command on TNT for state evolution on character 163. Arrows indicate the allowed transformation path initiating for the state [0], each stop on a state increases one step. A. *Rhina ancylostoma* Bloch and Schneider, 1801 (LACM 38117-38, https://sharksrays.org/, accessed on 20 Oct. 2023), B. *Torpedo fuscomaculata* Peters, 1855 (https://sharksrays.org/, accessed on 20 Oct. 2023), C. *Mobula munkiana* Notarbartolo-di-Sciara, 1987 (SIO 85-34) (https://sharksrays.org/, accessed on 20 Oct. 2023).

164. Sup Primary calcification of vertebrae: [0] absent, **[1]** present. Landemaine *et al*. (2018, Char. 183), Shirai (1996, Char. 75), **Shirai (1996, Char. 151 & 152)**.

165. Sub Primary calcification of vertebrae: [0] restricted terminally, **[1]** developed. Landemaine *et al*. (2018, Char. 183), Shirai (1996, Char. 75)**, Shirai (1996, Char. 151 & 152)**.

166. Sup Secondary calcification of vertebrae: [0] absent, **[1]** present. **Shirai (1996, Char. 155).**

167. Sub Secondary calcification of vertebrae: [0] endochordal radii radiating from the notochordal sheath, [1] with developed solid medialia and diagonal calcified lamellae, [2] compact mass. Landemaine *et al*. (2018, Char. 184), **Shirai (1996, Char. 76)**, Jambura *et al*. (2023, Char. 130).

Remarks: Reductive coding was applied to characters 164–167 to add the grouping information on the presence and absence, which was overlooked under the previous unordered polymorphic scoring.

168. Hemal arch: [0] not arched at anterior precaudal tail vertebrae, [1] almost complete in the entire region of the precaudal tail. Landemaine *et al*. (2018, Char. 96), Klug (2010, Char. 97(42)), de Carvalho (2004, Char. 47), Shirai (1996, Char. 78), **Shirai (1996, Char. 159**).

169. Sup Supraneurals: [0] absent [1] present. Landemaine *et al*. (2018, Char. 62), & 91(39) Klug (2010, Char. 62(38)), **de Carvalho and Maisey (1996, Char. 69), Shirai (1996, Char. 156**).

170. Sup Supraneurals (plate-like supraneurals): [0] enlarged at least in front of the second dorsal fin, [1] also enlarged in the abdominal region. †*Ptychodus***[-]**. (Landemaine *et al*. (2018, Char. 62 & 90), Klug (2010, Char. 62(38) & 91(39)), de Carvalho and Maisey (1996, Char. 70)***, Shirai (1996, Char. 157**).

171. Vertebral ribs: [0] absent, [1] present [2] reduced. Villalobos-Segura *et al*. (2022, Char. 90), Aschliman *et al*. (2012, Char. 44), Klug (2010, Char. 105), McEachran and Aschliman (2004, Char. 49), McEachran *et al*. (1996, Char. 44), Shirai (1996, Char. 74), **Shirai (1992, Char. 158)**, Nishida (1990, Char. 64).

Scoring: Considering that the presence of vertebral ribs is the most common state across the neoselachians, it was placed as the basal state for the group using the "cstree" command and it was followed by the reduction of the structure in some groups (see, matrix in supplementary file).

172. Pleural ribs: [0] absent, [1] present. New (modified from Maisey, 1982).

Remarks: According to Maisey (1982), the "ribs" of elasmobranchs and hybodontiforms are not homologous. In hybodonts, the ribs are placed on the mesial wall of the body cavity, whereas in elasmobranchs, the ribs are inserted in the horizontal myoseptum between the epaxial and hypaxial body muscles.

173. Arcualia dorsalis: [0] absent, [1] present. Villalobos-Segura *et al*. (2022, Char. 54), **Brito *et al*. (2013, Char. 30)**.

174. Number of dorsal fins: [0] one, **[1] two**, [2] reduced. Landemaine *et al*. (2018, Char. 145), Klug (2010, Char. 149(89)), de Carvalho (2004, Char. 50), **de Carvalho and Maisey (1996, Char. 83)**, Shirai (1996, Char. 80).

175. Dorsal fin: [0] aplesodic, [1] plesodic. Jambura *et al*. (2023, Char. 152).

176. Dorsal fin endoskeleton: [0] composed of a triangular or rectangular basal cartilage and radials separated from vertebral column, [1] composed of a triangular or rectangular basal cartilage and radials close to vertebral column, **[2]** radials only (no basal), [3] at least two large plates, [4] small radials (variously arranged), elongate basal with radials [5]. Modified from Jambura *et al*., (2013, Char. 155), **Shirai (1996, Char. 162-166**).

177. Caudal fin: [0] with a developed lower lobe to make a "lunate" form, [1] heterocercal, [2] reduced to the plesodic or tail folds, [3] without any tail folds or finlet. **Shirai (1996, Char. 86)**, Nishida (1990, Char. 56).

178. Caudal lower lobe: [0] without radials, [1] with radials. **Frey *et al*. (2020, Char. 213**).

179. Scapular process with posterodorsal process: [0] absent, [1] present. Coates and Sequeira (2001a); Davis *et al*. (2012); Zhu *et al*. (2013), **Frey *et al*. (2020, Char. 193**).

180. Procoracoid mineralisation: [0] absent, [1] present. Davis (2002), Brazeau (2009), **Frey *et al*. (2020, Char. 196**).

181. Posterior dorsal fin with delta-shaped cartilage: [0] absent, [1] present. Coates and Sequeira (2001), **Frey *et al*. (2020, Char. 209**).

External features

182. Cephalic lobes: [0] absent, [1] present. Villalobos-Segura *et al*. (2022, Char. 61), Aschliman *et al*. (2012, Char. 10), McEachran *et al*. (1996, Char. 9), **Nishida (1990, Char. 96)**.

183. Upper eyelid: [0] present, [1] absent. †*Ptychodus***[?]**. Villalobos-Segura *et al*. (2022, Char. 1), Aschliman *et al*. (2012, Char. 1), **McEachran *et al*. (1996, Char. 1)**. In rays, the cornea is fused with the skin of the skull dorsally and therefore no upper eyelid is present in this group.

184. Nictitating eyelid: [0] absent, [1] present. †*Ptychodus***[?]**. **Shimada (2005, Char. 25)**. According to Compagno (1977), the nictitating eyelid is a synapomorphy for Carcharhiniformes.

185. Nostrils: [0] separated, [1] close together. †*Ptychodus***[?]**. **Villalobos-Segura *et al*. (2022, Char. 36).**

186. Anterior nasal lobe: [0] fails to reach mouth, [1] reaches the mouth. †*Ptychodus***[?]**. Villalobos-Segura *et al*. (2022, Char. 31), **Aschliman *et al*. (2012, Char. 11)**.

187. Anterior nasal lobe: [0] fails to cover most of the medial half of the naris, [1] well-developed. †*Ptychodus***[?]**. **Villalobos-Segura *et al*. (2022, Char. 32)**, Aschliman *et al*. (2012, Char. 11).

188. Nasal curtain fringes: [0] absent, [1] present. †*Ptychodus***[?]**. Villalobos-Segura *et al*. (2022, Char. 33).

189. Infraorbital loop of suborbital and infraorbital canals: [0] absent, [1] present. †*Ptychodus***[?]**. Villalobos-Segura *et al*. (2022, Char. 81), Aschliman *et al*. (2012, Char. 21), **McEachran *et al*. (1996, Char. 15**).

190. Subpleural loop of the hyomandibular canal: [0] broad rounded, [1] loop forms a lateral hook, [2] lateral aspects of subpleural loop are nearly parallel. †*Ptychodus***[?]**. Villalobos-Segura *et al*. (2022, Char. 82), Aschliman *et al*. (2012, Char. 22), **McEachran *et al*. (1996, Char. 16).**

191. Sup_Abdominal canal on coracoid bar: [0] absent, [1] present. †*Ptychodus***[?]**. **Villalobos-Segura *et al*. (2022, Char. 83),** Aschliman *et al*. (2012, Char. 24), McEachran *et al*. (1996, Char. 18).

192. Sub_Abdominal canal on coracoid bar (if present): [0] groove-cephalic lateral line forms abdominal canal on coracoid bar, [1] pores. †*Ptychodus***[?]**. **Villalobos-Segura *et al*. (2022, Char. 84)**.

193. Scapular loops of scapular canals: [0] absent, [1] present. †*Ptychodus***[?]**. Villalobos-Segura *et al*. (2022, Char. 86), Aschliman *et al*. (2012, Char. 25), **McEachran *et al*. (1996, Char. 19)**.

194. Cephalic lateral line canals on ventral surface: [0] present, [1] absent. †*Ptychodus***[?]**. Villalobos-Segura *et al*. (2022, Char. 87), Aschliman *et al*. (2012, Char. 20), McEachran *et al*. (1996, Char. 14).

195. Sup Cephalic spines: [0] absent, [1] present. (**Maisey, 1989, Char. 14**).

196. Sub Cephalic spines (Trilobed cephalic spine base): [0] absent, [1] present. †*Ptychodus***[-]**.

197. Sub Cephalic spines (Number of pairs): [0] one, [1] two. †*Ptychodus***[-]**. (**Maisey, 1989, Char. 35**).

Remarks: Character 196 is proposed based on Maisey (1989) observations regarding the shape of the base of the cephalic spines of †*Hamiltonichthys* Maisey, 1989. Character 197 Maisey (1989, Char. 35) includes observations made by Lane (2010) regarding the number of cephalic spines in †*Tribodus* Brito and Ferreira, 1989 and †*Egertonodus* Maisey, 1987.

198. Sub Cephalic spines (Multicuspid): [0] not multiple cuspid, [1] present and with multiple cuspids. †*Ptychodus***[-]**. (**Maisey, 1989, Char. 31**).

199. Placoid scales: [0] scarce or absent, **[1]** present. Villalobos-Segura *et al*. (2022, Char. 133)., Aschliman *et al*. (2012, Char. 15), **McEachran and Dunn (1998, Char. 11**).

200. Malar and alar thorns: [0] absent, [1] present. Villalobos-Segura *et al*. (2022, Char. 134), Aschliman *et al*. (2012, Char. 17), **McEachran and Dunn (1998, Char. 22).**

201. Lateral rostral dermal denticles: [0] absent, [1] present. **Villalobos-Segura *et al*. (2022, Char. 136)**.

202. Sup Dorsal fin spines: [0] absent, [1] present. Villalobos-Segura *et al*. (2022, Char. 130), Goto (2001, Char. 12a), **de Carvalho (2004, Char. 49**).

203. Dorsal cephalic fin spines: [0] absent, [1] present. Frey *et al*. (2020, Char. 216).

204. Sub Dorsal fin spines (Vascularization): [0] vascularize, [1] unvascularize. †*Ptychodus***[-]**. (Maisey, 1977).

205. Sub Dorsal fin spines (posterior denticles): [0] absent, [1] present. †*Ptychodus***[-]**. Frey *et al*, (2020, Char. 229).

206. Sub Dorsal fin spines (Fin spines ornamentation): [0] absent, [1] present. †*Ptychodus***[-]**. **Frey *et al*., (2020, Chars. 227-228**).

207. Dorsal fin spine apex curved posteriorly: [0] absent, [1] present. †*Ptychodus***[-]. Frey *et al*., (2020, Chars. 218)**

Remarks: Character 156 includes the observations made by Maisey (1977) observations regarding the histology of the dorsal fin spines.

208. Serrated tail sting: [0] absent, [1] present. Villalobos-Segura *et al*. (2022, Char. 132), Aschliman *et al*. (2012, Char. 14), McEachran *et al*. (1996, Char. 13).

Dentition

209. Sup Three-layered enameloid structure: [0] absent, **[1]** present. Landemaine *et al*. (2018, Char. 159), Klug (2010, Char. 163(103)), Jambura *et al*. (2023, Char. 181).

210. Sub Three-layered enameloid structure (Secondary lost): [0] absent, [1] present.

Remarks: Character 210 is added to include the possible subsequent reduction of the enameloid layer observed in batomorphs. We agree with Jambura *et al*. (2023) that a multilayered enameloid was most likely present in the common ancestor of sharks and rays. The reduction of the enameloid layers still needs to be considered.

211. Ligual torus: [0] absent, [1] present. **Frey *et al*. (2020, Char. 71)**.

212. Differentiated lateral uvulae on teeth: [0] absent, [1] present. Villalobos-Segura *et al*. (2022, Char. 56), Claeson *et al*. (2013, Char. 22).

213. Crown dentine: [0] orthodentine, **[1]** osteodentine, [2] pseudoostedentine (ortho + osteodentine). **Jambura *et al*. (2023, Char. 193).**

214. Sup Basal furrows on root: [0] absent, [1] present. Modified from Klug (2010, Char. 166(106)).

215. Sub Basal furrows on root (Compression): [0] absent, [1] present. †*Ptychodus***[-]**. New. Based on Cappetta (2012) observations.

216. Teeth with distal heel [0] absent, [1] present. Pollerspöck and Straube (2022, Char. 20), Flammensbeck *et al*. (2018, Char. 10).

217. Labial root depression: [0] absent, [1] present. (Klug, 2010, Char. 170 (110).

218. Root dentine: [0] osteodentine, [1] orthodentine. Villalobos-Segura *et al*. (2022, Char. 57), Aschliman *et al*. (2012, Char. 19), Jambura *et al*. (2023, Char. 195).

219. Teeth with three slim main cusps almost equal to each other, strongly recurved: [0] absent, [1] present. **Frey *et al*. (2020, Char. 73).**

220. Toothplates: [0] absent, [1] present. Patterson (1965); Stahl (1999), **Frey *et al*. (2020, Char. 74).**

221. Tubular dentine: [0] absent, [1] present. Stahl (1999), see also Patterson (1965). **Frey *et al*. (2020, Char. 5).**

Part F. Institutional abbreviations

AC.UERJ: Fish Collection of the Departamento de Zoologia, Universidade do Estado do Rio de Janeiro, Rio de Janeiro, Brazil; **AMNH**: American Museum of Natural History, New York, USA; **AMS**: Australian Museum, Sydney, Australia; **ANSP**: Academy of Natural Sciences of Drexel University, Philadelphia, USA; **BMB**: Booth Museum, Brighton, UK; **CAS**: California Academy of Sciences, San Francisco, USA; **CNPE-IBUNAM**: Colección Nacional de Peces del Instituto de Biología, Universidad Nacional Autónoma de México, México; **CSIRO**: Commonwealth Scientific and Industrial Research Organization, Canberra, Australia; **FHSM**: Stenberg Museum of Natural History, Fort Hays State University, Hays, USA; **FMNH**: Field Museum of Natural History, Chicago, USA; **FSFL**: Far Seas Fisheries Research Laboratory, Orido, Japan; **GMBL**: Grice Marine Biological Laboratory, College of Charleston, USA; **HUMZ**: Hokkaido University Laboratory of Marine Zoology, Japan; **KUVP**: Museum of Natural History, University of Kansas, Vertebrate Paleontology Collection, Lawrence, USA; **LACM**: Los Angeles County Museum of Natural History, USA; **LJVC**: L.J.V. Compagno cataloged collection; **MCSNV**: Museo Civico di Storia Naturale di Verona, Italy; **MCZ**: Museum for Comparative Zoology, Cambridge, USA; **MGL**: Collection Géologique, Muséum d'Histoire Naturelle de Lille, France; **MNHN** Muséum National d'Histoire Naturelle, Paris, France; **MPPSA**: Museo Preistorico e Paleontologico di Sant'Anna d'Alfaedo, Verona, Italy; **MSM**: Marine Science Museum, Tokai University, Japan; **MSNUP**: Museo di Storia Naturale dell'Università di Pisa, Italy; **MZUSP**: Universidade de Sao Paulo, Museu de Zoologia, Brazil; **NBMG**: New Brunswick Museum, Saint-John, Canada; **NMMB(HO)**: National Museum of Marine Biology and Aquarium, Checheng, Taiwan; **NMMNH**: New Mexico Museum of Natural History and Science, Albuquerque, USA; **NHMUK**: Natural History Museum United Kingdom, London, UK; **NSMT**: National Science Museum, Department of Zoology, Tokyo, Japan; **PIMUZ**: Palaeontological Institute and Museum of the University of Zurich, Switzerland; **ROM**: Royal Ontario Museum, Toronto, Canada; **RUSI**: South African Institute for Aquatic Biodiversity (SAIAB), formerly J.L.B. Smith Institute of Ichthyology, Grahamstown, South Africa; **RSM**: Royal Scottish Museum, Edinburgh, Scotland; **SIO**: Scripps Institution of Oceanography, San Diego, USA; **SMNS**: Staatliches Museum für Naturkunde Stuttgart, Germany; **SMU-SMP**: Shuler Museum of Paleontology, Southern Methodist University, Dallas, USA; **UF:** University of Florida, Florida Museum, Gainesville, USA; **UNSM**: University of Nebraska State Museum, Lincoln, USA; **USNM**: Smithsonian National Museum of Natural History, Washington, USA; **ZMB**: Museum für Naturkunde, Berlin, Germany; **ZMUC**: Kobenhavns Universitet Zoologisk Museum (Zoological Museum, University of Copenhagen), Denmark.

Part G. Supplementary references

Agassiz LJR. 1833-1844 *Recherches sur les Poissons Fossiles*; Petitpierre: Neuchâtel, Switzerland; Volumes 1–5.

Allis EP. 1914 The pituitary fossa and trigemino-facialis chamber in selachians. *Anat. Anz.* **46**, 225–253

Allis EP. 1923 The cranial anatomy of *Chlamydoselachus anguineus*. *Acta Zool*. **4,** 123–221.

Aschliman NC, Claeson KM, McEachran JD. 2012 Phylogeny of Batoidea. In *Biology of Sharks and Their Relatives*, 2nd ed. (ed. JC Carrier, JA Musick, MR Heithaus), pp. 57–97. Boca Raton, FL: CRC Press.

Amadori M, Amalfitano J, Giusberti L, Fornaciari E, Carnevale G, Kriwet J. 2020a A revision of the Upper Cretaceous shark *Ptychodus mediterraneus* Canavari, 1916 from northeastern Italy, with a reassessment of *P. latissimus* and *P. polygyrus* Agassiz, 1835 (Chondrichthyes, Elasmobranchii). *Cret. Res.* **110**, 104386.

Amadori M, Amalfitano J, Giusberti L, Fornaciari E, Carnevale G, Kriwet J. 2020b The Italian record of the Cretaceous shark, *Ptychodus latissimus* Agassiz, 1835 (Chondrichthyes, Elasmobranchii). *PeerJ* **8**, e10167.

Amadori M, Kindlimann R, Fornaciari E, Giusberti L, Kriwet J. 2022a A new cuspidate ptychodontid shark (Chondrichthyes; Elasmobranchii), from the Upper Cretaceous of Morocco with comments on tooth functionalities and replacement patterns. *J. Afr. Earth Sci.* **187**, 104440.

Amadori M, Solonin SV, Vodorezov AV, Shell R, Niedźwiedzki R, Kriwet J. 2022b The extinct shark, *Ptychodus* (Elasmobranchii: Ptychodontidae) in the Upper Cretaceous of central-western Russia—The road to easternmost peri-Tethyan seas. *J. Vert. Paleontol.* **42**, e2162909.

Ayres WO. 1854 Description of new fishes from California. *Proc. Calif. Acad. Sci*. **1**, 3–22.

Ayres WO. 1855 [Descriptions of new species of Californian fishes.] A number of short notices read before the Society at several meetings in 1855. *Proc. Calif. Acad. Sci*. 1, 23–77.

de Beer GR, Moy–Thomas JA. 1935 VI—On the skull of Holocephali. *Philos. Trans. R. Soc. B.* **224**, 287–312.

de Beer GR. 1937 *The development of the vertebrate skull*. Oxford: Clarendon Press.

Bennett ET. 1830 Class Pisces. In *Memoir of the Life and Public Services of Sir Thomas Stamford Raffles* (ed. Lady Stamford Raffles), pp. 686–694. London, UK: John Murray.

Beyrich E. 1848 Über *Xenacanthus decheni* und *Holacanthus gracilis*, zwei Fische aus der Formation des Rothliegenden in Norddeutschland. *Berichte der Königlich-Preussischen Akademie der Wissenschaften* **1848**, 24–33.

Blanco A, Cavin L. 2003 New Teleostei from the Agua Nueva Formation (Turonian), Vallecillo (NE Mexico). *C. R. Palevol.* **2**, 299–306.

Blanco A, Stinnesbeck W, López-Oliva JG, Frey E, Adatte T, González AH. 2001 Vallecillo, Nuevo León: una nueva localidad fosilífera del Cretácico Tardío en el noreste de México. *Rev. Mex. Cienc. Geol.* **18**, 186–199.

Bleeker P. 1858 Vierde bijdrage tot de kennis der ichthyologische fauna van Japan. *Verhandelingen der Natuurkundige Vereeniging in Nederlandsch Indië* **3**, 1–46.

Bleeker P. 1867. Description et figure d'une espèce inédite de *Crossorhinus* de l'archipel des Moluques. In *Archives néerlandaises des sciences exactes et naturelles.* 2 vol. (eds EH von Baumhauer, RMM van Rees, J van der Hoeven, D Bierens de Haan, CAJA Oudemans, W Koster), pp. 400–402. The Hague, Netherlands: Martinus Nijhoff.

Bloch ME, Schneider JG. 1801. *M.E. Blochii Systema Ichthyologiae iconibus ex illustratum. Post obitum auctoris opus inchoatum absolvit, correxit, interpolavit.* Saxo.

de Blainville H. 1816 Prodrome d'une nouvelle distribution systématique du règne animal. *Bull. Sci. Soc. Philom. Paris* **8**, 105–112.

Brazeau MD. 2009 The braincase and jaws of a Devonian ‘acanthodian’ and modern gnathostome origins. *Nature* **457**, 305–308.

Brito PM, Ferreira PLN. 1989 The first Hybodont shark, *Tribodus limae* n. gen., n. sp., from the Lower Cretaceous of Chapada do Araripe (North-East Brazil). *An. Acad. Bras. Cienc.* **61**, 53–57.

Brito PM, Leal M, Gallo V. 2013 A new lower Cretaceous guitarfish (Chondrichthyes, Batoidea) from the Santana Formation, Northeastern Brazil. *Bol. Mus. Nac. Rio de J.* **75**, 1–13.

Brito PM, Seret B. 1996 The new genus *Iansan* (Chondrichthyes, Rhinobatoidea) from the Early Cretaceous of Brazil and its phylogenetic relationships. In *Mesozoic fishes - Systematics and Paleoecology*, vol. 1 (eds G Arritia, V Gunther), pp. 47–63. Munich, Germany: Verlag Dr. Friedrich Pfeil.

Bonnaterre JP. 1788. *Ichthyologie. Tableau encyclopédique et méthodique des trois règnes de la nature.* Paris: Chez PANCKOUCKE, Libraire, Hotel de Thou, rue des Poitevins.

Bory de Saint-Vincent JBGM. 1823 Dictionnaire Classique d'Histoire Naturelle. Paris: Imprimeurs de la Société d'Histoire Naturelle, rue de Vaugirard.

Böttcher R, Duffin CJ. 2000 The neoselachian shark †*Sphenodus* from the Late Kimmeridgian (Late Jurassic) of Nusplingen and Egesheim (Baden-Württemberg, Germany). *Stutt. Beitr. Naturkd. B (Geologie und Paläontologie)*. **283**, 1–31.

Burrow CJ, den Blaauwen J, Newman M, Davidson R. 2016 The diplacanthid fishes (Acanthodii, Diplacanthiformes, Diplacanthidae) from the Middle Devonian of Scotland. *Palaeont. Electr*. **19**, 1–83.

Cadenat J. 1963 Notes d'ichtyologie ouest-africaine. XXXIX. Notes sur les requins de la famille des Carchariidae et formes apparentées de l'Ouest-africain (Avec la description d'une espèce nouvelle: *Pseudocarcharias pelagicus*, classée dans un sous-genre nouveau). *Bull. Inst. fr. Afr. Noire (A)* **25**, 526–537.

Cappetta H. 2012 Chondrichthyes. Mesozoic and Cenozoic Elasmobranchii: Teeth. In *Handbook of paleoichthyology*, vol. 3E (ed. H-P Schultze), München, Germany: Pfeil.

de Carvalho MR. 1996 Higher-Level Elasmobranch Phylogeny, Basal Squaleans and Paraphyly. In *Interrelationships of fishes* (eds MLJ Stiassny, LR Parenti, DG Johnson), pp. 35–60. San Diego, CA: Academic Press.

de Carvalho MR. 2004 Late Cretaceous thornback ray from southern Italy, with a phylogenetic reappraisal of the Platyrhinidae (Chondrichthyes: Batoidea). In *Mesozoic Fishes 3 - Systematics, Paleoenvironments and Biodiversity*, vol. 3 (ed. G Arratia, A Tintori), pp. 75–101. Munich, Germany: Verlag Dr. Friedrich Pfeil.

de Carvalho MR, Maisey JG. 1996 Phylogenetic Relationships of the Late Jurassic Shark *Protospinax Woodward* 1919 (Chondrichthyes: Elasmobranchii). In *Mesozoic fishes - Systematics and Paleoecology*, vol. 1 (eds G Arratia, V Gunther), pp. 9–47. Munich, Germany: Verlag Dr. Friedrich Pfeil.

Castex MN, Castello HP. 1970 *Potamotrygon yepezi*, n. sp. (Condrichthyes, (sic) Potamotrygonidae), a new species of freshwater sting-ray from Venezuelan rivers. *Acta Scientifica, Universidad del Salvador*. **8**, 15–39

Claeson KM. 2011 The synarcual cartilage of batoids with emphasis on the synarcual of Rajidae. *J. Morphol*. **272**, 1444–1463.

Claeson KM, Hilger A. 2011 Morphology of the anterior vertebral region in elasmobranchs: special focus, Squatiniformes. *Foss. Rec*. **14**, 129–140.

Claeson KM, Underwood CJ, Ward DJ. 2013 †*Tingitanius tenuimandibulus*, a New Platyrhinid Batoid from the Turonian (Cretaceous) of Morocco and the Cretaceous Radiation of the Platyrhinidae. *J. Vertebr. Paleontol*. **33**, 1019–1036.

Coates MI, Gess RW, Finarelli JA, Criswell KE, Tietjen K. 2017 A Symmoriiform Chondrichthyan Braincase and the Origin of Chimaeroid Fishes. *Nature* **541**, 208–211.

Coates MI, Finarelli JA, Sansom IJ, Andreev PS, Criswell KE, Tietjen K, Rivers ML, La Riviere PJ. 2018 An early chondrichthyan and the evolutionary assembly of a shark body plan. *Proc. R. Soc. B.* **285**, 20172418.

Coates MI, Sequeira SEK. 1998 The braincase of a primitive shark. *Earth Environ. Sci. Trans. R. Soc. Edinb*. **89**, 63–85.

Coates MI, Sequeira SEK. 2001 A new stethacanthid chondrichthyan from the Lower Carboniferous of Bearsden, Scotland. *J. Vertebr. Paleontol*. **21**, 438–459.

Coates MI, Tietjen K. 2018 The neurocranium of the Lower Carboniferous shark *Tristychius arcuatus* (Agassiz, 1837). *Earth Environ. Sci. Trans. R. Soc. Edinb*. **108**, 19–35.

Compagno LJV. 1977 Phyletic Relationships of Living Sharks and Rays. *Am. Zool*. **17**, 303–322.

Compagno LJV. 1984a Sharks of the world. An annotated and illustrated catalogue of shark species known to date. Volume 4, Part 1. Hexanchiformes to Lamniformes. *FAO Fish. Synop.* **125**, 1–249.

Compagno LJV. 1984b Sharks of the world. An annotated and illustrated catalogue of shark species known to date. Volume 4, Part 2. Carcharhiniformes. *FAO Fish. Synop.* **125**, 251–655.

Compagno LJV. 1990a Alternative life-history styles of cartilaginous fishes in time and space. *Environ. Biol. Fishes* **28**, 33–75.

Compagno LJV. 1990b Relationships of the megamouth shark, *Megachasma pelagios* (Lamniformes: Megachasmidae), with comments on its feeding habits. *NOAA Tech. Rep. NMFS*. **90**, 357–379.

Compagno LJV. 2001 Sharks of the world. An annotated and illustrated catalogue of shark species known to date. Volume 2. Bullhead, mackerel and carpet sharks (Heterodontiformes, Lamniformes and Orectolobiformes). *FAO Species Cat. Fish. Purp.* **1**, 1–269.

Compagno LJV, Last PR. 2010 A new species of wedgefish, *Rhynchobatus springeri* (Rhynchobatoidei, Rhynchobatidae), from the western Pacific. In: Descriptions of new sharks and rays from Borneo. *CSIRO Marine and Atmospheric Research Paper* **32**, 77–88.

Cope ED. 1894 New and little known Paleozoic and Mesozoic fishes. *J. Acad. Nat. Sci. Phila.* **2**, 427–448.

Daniel JF. 1934. The elasmobranch fishes. Berkeley, CA: University of California Press, 3rd ed., 332 p.

Davis SP, Finarelli JA, Coates MI. 2012 *Acanthodes* and shark-like conditions in the last common ancestor of modern gnathostomes. *Nature* **486**, 247–250.

Dick JR. 1981. *Diplodoselache woodi* gen. et sp. nov., an early Carboniferous shark from the Midland Valley of Scotland. *Earth Environ Sci Trans R Soc Edinb.* **72**, 99–113.

Dupret V, Sanchez S, Goujet D, Tafforeau P, Ahlberg PE. 2014 A primitive placoderm sheds light on the origin of the jawed vertebrate face. *Nature* **507**, 500–503.

Ebert DA. 2014 *On board guide for the identification of pelagic sharks and rays of the Western Indian Ocean*. Roma, Italy: FAO.

Egerton P. 1844 Description of the mouth of a *Hybodus* found by Mr. Boscawen Ibbetson in the Isle of Wight. *Proc. Geol. Soc. Lond*. **4**, 414–416

El-Toubi MR. 1949 The development of the chondrocranium of the spiny dogfish, *Acanthias vulgaris* (*Squalus acanthias*). Part I. Neurocranium, mandibular and hyoid arches. *Jour. Morph*. **84**, 227–280.

Flammensbeck CK, Pollerspöck J, Schedel FDB, Matzke NJ, Straube N. 2018 Of Teeth and Trees: A Fossil Tip-Dating Approach to Infer Divergence Times of Extinct and Extant Squaliform Sharks. *Zool. Scr*. **47**, 539–557.

Frey E, Mulder EWA Stinnesbeck W, Rivera-Sylva HE, Padilla-Gutiérrez, González-González. 2017 A new polycotylid plesiosaur with extensive soft tissue preservation from the early Late Cretaceous of northeast Mexico. *Bol. Soc. Geol. Mex.* **69**, 86–134.

Frey L, Coates MI, Tietjen K, Rücklin M, Klug C. 2020 A Symmoriiform from the Late Devonian of Morocco Demonstrates a Derived Jaw Function in Ancient Chondrichthyans. *Commun. Biol*. **3**, 1–10.

Fraas E. 1896 Neue Selachier-Reste aus dem oberen Lias von Holzmaden in Württemberg. *Jahresh. Ver. vaterl. Naturkd. Wb*. **52**, 1–25.

Gardiner BG. 1984 The relationships of the palaeoniscid fishes, a review based on new specimens of Mimia and Moythomasia from the Upper Devonian of Western Australia. *Bull.br.Mus.nat.Hist.Geol*. **3**, 173–428.

Garman S. 1884 An extraordinary shark. *Bull. Essex Inst*. **16**, 47–55.

Garman S. 1880 New species of selachians in the museum collection. *Bull. Mus. comp. Zool*. **6**, 167–172.

Garman S. 1877 On the pelvis and external sexual organs of selachians, with especial references to the new genera *Potamotrygon* and *Disceus* (with descriptions). *Proc. Boston Soc. Nat. Hist*. **19**, 197–214.

Giles S, Friedman M, Brazeau MD. 2015 Osteichthyan-like cranial conditions in an Early Devonian stem gnathostome. *Nature* **520**, 82–85.

Girard CF. 1855 Characteristics of some cartilaginous fishes of the Pacific coast of North America. *Proc. Acad. Nat. Sci. Phila.* **7**, 196–197

Goloboff P, De Laet J, Ríos-Tamayo D, Szumik CA. 2021 A reconsideration of inapplicable characters, and an approximation with step- matrix recoding. *Cladistics* **37**, 596–629.

Goodrich ES. 1930. *Studies on the Structure and Development of Vertebrates.* London, UK: Macmillan and Co., Limited.

Goto T. 2001 Comparative Anatomy, Phylogeny and Cladistic Classification of the Order Orectolobiformes (Chondrichthyes, Elasmobranchii). *Mem. Grad. Sch. Fish. Sci. Hokkaido Univ*. **48**, 1–100.

Günther A. 1870 *Catalogue of the fishes in the British Museum*. London, UK: Taylor and Francis.

Günther A. 1877 Preliminary notes on new fishes collected in Japan during the expedition of H. M. S. `Challenger.' *Ann. Mag. Nat. Hist*. **119**, 433–446.

Günther A. 1880. *Report on the shore fishes procured during the voyage of H. M. S. Challenger in the years 1873-1876.* In: Report on the scientific results of the voyage of H. M. S. Challenger during the years 1873-76. Zoology, Vol 1.

Gray JE. 1831 Description of three new species of fish, including two undescribed genera, discovered by John Reeves, Esq., in China. *Zool. Misc*. **6**, 4–5.

Haacke W. 1885 Diagnosen zweier bemerkenswerther südaustralischer Fische. *Zool. Anz*. **8**, 508–509.

Hamm SA. 2020 Stratigraphic, geographic and paleoecological distribution of the Late Cretaceous shark genus *Ptychodus* within the Western Interior Seaway, North America. *Bull. N. M. Mus. Nat. Hist. Sci.* **81**, 1–94.

Hamm SA, Shimada K. 2004 A Late Cretaceous durophagous shark, *Ptychodus martini* Williston, from Texas. *Texas J. Sci.* **56**, 215–222.

Hodnett JPM, Grogan E, Lund R, Lucas SG, Suazo T, Elliott DK, Pruitt J. 2021 Ctenacanthiform sharks from the Late Pennsylvanian (Missourian) Tinajas member of the Atrasado Formation, central New Mexico. *Bull. N. M. Mus. Nat. Hist. Sci*. **84**, 391–424.

Holmgren N. 1940 Studies on the head in fishes. Part I: Development of the skull in sharks and rays. *Acta Zool*. **21**, 51–266.

Holmgren N. 1941 Studies on the Head in Fishes. Embryological, Morphological, and Phylogenetical Researches. Part II: Comparative Anatomy of the Adult Selachian Skull, with Remarks on the Dorsal Fins in Sharks. *Acta Zool*. **22**, 1–100.

Ifrim C. 2006 The fossil *Lagerstätte* at Vallecillo, north-eastern Mexico: Pelagic *Plattenkalks* related to Cenomanian–Turonian boundary anoxia. PhD thesis, University of Karlsruhe, Germany.

Ifrim C. 2013 Paleobiology and paleoecology of the early Turonian (Late Cretaceous) ammonite *Pseudaspidoceras flexuosum*. *Palaios* **28**, 9–22.

Ifrim C. 2015 Fluctuations of the oxygen minimum zone at the end of the Oceanic Anoxic Event 2 in the Gulf of Mexico and the response of ammonites. *Swiss J. Palaeontol.* **134**, 217–225.

Ifrim C, Stinnesbeck W. 2008 Cenomanian–Turonian hig-resolution biostratigraphy of north-eastern Mexico and its correlation with the GSSP and Europe. *Cret. Res.* **29**, 943–956.

Ifrim C, Götz S, Stinnesbeck W. 2011 Fluctuations of oxygen minimum zone at the end of Oceanic Anoxic Event 2 reflected by benthic and planktic fossils. *Geology* **39**, 1043–1046.

Ifrim C, Stinnesbeck W, Frey E. 2007 Upper Cretaceous (Cenomanian–Turonian and Turonian–Coniacian) open marine plattenkalk deposits in NE Mexico. *N. Jb. Geol. Paläont. Abh.* **245**, 71–81.Jaekel O. 1921 Die Stellung der Palaöntologie zu einigen Problemen der Biologie und Phylogenie. *Paläontol. Z.* **3**, 213–239.

Jambura PL, Villalobos-Segura E, Türtscher J, Begat A, Staggl MA, Stumpf S, Kindlimann R, Klug S, Lacombat F, Pohl B, Maisey GJ, Naylor GJP, Kriwet J. 2023 Systematics and phylogenetic interrelationships of the enigmatic Late Jurassic shark *Protospinax annectans* Woodward, 1918 with comments on the shark–ray sister group relationship. *Diversity* **15**, 311.

Jensen CF, Natanson LJ, Pratt Jr HL, Kolher NE, Campana SE. 2002 The reproductive biology of the porbeagle shark (*Lamna nasus*) in the western North Atlantic Ocean. *Fish. Bull.* **100**, 727–738.

Jollie M. 1962 *Chordate morphology*. London, UK: Chapman and Hall.

Jordan DS, Gilbert CH. 1880 Description of a new ray (*Platyrhina triseriata*), from the coast of California. *Proc. U. S. Natl. Mus*. **3**, 36–38.

Jordan DS. Gilbert CH. 1883 Description of a new species of *Rhinobatus* (*Rhinobatus glaucostigma*) from Mazatlan, Mexico. *Proc. U. S. Natl. Mus*. **6**, 210-211.

Jordan DS, Fowler HW. 1903 A review of the elasmobranchiate fishes of Japan. *Proc. U. S. Natl. Mus*. **26**, 593–674.

Klug S. 2010 Monophyly, Phylogeny and Systematic Position of the †Synechodontiformes (Chondrichthyes, Neoselachii). *Zool. Scr.* **39**, 37–49.

Lacepède BGE. 1798 Histoire Naturelle des Poissons. Plassan, Paris.

Landemaine O, Thies D, Waschkewitz J. 2018 The Late Jurassic Shark *Palaeocarcharias* (Elasmobranchii, Selachimorpha) – Functional Morphology of Teeth, Dermal Cephalic Lobes and Phylogenetic Position. *Palaeontogr. Abt. A.* **312**, 103–165.

Lane JA. 2010 Morphology of the braincase in the Cretaceous hybodont shark *Tribodus limae* (Chondrichthyes: Elasmobranchii), based on CT scanning. *Am. Mus. Novit*. **2010**, 1–70.

Linnaeus C. 1758. *Systema Naturae per regna tria naturae, regnum animale, secundum classes, ordines, genera, species, cum characteribus differentiis synonymis, locis. Tomus I. Editio decima, reformata.* Stockholm: Laurentii Salvii.

Lu J, Giles S, Friedman M, den Blaawen JL, Zhu M. 2016. The oldest actinopterygian highlights the cryptic early history of the hyperdiverse ray-finned fishes. *Curr. Biol.* **26**, 1602–1608.

Lund R. 1985 The morphology of *Falcatus falcatus* (St. John and Worthen), a Mississippian stethacanthid chondrichthyan from the Bear Gulch Limestone of Montana. *J. Vertebr. Paleontol*. **5**, 1–19.

Lund R. 1986 On *Damocles serratus*, nov. gen. et sp. (Elasmobranchii: Cladodontida) from the Upper Mississippian Bear Gulch Limestone of Montana. *J. Vertebr. Paleontol*. **6**, 12–19.

Maisey JG. 1977 The fossil selachian fishes *Palaeospinax* Egerton, 1872 and *Nemacanthus* Agassiz, 1837. *Zool. J. Linn. Soc*. **60**, 259–273.

Maisey JG. 1980 An evaluation of jaw suspension in sharks. *Am. Mus. Nov*. **2706**, 1–17.

Maisey JG. 1982 The Anatomy and Interrelationships of Mesozoic Hybodont Sharks. *Am. Mus. Novit*. **2724**, 1–48.

Maisey JG. 1983. Cranial anatomy of *Hybodus basanus* Egerton from the Lower Cretaceous of England. *Am. Mus. Novit.* **1983**, 1–64.

Maisey JG. 1984 Higher elasmobranch phylogeny and biostratigraphy. *Zool. J. Linn. Soc*. **82**, 33–54.

Maisey JG. 1985 Cranial Morphology of the Fossil Elasmobranch *Synechodus dubrisiensis*. *Am. Mus. Novit.* **2804**, 1–28.

Maisey JG. 1986 The Upper Jurassic hexanchoid elasmobranch *Notidanoides* n. g. *Neues Jahrb. Geol. Paläontol. Abh*. **172**, 83–106.

Maisey JG. 1987 Cranial anatomy of the Lower Jurassic shark *Hybodus reticulatus* (Chondrichthyes, Elasmobranchii): with comments on hybodontid systematics. *Am. Mus. Novit*. **2878**. 1–39.

Maisey JG. 1989 *Hamiltonichthys mapesi*, g. & sp. nov. (Chondrichthyes, Elasmobranchii), from the Upper Pennsylvanian of Kansas. *Am. Mus. Novit*. **2931**, 1–44.

Maisey JG. 2001 A primitive chondrichthyan braincase from the Middle Devonian of Bolivia. In *Major events in early vertebrate evolution* (ed. PE Ahlberg), pp. 263–288. London, UK: Taylor & Francis.

Maisey JG. 2004. Morphology of the braincase in the broadnose sevengill shark *Notorynchus* (Elasmobranchii, Hexanchiformes), based on CT scanning. *Am. Mus. Novit*. **3429**, 1–52.

Maisey JG. 2005 Braincase of the Upper Devonian shark *Cladodoides wildungensis* (Chondrichthyes, Elasmobranchii), with observations on the braincase in early chondrichthyans. *Bull. Am. Mus. Nat. Hist.* **288**, 1–103.

Maisey JG. 2007 The braincase in Paleozoic symmoriiform and cladoselachian sharks. *Bull. Am. Mus. Nat. Hist.* **307**, 1–122.

Maisey JG. 2008 The postorbital palatoquadrate articulation in elasmobranchs. *J. Morphol.* **269**, 1022–1040.

Maisey JG, Miller R, Pradel A, Denton JS, Bronson A, Janvier P. 2017. Pectoral morphology in *Doliodus*: bridging the 'acanthodian'-chondrichthyan divide. *Am. Mus. Nat. Hist.* **3875**, 1–15.

Maisey JG, Janvier P, Pradel A, Denton JSS, Bronson A, Miller R, Burrow CJ. 2019 *Doliodus* and pucapampellids: Contrasting perspectives on stem chondrichthyan morphology. In *Evolution and Development of Fishes* (eds Z Johanson, C Underwood, M Richter), pp. 87–109. Cambridge, UK: Cambridge University Press.

Maisey JG, Lane JA. 2010 Labyrinth morphology and the evolution of low-frequency phonoreception in elasmobranchs. *C R Palevol* **9**, 289–309.

Maisey JG, Springer VG. 2013 Chondrocranial morphology of the Salmon Shark, *Lamna ditropis*, and the Porbeagle, *L. nasus* (Lamnidae). *Copeia* **2013**, 378–389.

Marini TL. 1936 Revisión de las especies de la familia "Squatinidae" en las aguas argentinas ("*S. guggenheim*" n. sp.). *Physis (Buenos Aires)* **12**, 19–30.

Marramà G, Klug S, De Vos J, Kriwet J. 2018 Anatomy, relationships and palaeobiogeographic implications of the first Neogene holomorphic stingray (Myliobatiformes: Dasyatidae)

from the early Miocene of Sulawesi, Indonesia, SE Asia. *Zool. J. Linn. Soc.* **184**, 1142–1168.

Matsubara K. 1936 A new carcharoid shark found in Japan. *Zool. Mag. Tokyo* **48**, 380–382.

McCulloch AR. 1911 *Report on the fishes obtained by the F. I. S. "Endeavour," on the coasts of New South Wales, Victoria, South Australia and Tasmania. Part I. Biological Results Endeavour*.

McEachran JD, Aschliman N. Phylogeny of Batoidea. 2004 In *Biology of Sharks and their Relatives*, (eds JC Carrier, JA Musick, MR Heithaus), pp. 79–109. Boca Raton, FL: CRC Press.

McEachran JD, Dunn KA. 1998 Phylogenetic Analysis of Skates, a Morphologically Conservative Clade of Elasmobranchs (Chondrichthyes: Rajidae). *Copeia* **1998**, 271–290.

McEachran JD, Dunn KA, Miyake T. 1996 Interrelationships of the batoid fishes (Chondrichthyes: Batoidea). In *Interrelationships of fishes* (eds ML Stiassny, LR Parenti, GD Johnson), pp. 63–83. New York, NY: Atlantic Press.

McEachran JD, Miyake T. 1988 A new species of skate from the Gulf of California (Chondrichthyes, Rajoidei). *Copeia* **1988**, 877–886.

de Miranda Ribeiro A. 1907 Fauna Braziliense. Peixes. II. Desmobranchios. *Arch. Mus. Nac. (Rio de J.)* **14**, 131–217

Moreira RA, Gomes UL, de Carvalho MR. 2017 Clasper morphology of skates of the tribe Riorajini (Chondrichthyes: Rajiformes: Arhynchobatidae) and its systematic significance. *J. Morphol.* **278**, 1185–1196.

Moreira RA, de Carvalho MR. 2021 Phylogenetic significance of clasper morphology of electric rays (Chondrichthyes: Batoidea: Torpediniformes). *J. Morphol.* **282**, 438–448.

Mori O. 1924 Uber die Entwicklung des Schadelskelettes des Dornhaies, Acanthias vulgaris. *Z. Anat. Entw. Gesch*. **73**, 389–430.

Müller J, Henle FGJ. 1837 Gattungen der Haifische und Rochen nach einer von ihm mit Hrn. Henle unternommenen gemeinschaftlichen Arbeit über die Naturgeschichte der Knorpelfische. *Monatsb. K. Preuss. Akad. Wiss. Berlin* **1837**, 111–118.

Müller J, Henle FGJ. 1841 Systematische Beschreibung der Plagiostomen. *Berlin, Verlag Von Veit und Comp*. **1841**, 1–200.

Nakaya K. 1975 Taxonomy, comparative anatomy and phylogeny of Japanese catsharks, Scyliorhinidae. *Mem. Fac. Fish., Hokkaido Univ*. **23**, 1–94

Newberry JS. 1889 The Paleozoic fishes of North America. *Monogr. U. S. Geol. Surv.* **16**, 1–340.

Niebuhr C. 1775. Descriptiones animalium, avium, amphibiorum, piscium, insectorum, vermium / quae in itinere orientali observavit Petrus Forskål. Post mortem auctoris edidit Carsten Niebuhr. Adjuncta est materia medica kahirina atque tabula maris Rubri geographica. Post mortem auctoris edidit Carsten Niebuhr. Hauniae. *Descriptiones animalium quae in itinere ad Maris Australis terras Pisces*.

Nishida K. 1990 Phylogeny of the Suborder Myliobatidoidei. *Mem. Fac. Fish. Sci. Hokkaido Univ.* **37**, 1–108.

Notarbartolo di Sciara G. 1987 A revisionary study of the genus *Mobula* Rafinesque, 1810 (Chondrichthyes: Mobulidae), with the description of a new species. *Zool. J. Linn. Soc.* **91**, 1–91.

Ogilby JD. 1893 Description of a new shark from the Tasmanian coast. *Rec. Aust. Mus.* **2**, 62–63.

von Olfers JFM. 1831 *Die Gattung Torpedo in ihren naturhistorischen und antiquarischen Beziehungen erläutert*. Berlin.

de Oliveira Lana F, Soares KD, Hazin FHV, Gomes UL. 2021 Description of the chondrocranium of the silky shark *Carcharhinus falciformis* with comments on the cranial terminology and phylogenetic implications in carcharhinids (Chondrichthyes, Carcharhiniformes, Carcharhinidae). *J. Morphol.* **282**, 685–700.

Palmer G. 1950 A new species of electric ray of the genus *Diplobatis* from British Guiana. *Ann. Mag. Nat. Hist.* **3**, 480–484.

Patterson C. 1965 The phylogeny of the chimaeroids. *Philos. Trans. R. Soc. B.* **249**, 101–219.

Péron F. 1807 Voyage de Découvertes aux Terres Australes, exécuté par ordre de sa majesté l'Empereur et Roi, sur les Corvettes la Géographe, la Naturaliste et la Goulette le Casuarina, pendant les années 1800, 1801, 1803 et 1804. Paris. *Voyage de Découvertes aux Terres Australes* **1**, 1–496.

Peters WCH. 1855 Übersicht der in Mossambique beobachteten Seefische. *Monatsb. K. Preuss. Akad. Wiss. Berlin* **1855**, 428–466.

Pilgrim BL, Franz-Odendaal TA. 2009 A comparative study of the ocular skeleton of fossil and modern chondrichthyans. *J. Anat.* **214**, 848–858.

Pollerspöck J, Straube N. 2022 Phylogenetic placement and description of an extinct genus and species of kitefin shark based on tooth fossils (Squaliformes: Dalatiidae). *J. Syst. Palaeontol*. **19**, 1083–1096.

Pradel A. 2010 Skull and brain anatomy of Late Carboniferous Sibyrhynchidae (Chondrichthyes, Iniopterygia) from Kansas and Oklahoma (USA). *Geodiversitas* **32**, 595–661.

Pradel A, Tafforeau P, Maisey JG, Janvier P. 2011 A new Paleozoic Symmoriiformes (Chondrichthyes) from the Late Carboniferous of Kansas (USA) and cladistic analysis of early chondrichthyans. *PLoS One* **6**, e24938.

Pradel A, Didier D, Casane D, Tafforeau P, Maisey JG. 2013 Holocephalan embryo provides new information on the evolution of the glossopharyngeal nerve, metotic fissure and parachordal plate in gnathostomes. *PLoS One* **8**, e66988.

Qiao T, King B, Long JA, Ahlberg PE, Zhu M. 2016 Early Gnathostome Phylogeny Revisited: Multiple Method Consensus. *PLoS One* **11**, e0163157.

Rafinesque CS. 1810 *Caratteri di alcuni nuovi generi e nuove specie di animali e pinate della Sicilia, con varie osservazioni sopra i medisimi*. Part 1.

Regan CT. 1906 Descriptions of new or little-known fishes from the coast of Natal. *Ann. Natal Mus*. **1**, 1–6.

Richardson J. 1846 Report on the ichthyology of the seas of China and Japan. *Report of the British Association for the Advancement of Science 15th meeting*. 187–320.

Riley C, Cloutier R, Grogan ED. 2017 Similarity of morphological composition and developmental patterning in paired fins of the elephant shark. *Sci. Rep*. **7**, 1–10.

Schaeffer B. 1981 The xenacanth shark neurocranium, with comments on elasmobranch monophyly. *Bull. Am. Mus*. **169**, 1–72.

Schultze H-P, Fuchs D, Giersch S, Ifrim C, Stinnesbeck W. 2010 Palaeoctopus pelagicus from the Turonian of Mexico reinterpreted as a coelacanth (sarcopterygian) gular plate. *Palaeontology* **53**, 689–694.

Sewertzoff AN. 1897 Beitrag zur Entwicklungsgeschichte des Wirbeltierschadels. *Anat. Anz*. **13**, 409–425.

Shimada K. 2005 Phylogeny of lamniform sharks (Chondrichthyes: Elasmobranchii) and the contribution of dental characters to lamniform systematics. *Paleontol. Res*. **9**, 55–72.

Shimada K. 2012 Dentition of Late Cretaceous shark, *Ptychodus mortoni* (Elasmobranchii, Ptychodontidae). *J. Vert. Paleontol.* **32**, 1271–1284.

Shimada K, Rigsby, CK, Kim S. 2009 Partial skull of the Late Cretaceous durophagous shark, *Ptychodus occidentalis* (Elasmobranchii: Ptychodontidae), from Nebraska, U.S.A. *J. Vert. Paleontol.* **29**, 336–349.

Shimada K, Everhart MJ, Decker R, Decker PD. 2010 A new skeletal remain of the durophagous shark, *Ptychodus mortoni*, from the Upper Cretaceous of North America: an indication of gigantic body size. *Cret. Res.* **31**, 249–254.

Shirai S. 1992 *Squalean Phylogeny: A New Framework of "Squaloid" Sharks and Related Taxa*. Hokkaido University Press.

Shirai S. 1996 Phylogenetic Interrelationships of Neoselachians (Chondrichthyes: Euselachii). In *Interrelationships of Fishes* (eds MLJ Stiassny, LR Parenti, DG Johnson), pp. 9–34. San Diego, CA: Academic Press.

da Silva JPCB, de Carvalho MR. 2015 Morphology and phylogenetic significance of the pectoral articular region in elasmobranchs (Chondrichthyes). *Zool. J. Linn. Soc*. **175**, 525-568.

da Silva JPCB, Datovo A. 2020 The coracoid bar and its phylogenetic importance for elasmobranchs (Chondrichthyes). *Zool. Anz*. **287**, 167-177.

Soares KD, Gomes UL, Carvalho MR. 2016 Taxonomic review of catsharks of the *Scyliorhinus haeckelii* group, with the description of a new species (Chondrichthyes: Carcharhiniformes: Scyliorhinidae). *Zootaxa*, **4066**, 501-534.

Soares KD, de Carvalho MR. 2020 Phylogenetic relationship of catshark species of the genus *Scyliorhinus* (Chondrichthyes, Carcharhiniformes, Scyliorhinidae) based on comparative morphology. *Zoosystematics Evol.* **96**, 345–395.

Smith KT, Buchy M-C. 2008 A new aigialosaur (Squamata: Anguimorpha) with soft tissue remains from the Upper Cretaceous of Nuevo León, Mexico. *J. Vert. Paleontol.* **28**, 85–94.

Stahl BJ. 1999 Chondrichthyes III: Mesozoic and Cenozoic Elasmobrachii: Teeth. In *Handbook of Paleoichthyology*, (ed. H-P Schultze). München, Germany: Verlag Dr. Friedrich Pfeil.

Stehmann MFW. 2002 Proposal of a maturity stages scale for oviparous and viviparous cartilaginous fishes (Pisces, Chondrichthyes). *Arch. Fish. Mar. Res.* **50**, 23–48.

Temminck CJ, Schlegel H. 1850 Pisces. In *Fauna Japonica, sive descriptio animalium quae in itinere per Japoniam suscepto annis 1823–30 collegit, notis observationibus et adumbrationibus illustravit* (ed. PF de Siebold), vol. 2, pp. 1–323: Lugduni Batavorum [Leiden], Netherlands: Apud Auctorem.

Thiollière V. 1852 Troisième notice sur les gisements à poissons fossiles situés dans le Jura du département de l'Ain. *Ann. Sci. Phys. Nat. Agric. Indust., 2ème série* **4**, 353–446.

Villalobos-Segura E, Marramà G, Carnevale G, Claeson KM, Underwood CJ, Naylor GJP, Kriwet J. 2022 The Phylogeny of Rays and Skates (Chondrichthyes: Elasmobranchii) Based on Morphological Characters Revisited. *Diversity*. **14**, 1–65.

Villalobos-Segura E, Underwood CJ, Ward DJ, Claeson KM. 2019 The First Three-Dimensional Fossils of Cretaceous Sclerorhynchid Sawfish: *Asflapristis cristadentis* gen. et sp. nov., and Implications for the Phylogenetic Relations of the Sclerorhynchoidei (Chondrichthyes). *J. Syst. Palaeontol*. **17**, 1847–1870.

de Vis CW. 1883 Description of new genera and species of Australian fishes. *Proc. Linn. Soc. N. S. W.* **8**, 283-289.

Vullo R, Frey E, Ifrim C, González González MA, Stinnesbeck ES, Stinnesbeck W. 2021 Manta-like planktivorous sharks in Late Cretaceous oceans. *Science* **371**, 1253–1256.

Woodward AS. 1887 On the dentition and affinities of the selachian genus *Ptychodus*, Agassiz. *Quart. J. Geol. Soc.* **43**, 121–131.

Woodward AS. 1892 On the Lower Devonian fish-fauna of Campbellton, New Brunswick. *Geol. Mag.* **9**, 16.

Woodward AS. 1904 On the jaws of *Ptychodus* from the Chalk. *Quart. J. Geol. Soc.* **60**, 133–136.

Woodward AS. 1912 The fossil fish of the English Chalk, Part VII. *Monogr. Palaeontogr. Soc.* **65**, 225–264.

Zangerl R. 1973 Interrelationships of early chondrichthyans. In *Interrelationships of fishes* (eds PH Greenwood, RS Miles, C Patterson), pp. 1–14. London, UK: Academic Press.

Zangerl R, Case GR. 1976 *Cobelodus aculeatus* (Cope) an anacanthous shark from Pennsylvanian black shales of North America. *Palaeontograph. Abt. A.* **154**, 107–157.

Zhu M, Ahlberg P, Pan Z, Zhu Y, Qiao T, Zhao W, Jia L, Lu J. 2016 A Silurian maxillate placoderm illuminates jaw evolution. *Science* **354**, 334–336.

Zhu M, Zhao W, Jia L, Lu J, Qiao T, Qu Q. 2009 The oldest articulated osteichthyan reveals a mosaic of gnathostome characters. *Nature* **458**, 469–474.

Zhu M, Yu X, Ahlberg PE, Choo B, Lu J, Qiao Q, Zhao LJ, Blom H, Zhu Y. 2013 A Silurian placoderm with osteichthyan-like marginal jaw bones. *Nature* **52**, 188–193.